Multiple-Output Power Converter Topologies for LED Driver Application

Submitted in partial fulfillment of the requirements
for the award of the degree of

Doctor of Philosophy

By
Hemasundara Rao Kolla
(Roll No. 716112)

Supervisor
Dr. Bhagwan K Murthy
Professor

Department of Electrical Engineering
National Institute of Technology
Warangal
November - 2022

Dedicated to

My beloved Father **K Govindarao**

and to my wife **K Sri Vidya**

and to my sons **K Chahan & K Adhvit**

APPROVAL SHEET

This thesis entitled **"Multiple-Output Power Converter Topologies for LED Driver Application"** by **Hemasundara Rao Kolla** is approved for the degree of Doctor of Philosophy.

Examiners

.....

.....

.....

Supervisor

Dr. Bhagwan K Murthy

Professor,

Department of Electrical Engineering, NIT Warangal.

Chairman

Dr. M. Sailaja Kumari

Professor & Head,

Department of Electrical Engineering, NIT Warangal.

Date:.....

Department of Electrical Engineering
National Institute of Technology Warangal
Warangal - 506004, Telangana State, India.

DEPARTMENT OF ELECTRICAL ENGINEERING

NATIONAL INSTITUTE OF TECHNOLOGY WARANGAL

WARANGAL-506004

CERTIFICATE

This is to certify that the thesis entitled **"Multiple-Output Power Converter Topologies for LED Driver Application "**, which is being submitted by **Mr. Hemasundara rao Kolla** (Roll No: 716112), is a bonafide work submitted to National Institute of Technology Warangal in partial fulfillment of the requirements for the award of the degree of **Doctor of Philosophy** in Department of Electrical Engineering. To the best of my knowledge, the work incorporated in this thesis has not been submitted elsewhere for the award of any degree.

Date:
Place: NIT-Warangal

Dr. Bhagwan K Murthy
(Supervisor)
Professor
Department of Electrical Engineering
National Institute of Technology Warangal
Warangal - 506004

DECLARATION

This is to certify that the work presented in the thesis entitled **"Multiple-Output Power Converter Topologies for LED Driver Application"** is bonafide work done by me under the supervision of **Dr. Bhawan K Murthy**, Professor, Department of Electrical Engineering, National Institute of Technology, Warangal, India and was not submitted elsewhere for the award of any degree.

I declare that this written submission represents my ideas in my own words and where others ideas or words have been included, I have adequately cited and referenced the original sources. I also declare that I have adhered to all principles of academic honesty and integrity and have not misrepresented or fabricated or falsified any idea/date/fact/source in my submission. I understand that any violation of the above will be cause for disciplinary action by the institute and can also evoke penal action from the sources which have thus not been properly cited or from whom proper permission has not been taken when needed.

Date:
Place: NIT-Warangal

Hemasundara Rao Kolla
(Roll no: 716112)

ABSTRACT

In present lighting industry, Light Emitting Diode (LED) becomes a prominent light source for wide range of residential, industrial and commercial lighting applications. LED based lighting systems have gained remarkable attention over conventional lighting systems due to their several advantages such as energy efficient, high operating life, high brightness, environment friendly nature, and compactness. LEDs are current controlled or current driven devices. Hence LED based lighting systems require efficient constant current regulators. The essential requirements of LED driver circuits are: high efficiency, LED load current regulation, dimming control, compact size, high reliability etc.

Keeping in view the requirements of LED driver circuits, THREE driver circuit configurations for LED based lighting applications have been proposed in this thesis. The objectives are to provide high power conversion efficiency, reduced device current, powering of multiple lighting loads with dimming, zero-voltage switching, driving LED lamps of different power ratings, regulation of LED lamp current against input voltage variations and configurations suitable for high power lighting application.

The first work proposed a phase shift controlled full-bridge series resonant converter (SRC) integrated with buck converters for light-emitting diode (LED) driver application. This LED driver supplies four LED loads simultaneously. The current through LED loads is controlled by phase shift control of the SRC, and its output is added to the input voltage. Zerovoltage switching (ZVS) switching of all the switches is achieved by operating the SRC at lagging power factor for all input voltage variations. In this converter only part of the output power is processed through the SRC. The peak-efficiency of the converter is 95.7%. This configuration also provides reduced components count per lamp and hence reduction in cost.This configuration is suitable for street lighting as well as domestic lighting applications.

The second proposed converter configuration consists of a Dual frequency resonant converter. This configuration is powering two LED lamps of different power ratings. In this configuration, two series resonant circuits with different resonant frequencies are used to power two LED lamps. This circuit operates simultaneously at two different frequencies. This configuration provides regulation of LED lamp currents and independent PWM dimming control of LED

lamps. It also provides partial ZVS operation.

The third work proposed a dual output series resonant converter-based LED driver which utilizes three switches to form two half-bridge networks. The proposed three switch two half-bridge structure provides reduced switch count and independent control. It uses asymmetric duty cycle control to regulate the LED operating currents and utilizes a lowfrequency pulse width modulation (PWM) dimming scheme for each half-bridge to control the illumination of each LED load independently. All the switches in the proposed converter operate with Zero voltage turn-on to reduce the switching losses. This configuration is suitablefor applications like colour mixing, multi-colour light systems etc.

Contents

List of Figures

List of Tables

Abbreviations & Symbols

δ	Phase shift angle
Φ	Phase angle
C_r	Resonant capacitor
C_{o1}	Output filter capacitor-1
C_{o2}	Output filter capacitor-2
C_o	Output filter capacitor of full-bridge SRC
C_{r1}	SRC-1 resonant capacitor
C_{r2}	SRC-2 resonant capacitor
C_{rh}	High frequency resonant capacitor
C_{rl}	Low frequency resonant capacitor
D_1	Duty ratio of switch S_1
D_3	Duty ratio of switch S_3
D_{HF}	Duty ratio of high frequency switch
D_{LF}	Duty ratio of low frequency switch
f_d	Dimming frequency
f_H	High switching frequency
f_L	Low switching frequency
f_{r1}	Resoant frequency of SRC-1

f_{r2}	Resoant frequency of SRC-2
f_{rh}	High Resoant frequency
f_{rl}	Low resoant frequency
f_r	Resoant frequency
f_s	Switching frequency
G	Gain of SRC
i_r	Resoant circuit current
i_{d1}	Switch S_1 current
i_{d2}	Switch S_2 current
i_{d3}	Switch S_3 current
i_{d4}	Switch S_4 current
i_{dcbus}	DC bus current
I_{o1}	Lamp-1 output current
I_{o2}	Lamp-2 output current
I_{o3}	Lamp-3 output current
I_{o4}	Lamp-4 output current
i_{r1}	Resonant circuit-1 current
i_{r1}	Resonant circuit-2 current
i_{rh}	High frequency resonant circuit current
i_{rl}	Low frequency resonant circuit current
L_{r1}	SRC-1 resonant inductror

L_{r2}	SRC-2 resonant inductror
L_{rh}	High frequency resonant inductror
L_{rl}	Low frequency resonant inductror
L_r	Resonant inductror
R_{eff}	Effective resistance seen by SRC
V_{dcbus}	DC bus voltage
V_{DC}	DC input voltage
V_{ds1}	Drain source voltage of switch S_1
V_{ds2}	Drain source voltage of switch S_2
V_{ds3}	Drain source voltage of switch S_3
V_{ds4}	Drain source voltage of switch S_4
V_{gs1}	Gate source voltage of switch S_1
V_{gs2}	Gate source voltage of switch S_2
V_{gs3}	Gate source voltage of switch S_3
V_{gs4}	Gate source voltage of switch S_4
V_{o1}	Lamp-1 voltage
V_{o2}	Lamp-2 voltage
V_{o3}	Lamp-3 voltage
V_{o4}	Lamp-4 voltage
AC	Alternating current
ADC	Asymetric duty cycle control

AM	Amplitude modulation
CFL	Compact fluorescent lamps
CI	Coupled indutor
DC	Direct current
DCM	Discontinous conductiom mode
EMI	Electromagnetic interference
FBI	Full-bridge inverter
FFT	Fast fourier transform
HBI	Half-bridge inverter
HBLED	High brightness light emitting diode
HF	High frequency
HFT	High frequency transformer
HID	High-intensity discharge
IR	Infrared
LCD	Liquid crystal display
LED	Light emitting diode
LF	Low frequency
MOSFET	Metal-oxide-semiconductor field-effect transistor
MOSPI	Ministry of statistics and program implementation
PCM	Pulse code modulation
PF	Power factor

PFC	Power factor correction
PV	Photovoltaic
PWM	Pulse width modulation
S-type	Switched mode
S1	Single-stage
S2	Two-stage
S2A	Two-stage type-A
S2B	Two-stage type-B
S3	Three-stage
SRC	Series resonant converter
SSL	Solid state lighting
TDM	Time division multiplexing
THD	Total harmonic distortion
UV	Ultraviolet
VI	Variable inductor
ZVS	Zero voltage switching

Chapter 1

Introduction

Chapter 1

Introduction

1.1 General introduction

Since the development of elctrical bulb, lighting became key to productivity and development. Recently electrified communities and industrialized countries both regarded lighting as the foremost most important electrical load to be connected. In 2020, lighting consumed 20% of the total Indian electrical usage [1]. As result, there is a need to improve the performance of lighting technology. For the industry, this means increasing the efficiency and efficacy of industrial and domestic lighting.

The lighting industry has evolved through several technologies over the last century. The first electric lamp was invented by Thomas Alva Edison in 1879. The world described this electric lamp as an incandescent lamp and human entered into electric era. The incandescent lamp is oldest and universal type of light source. Since from Edison invention, the lighting technology has been started growing explosively. In the global market, the incandescent lamp is a prime element in lighting technology. The light is produced by heating up the tungsten by passing the electric current, which can turn on instantly and it does not require electronic ballast, hence results in less cost. However, only 10% of electrical energy is converted into light and rest of energy is wasted as heat, hence incandescent lamps are energy inefficient. Further, incandescent lamps suffer from short life-span (750-2000 hrs) and low luminous efficacy (4-18 lm/W).

The industries and researchers have been exploring widely to develop new lighting technologies to improve efficiency, life-span, and to reduce the cost. The fluorescent lamp is invented in 1903 which replace the conventional incandescent lamp. A fluorescent lamp is a low weight mercury vapor lamp, which uses electricity to excite mercury vapor to generate ultraviolet (UV) radiation, then it causes a phosphor to produce a visible light. As compared to incandescent lamps, the fluorescent lamps are high luminous efficacy (50-80 lm/W), long

life (5000-8000 hrs) and generate less heat. However, the fluorescent lamps are harmful to the environment and human health due to the presence of toxic gas.

Subsequently, high-intensity discharge (HID) lamps have been developed in contrast to incandescent and fluorescent lamps. The HID lamps or bulbs are a family of gas-discharge arc lamps which produces light by sending electrical discharge between two electrodes and plasma or ionized gas. Based on the type of gas used in the lamp, these HID lamps are classified as sodium, mercury and metal halide lamps. HID lamps can provide high luminous efficacy and long life in comparison with incandescent and fluorescent lamps. Like in fluorescent lamps, the HID lamps also use toxic gas to produce light and hence, results in environmental issues.

In order to overcome the various drawbacks and limitations of the conventional lighting system, the development of clean and energy efficient lighting is most desired. Therefore, the research is progressively exploring significant developments in the lighting industry. The light emitting diode (LED) has become a promising lighting resource for a future generation due to its various advantages such as long life and high efficacy etc [2, 3].

The utilization of incandescent bulbs is 63%, compact fluorescent lamps (CFL) are 35%, HID lamps are 2% and solid-state lighting (SSL) is 0.08% as per ministry of statistics and program implementation (MOSPI) report. The researchers have found that currently the incandescent bulbs are being used approximately 63% for industrial, commercial and residential lighting systems. These incandescent bulbs are less luminous efficacy, poor efficient and also oldest in lighting technology. Therefore, the energy efficient lighting sources need be developed to save energy in lighting technology by using high-brightness LED (HB-LED) device and high efficient power converters. LED technology is growing enormously due to its significant advantages and applications as follows;

1.1.1 Advantages and disadvantages of LEDs

- **Efficency:** They have estimated energy efficiency of 80%-90% when compared to conventional lighting.
- **Lifetime:** LED bulbs have an outstanding operational lifetime of over 50,000 hrs.
- **Response time:** Response time of LED is in the order of micro seconds. Hence, LEDs

can be used in high frequency ON-OFF applications.

- **Color LEDs:** LEDs can emit light of the desired colour without the use of colour filters, as traditional lighting methods require .
- **Dimming:** LEDs are ideal for PWM or AM dimming.
- **Durability:** LEDs are physically more durable than incandescent or fluorescent bulbs because they are solid-state devices.
- **Ecologically Friendly:**LED lights are clean and eco-friendly. It doesn't emit any toxic gasses like in conventional lights.

1.1.2 Disadvantages of LEDs

- **Temperature dependence:** The temperature of the operating environment and thermal management properties have a significant impact on LED performance.
- **LED driver complexity:** LEDs are highly sensitive to voltage. A small voltage delta causes a significant change in current and life time. As a result, complex drivers are required to reglate the LED currents.

1.1.3 Applications of LEDs

LEDs are suitable for wide range of applications due to their several advantages like; energy efficient, high operating life, high brightness, environment friendly nature, and compactness. The applications of LED based lighting are listed as follows.

i) General illumination

ii) Residential lighting

iii) Automotive applications

iv) Street Lighting

v) Signal lighting

vi) Decorative lighting

vii) Liquid crystal display (LCD) panels

viii) Agriculture

ix) Communication applications

x) Biomedical applications

1.2 Over view of LEDs

1.2.1 Physical structure and Operation of LED

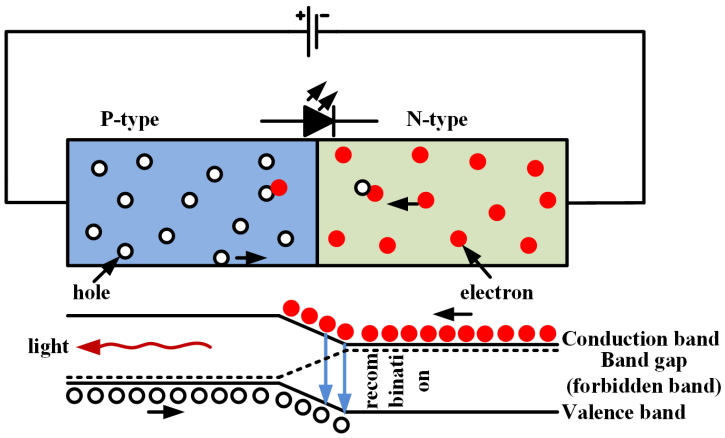

Figure 1.1: Operating principle of a LED

LED is a semiconductor device that produces light through electroluminescence. The principle of operation of LED is shown in Fig 1.1. Construction of LED is similar to normal p-n junction diode. LEDs are made up of a semiconductor chip doped with P-type impurities on one side and N-type impurities on the other, resulting in a p-n junction. When a sufficient forward voltage across the p-n junction is applied, electrons begin to move from cathode to anode and recombine with holes. When an electron recombines with a hole, it immediately falls to a lower energy level, releasing the energy difference in the form of light. The wavelength and color of the light dependes on the bandgap of the semiconductor material forming p-n junction. In indirect bandgap semiconductors like Si or Germanium (Ge) diodes, the recombination process is a non-radiative transition. Thus, no light is produced. LEDs are made from direct bandgap

materials like gallium arsenide (GaAs), indium gallium arsenide (InGaAs), etc. whose optical wavelengths in the range of visible, UV and IR of electromagnetic spectrum. The representation and electrical model of an LED are discussed in the following section.

1.2.2 Characteristics and Equivalent Model of LED

The typical I-V characteristic curves of different colour LEDs are shown in Fig. 1.2. When LED is reverse biassed or voltage applied across LED is less than the threshold voltage (V_{th}) than no current flows thorough the LED. The forward current increases exponentially as the forward voltage (V_F) applied across the LED crosses V_{th}. The voltage V_{th} depends on the wavelength of light emitted by LED. In order to simplify the analysis, LEDs are replaced with a piece-wise-linear model. Thus the LED can be modelled as a series connection of a dynamic resistance R_d, an thershold voltage V_{th}, and an ideal diode. LED symbol and its electrical equivalent model is shown in Fig. 1.3. Since the dynamic resistance of a LED is small, a small change in voltage across the it causes in a large variation in the current. In other words, an LED can often be thought of as a constant voltage load. Since the power output from LED is proportional to current flowing through LED, they must be powered from constant current power supplies to get constant illumination.

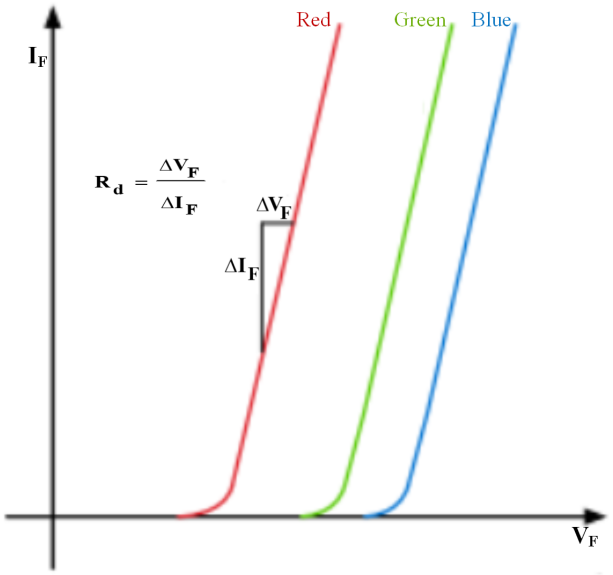

Figure 1.2: I-V Characteristics of different colour LEDs

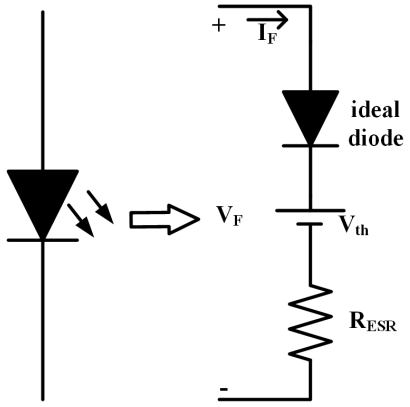

Figure 1.3: Symbol and Electrical equivalent circuit of LED

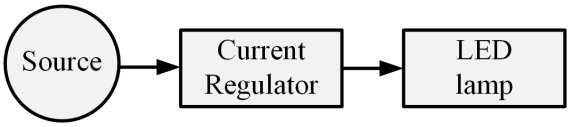

Figure 1.4: Schematic of LED driver

1.3 LED driver

Examining the characteristics of a LED as a load, we clearly understand that a LED currents needs to be regulated properly in order to provide the desired light output. Moreover, this desired light output has to be unperturbed by the tolerances in the electrical characteristics of the LED, and independent of the perturbations of the energy source. The current regulator and LED load together is generally called as LED driver circuit which is shown in Fig 1.4. Several types of driver circuits for LED lighting applications have been proposed by different researchers based on the availability of driving sources, such as AC fed LED drivers [4–29], DC fed LED drivers [30–57] etc. The requirements of AC fed LED drivers and DC fed LED drivers are different. However, high efficiency, LED load current regulation, dimming control, compact size, high reliability etc., are the main requirements to be met by LED driver circuit irrespective of the driving source.

In AC fed LED drivers, the required constant current is supplied by the utility ac mains supply. They are classified as passive LED drivers and switched mode LED drivers. Passive LED drivers consists of only passive devices like capacitors and inductor. LED loads are supplied with high ac ripple without active control. Hence they are simple, highly reliable, cost-effective and they produce low electromagnetic interference (EMI) [4–7]. However low

power factor (PF), lack of precise current regulation, high source current total harmonic distortion (THD), usage of large electrolytic capacitors and large size of inductors are the limitations of passive LED drivers. On the contrary, switched mode LED drivers overcome the limitations of passive LED drivers due to their high frequency operation. Due to active control of switched mode LED drivers, they achieve high PF, low THD, precise LED load current regulation, high efficiency, dimming control, compactness, isolation between LED load and input etc. [8–29]. Switched mode LED drivers are further classified as single-stage LED drivers [8–17], two-stage LED drivers [18–25] and three-stage LED drivers [26–29]. In single-stage LED drivers, both PFC and LED load current regulation are achieved with single dc-dc converter. Due to less components, single stage drivers are used in low and medium power lighting applications ($<$50 W). In two-stage LED drivers, PFC function and LED load current control are performed separately using two dc-dc converters. The performance of two stage drivers is better than single stage drivers. However, two stage drivers are complex and are costly. Hence two stage drivers are applicable for medium and high power lighting applications. In three-stage switched mode LED drivers, stage-1 and stage-2 perform PFC and dc-dc regulation respectively and stage-3 is a post regulator which features dimming control and current equalization in LED strings. Since each stage performs a single function, three stage drivers are mainly suitable for high power lighting applications ($>$100 W).

In DC fed LED drivers, driving source itself is dc voltage which can be obtained from PV, battery or dc grid. Since the driving input is dc source, PFC stage is not required. In addition, DC fed LED drivers are efficient and more reliable. In DC fed drivers, LED loads are supplied from either linear or switched mode dc-dc converters. The efficiency of switched mode dc-dc converters is high and are more preferred for LED drivers [30–32]. Basic isolated and non-isolated dc-dc converters are used for powering LED lighting loads [33–45]. Recently, usage of soft-switching converters in LED lighting applications is increasing due to their high efficiency, compactness and low EMI [46–57].

1.4 Thesis organization

The thesis work is organized into six chapters and presented as follows;

In Chapter 2, presents the comprehensive literature review of existing converter topologies and control techniques for LED lighting system. Thus, motivates for the research work

carried out in this thesis.

In Chapter 3, Input voltage contrlled full-bridge series resonat converter has been proposed for LED driver application. The circuit operation, analysis and design procedure are explained. Dimming control and current regulation are demonstrated. Simulation and experimental results are presented. Efficiency characteristic is presented.

In Chapter 4, Dual frequency series resonant converter based LED driver has been proposed. The circuit operating principle, analysis, design considerations of proposed configuration are explained. LED lamp current regulation and independent dimming operations are discused. Simulation and experimental results are presented.

In Chapter 5, Independently controllable dual output series resonant conevrter has been proposed to drive two LED lamps independently. The circuit operating principle, analysis, design considerations of proposed configuration are explained. LED lamp current regulation and independent dimming operations are discused. Simulation and experimental results and efficiency characterstics are presented.

In Chapter 6, highlights the brief conclusions and significant contribution of the thesis work and also, provides the scope for further research in this area.

Chapter 2

Literature review

Chapter 2

Literature review

2.1 Introduction

LEDs are being used in number of applications due to their performance indices such as high efficacy, high operating life, solid state characteristic and eco-friendliness. LEDs are dc operated devices and have non-linear voltage-current characteristics like a diode. The illumination level of an LED directly depends upon the forward current through it. In addition, they acts like a constant voltage load with low dynamic resistance. LED output characteristics clearly indicates that a small in its output voltage results in significant current variation which changes the light output. The variation or fluctuation in the lamp illumination is undesirable. To ensure uniform light output from an LED, it must be powered from constant current regulator which is called as LED driver. This chapter presents an overview of AC fed LED drivers [4–29], DC fed driver circuits for LED lighting applications [30–57] and LED illumination control methods [58–65]. The implementation of a LED driver depends on the energy source and the converter technology. LED drivers can be classified by the type of the input source, either dc power or ac-power (mains connected) drivers.

2.2 Classification of LED driver circuits

The implementation of a LED driver depends on the energy source and the converter technology. LED drivers can be classified by the type of the input source, either dc fed or ac-fed (mains connected) LED drivers.

2.2.1 AC fed LED drivers

LED lighting loads require regulated constant DC current for producing uniform brightness. In AC fed LED drivers, constant DC current is derived from AC utility line. These drivers

are classified as passive LED drivers [4–7] and switched mode LED drivers [8–29]

2.2.1.1 Passive LED drivers

Passive LED drivers consist of passive components (resistor, capacitor, and inductor/transformer) and diodes. They do not have semiconductor switches, associated gate driver and linear or active regulators. Without active control, they supply required dc current for LED load with large ac ripple. In these drivers, output current control function is realized either by lossy or lossless impedance at line frequency or double-line frequency. The limitations of passive LED drivers are low PF, high THD in source current, requirement of large filter capacitor to avoid flickering due to 100Hz ripple in LED load, large size of inductors, lack of precise output current control against input voltage variations etc. However, high reliability, simple structure, low cost and less electromagnetic interference (EMI) due to absence of high switching frequency operation are key features of passive LED drivers. They are suitable for applications where high priority is given to reliability such as outdoor lighting applications.

2.2.1.2 Switched mode LED drivers

Switched mode (S-type) LED drivers contain active switches and active switching regulators. Due to high switching frequency operation of S- type LED drivers, they overcome the limitations of passive LED drivers. S-type LED drivers use power factor correction (PFC) converter to attain high PF and low THD in source current. Active control of DC-DC switching converter in S-type LED drivers provide precise current control, high efficiency, and compactness. The features of S-type LED drivers such as good PF, ability to regulate LED load current against input voltage and load variations, dimming operation, isolation between LED load and input, and protection in all aspects make them suitable for wider range of applications in lighting industry. Good number of S-type LED drivers are available in literature to explore key issues of lighting systems [8–29] . S-type LED drivers are further classified based on power processing stages and applications such as single-stage (S1) LED drivers [8–17], twostage (S2) LED drivers [18–25] and three-stage (S3) LED drivers [26–29].

Single-stage (S1) LED drivers have only one power processing stage. The schematic representation of S1 LED drivers is shown in Fig. 2.1. In these LED drivers, ac is converted

into unregulated dc output by diode bridge rectifier which is given as input to dc-dc converter. With suitable high frequency operation of switches in dc-dc converter topology, PFC and output current control are realized simultaneously. The filter or energy storage capacitor C_O can be connected either on low frequency side or on the frequency side which does not affect its size. They have less component count due to single power conversion stage and are applicable for low and medium power lighting applications (<50 W). Conventional topologies based on buck [8], boost [9], buck-boost [10], SEPIC [12], flyback [13], half-bridge [16], push-pull [17] converters can be used as S1 LED drivers. However it is difficult to achieve good PF, high energy efficiency, high step-down conversion and constant output current simultaneously in S1 LED drivers.

Two-stage (S2) LED drivers contain two power processing stages. As each stage is designed for specific function, S2 driver's performance is better as compared to S1 drivers in terms of PFC, LED load current regulation, ac ripple and reliability. However, S2 drivers have some limitations such as low efficiency, high cost and require two isolated control circuits. The S2 drivers are suitable for medium and high power lighting applications, where the LED load current regulation and reliability issue are major priority than that of cost and size of lighting system. Depending on stage-2 configuration, the S2 drivers are further classified as two-stage type-A (S2A) drivers and two-stage type-B (S2B) drivers as shown in Fig. 2.2a and 2.2b. In S2A drivers, stage-1 performs PFC operation, whereas stage-2 which is a high step-down dc-dc converter performs dc-dc regulation [18–22]. Both stage-1 and stage-2 are connected in cascaded structure with LED load. Generally, boost converter in discontinuous conduction mode (DCM) is used to achieve good PF in stage-1. The major drawback of S2A drivers is that they require large size filter capacitor. In S2B drivers, stage-1 performs both PFC and output current regulation. And stage-2 which is connected in parallel with LED load extracts doubleline frequency power from dc-link to minimize flickering effect in LED load [23–25]. The size of filter capacitor in S2B drivers can be reduced by allowing large voltage variations. Three-stage

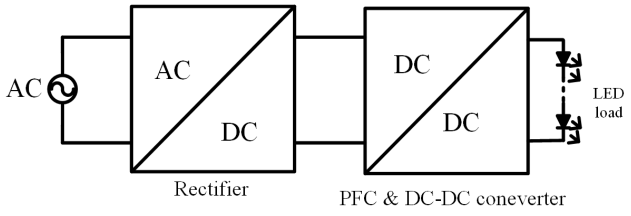

Figure 2.1: Single stage LED driver

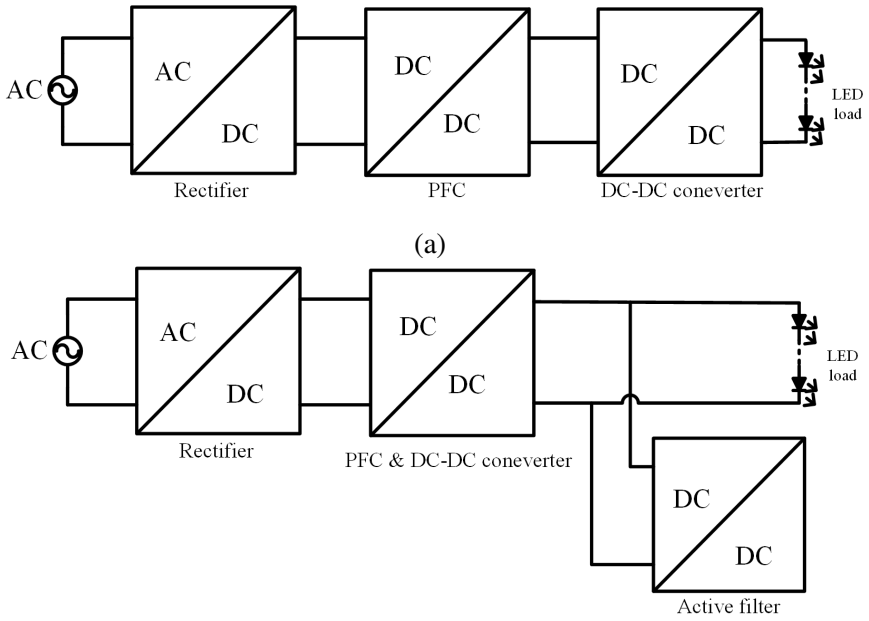

Figure 2.2: (a)Type-A two stage LED driver (b) Type-B two stage LED driver

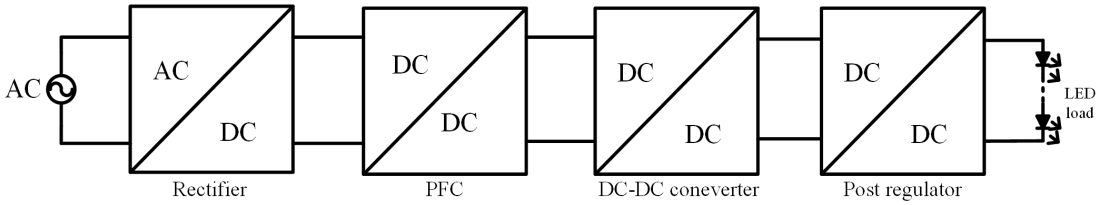

Figure 2.3: Three stage LED driver

(S3) switched mode LED drivers have three power processing stages as shown in Fig. 2.3. The function of stage-1 and stage-2 is same as the S2A drivers. And stage- 3 comprises a current post regulator that provides dimming operation and current equalization among the parallel connected LED strings [26–28]. Current post regulator can be linear or switched type depending upon lighting application. Since each stage is optimized for a single function, S3 drivers are used for high power lighting applications (>100 W). Further softswitching topologies are preferred in stage-2 to increase the efficiency of whole lighting system. The cost and component count of S3 LED drivers often increases for multi LED string application. To reduce the lighting system cost, single input multi output topologies are employed in stage-2 which eliminates current post regulator [29].

2.2.2 DC fed LED drivers

In dc fed LED drivers, dc input is obtained from PV or battery or dc grid. The advantages of dc fed LED driver are: PFC stage elimination, non-requirement of electrolytic capacitor, simplified converter design aspects, improved efficiency and reliability. The requirements of LED driver circuit are different for each application. However, high power conversion efficiency, regulation of LED load current, dimming operation, less component count, high operating life, simple structure, reliability etc., are the basic objectives of LED driver circuit. As the available input is dc source, LED lighting loads can be powered from either linear or switched mode dc-dc converters. Switching converters are more preferred due to their high efficiency [30–32]. These dc-dc converter topologies are classified according to the electrical isolation between input and output. The basic isolated dc-dc converter topologies are Flyback, Forward, Push-pull, Half-bridge, and Full-bridge converters. Similarly, basic non-isolated topologies are Buck, Boost, Buck-Boost, Cuk, SEPIC, and Zeta converters. Based on the available input voltage and required output voltage for LED lighting loads, both isolated and non-isolated topologies have been used for driving LED loads for all lighting applications [33–45]. Some of the converters used in S2 and S3 LED drivers in second stage can also be used for dc fed LED driver circuit configurations. Recently, soft-switching converters have gained significant popularity in LED lighting applications [46–57]. High power conversion efficiency and high frequency operation of soft switching converter makes the LED driver system compact with good dynamic response, which is desirable when PWM dimming is applied.

As this thesis work focuses on the development of dc operated LED drivers, this section describes the literature related to the different dc operated driver circuit configurations for LED based lighting applications.

Resonant converters are gaining popularity because they provide soft-switching, which leads to reduced EMI noise, high efficiency, increased power density and so on. Half-bridge (HB) and full-bridge (FB) based series, parallel & series-parallel resonant converters are commonly used for LED drivers. A multi-string LED driver based on FB LCLC resonant converter with current balancing is presented in [51]. A simple current controlled LED driver is presented in [66] using FB resonant converter, which requires an extra transformer, switch and three diodes. In [67],the input of the FB SRC is regulated by a front end converter, where the

power processed by the front end converter is low. But, the front end converter needs an extra source and opearted with hard switching, and the component count of the converter is also high. Many other LED driver topologies [68–73] used HB resonant converter because of their simple configuration, easy operating principle, small size [68] and high efficiency due to soft-switching operation, etc. Furthermore, these HB resonant converters are combined with some other converters to form single-stage AC-DC LED drivers [74–77] that attain multi-tasking with a lower device count and increased efficiency. In [52], a HB resonant convereter with magenetic control is presented to regulate LED currents . In [78, 79], a wide input HB resonant converter is presented in which Buck-boost converter is integrated with HB resonant converter. For low voltage applications isolation is not required, nonisolated converters are preferred to make implementation easy and less cost. In [80], asymmetrical duty cycle (ADC) controlled half-bridge parallel resonant converter based LED driver is reported. In [77], ADC controlled HB SRC is presented for improved efficiency. In [81], buck-boost integrated symmetrical half-bridge parallel LC resonant based LED driver is presented for increasing the gain, but the device count is higher, increasesing total cost and reduces the driver efficiency due to the hard switching buck-boost converter.

2.3 Multiple output LED drivers

In many applications such as auto-motive lighting, colour mixing, traffic signal lighting, LCD back lighting etc. needs multiple outputs which are driven from a single source.The most direct way to achieve multiple outputs is to use individual converter for each output. However, this parallel structure requires extra sets of components increasing the cost and complexity of the system. Hence, appropriate converter configurations with multiple outputs are preferable in these applications due to lesser component count, low cost, compact size, etc. in comparison to using an individual driver for each LED load. Some, multiple-output LED drivers [50, 52, 54, 70, 82–98] are discussed. Full-bridge configuration [82, 83] is used to drive multiple LED loads with less component count per lamp and conduction loss but can drive only similar loads (i.e., equal voltage and current). A high step-down buck converter [84](Fig. 2.4) to supply multiple loads is presented, which can drive loads with unequal voltage but with equal currents.

A coupled inductor (CI) based two output LED driver is discussed in [50](Fig. 2.5), wherein one LED load is directly energized through CI and the other load is powered from its

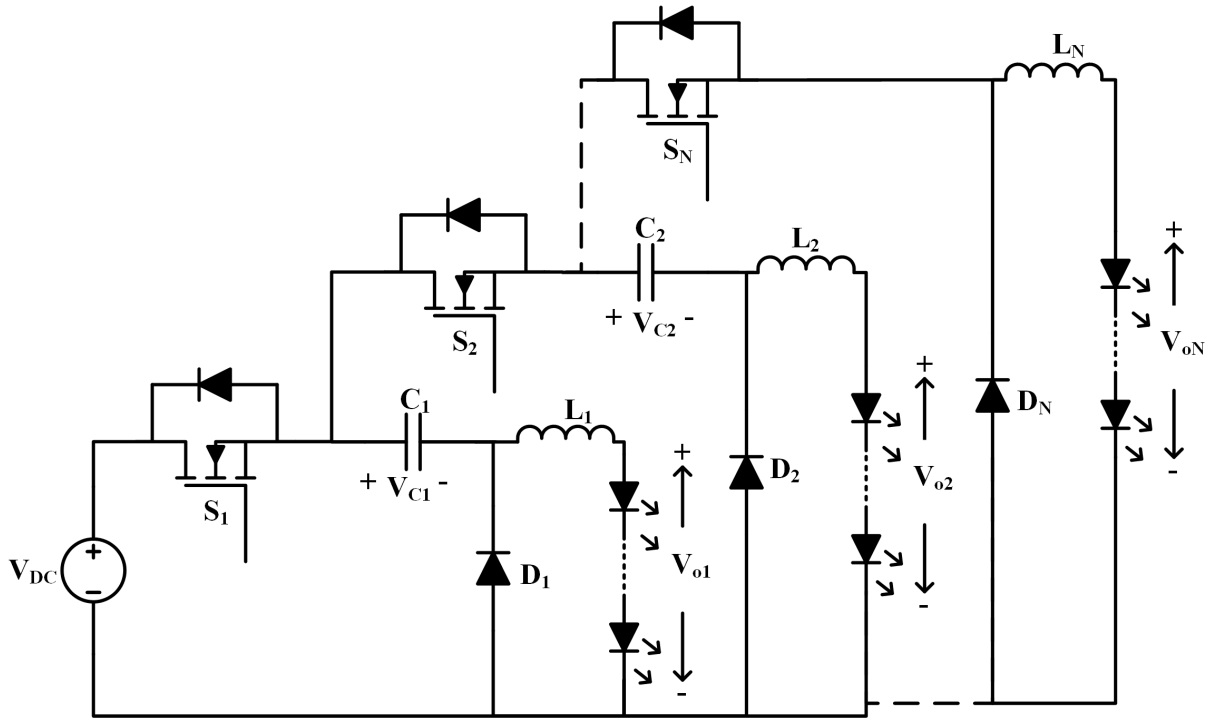

Figure 2.4: High step-down multiple output LED Driver

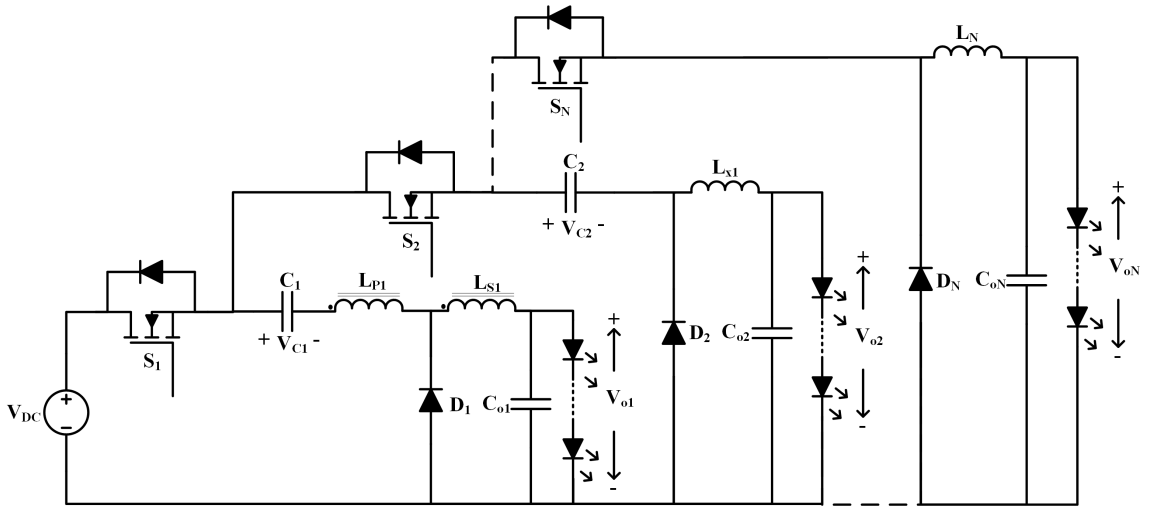

Figure 2.5: Coupled inductor based multiple output LED Driver

leakage energy. As the rating of one load is fractional of the other load and depends on the leakage inductance, hence it is difficult to decide the fractional load's rating. All the topologies presented in [50, 82–84] are able to drive multiple loads with identical or different ratings but fail to provide independent dimming. Multiple-output LED drivers [70, 85, 86](Fig. 2.6) with selective dimming are presented but can supply LED loads with equal currents. Single inductor multiple-output (SIMO) LED drivers are presented in [87–90](Fig. 2.7) to enable indepen-

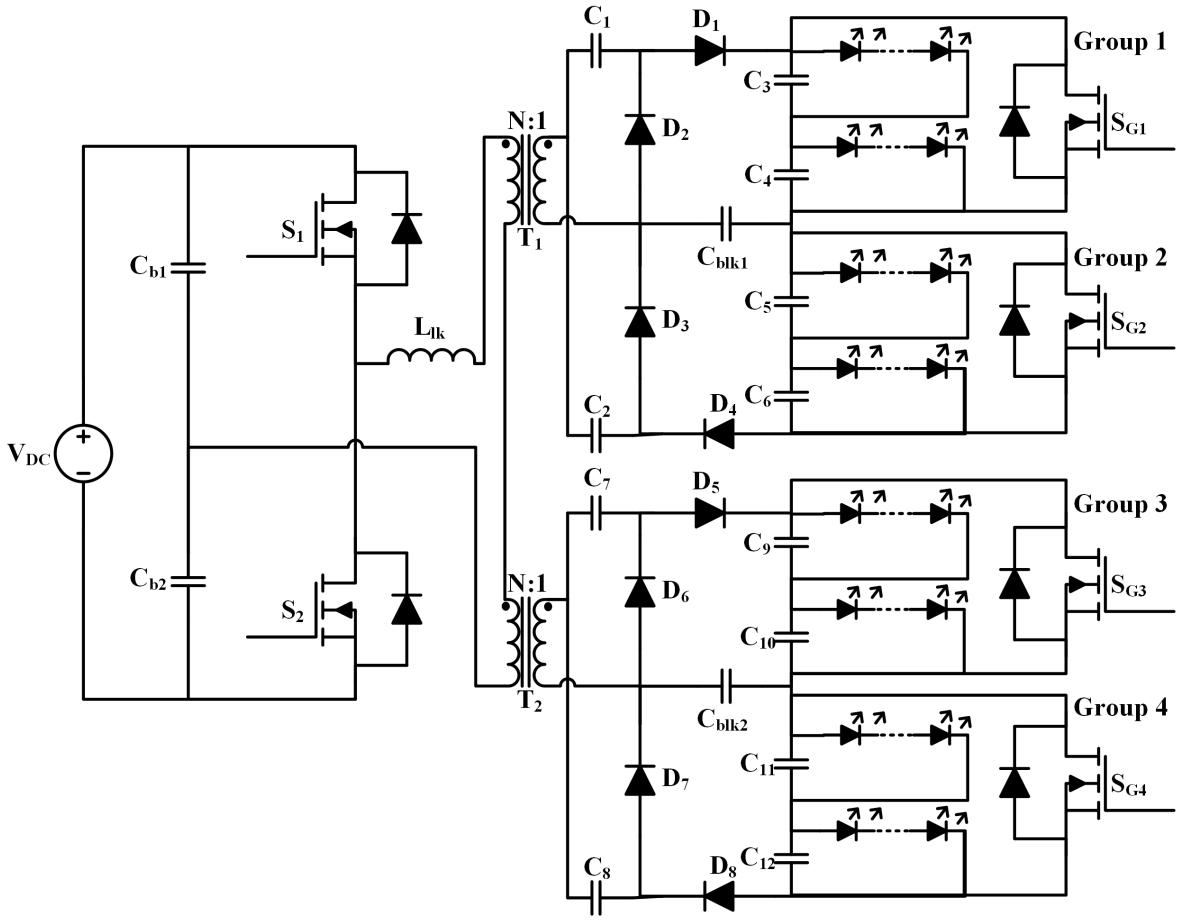

Figure 2.6: Selective dimming LED Driver

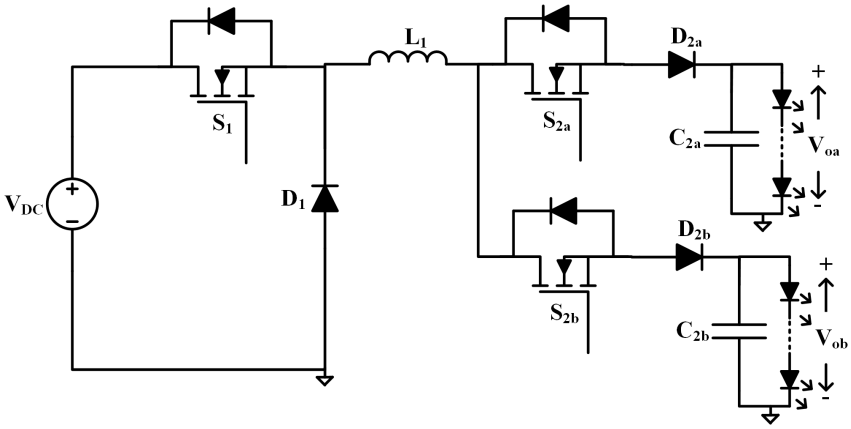

Figure 2.7: Single Inductor multiple output LED Driver

dent current control and dimming operation. In these converters, a single inductor is shared in time-division multiplexing (TDM) by different loads, which reduces the size, device count, and cost of the converter. However, TDM sharing and DCM operation of these converters reduce the operating frequency of the loads, which increases the output filter. Current source mode

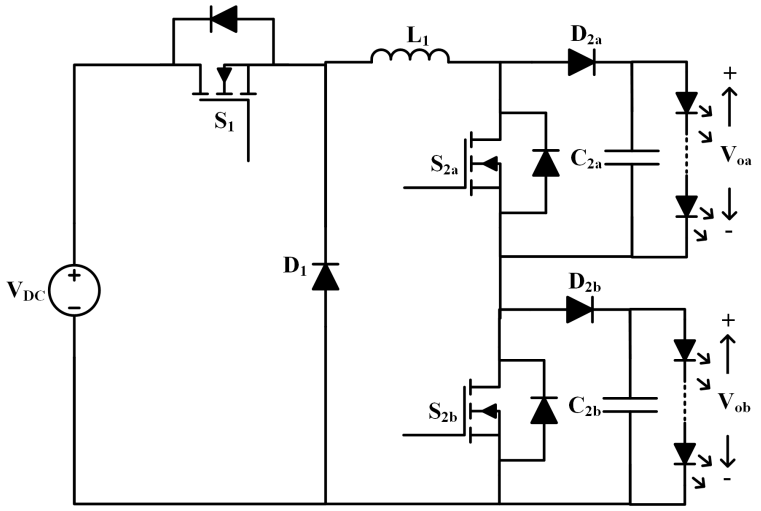

Figure 2.8: Current Source Mode multiple output LED Driver

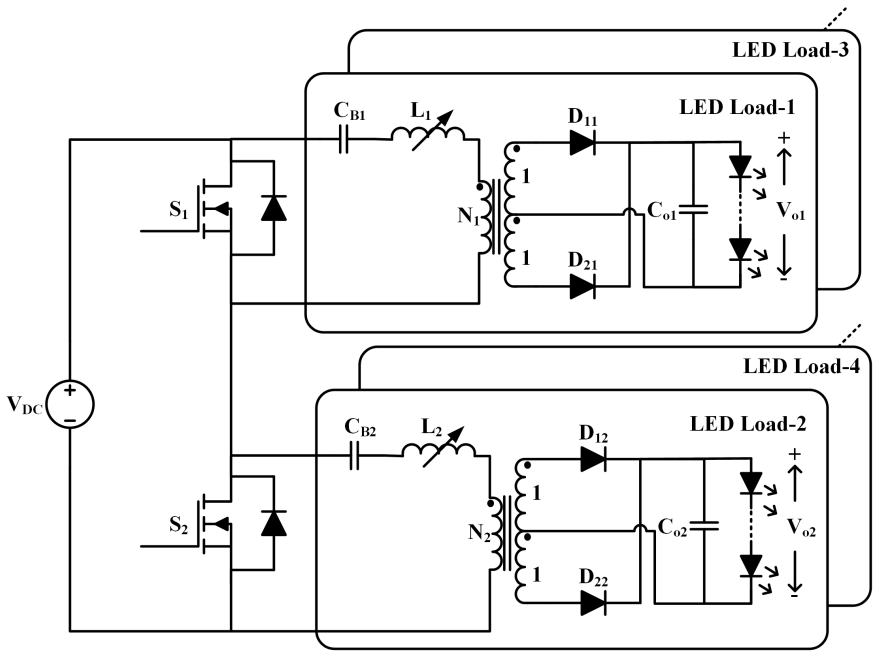

Figure 2.9: Variable Inductor controlled multiple output LED Driver

SIMO LED driver is presented in [91, 92](Fig. 2.8), uses simple control to implement independent dimming and regulation of different loads. However, the converter operating with hard switching, which reduces the efficiency. Variable inductor-based multiple output LED drivers are presented [52, 93, 94](Fig. 2.9) provide zero voltage switching (ZVS) along with independent current control and dimming operation But, the design and implementation of the variable inductor are complex and also decrease the overall efficiency of the converter. Switch controlled capacitor multiple output LED drivers are discussed in [54, 95, 96](Fig. 2.10), in which

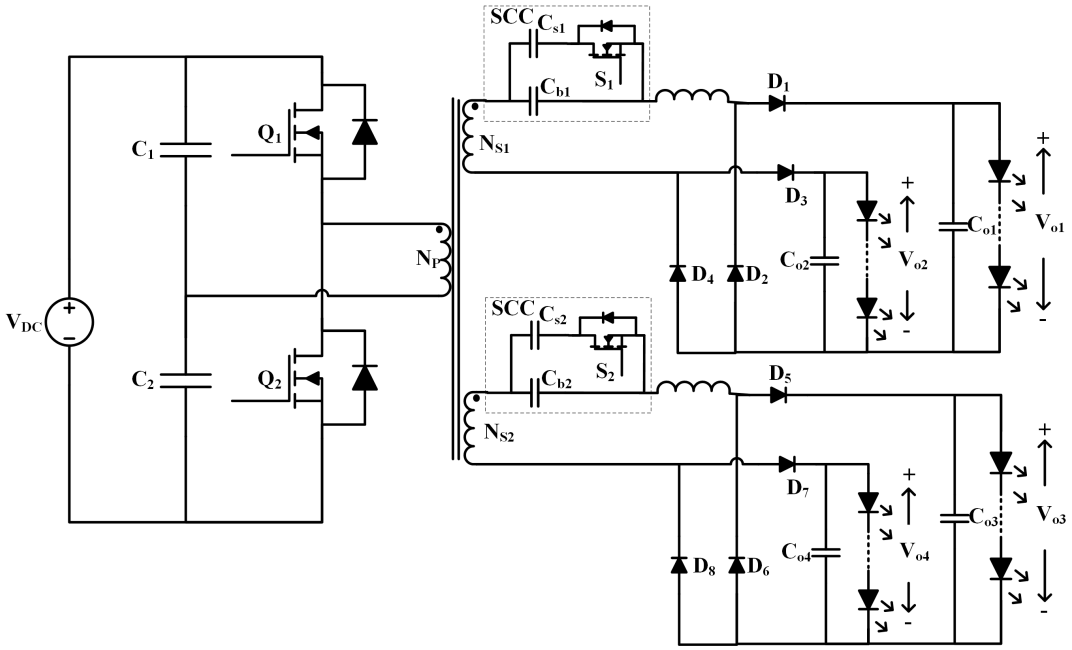

Figure 2.10: Switch-controlled capacitor multiple output LED Driver

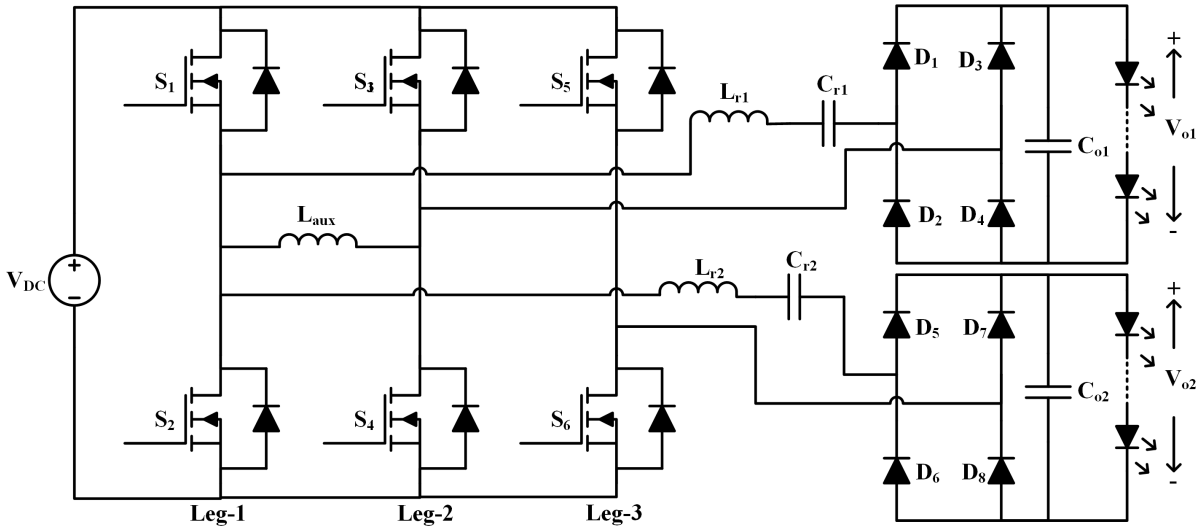

Figure 2.11: Three Leg LED Driver

switch controlled capacitor is used in each output channel to achieve independent dimming and regulation. But the implementation of switch controlled capacitor requires extra passive an-d active components, which increases cost and size of the converter. A three-leg series resonant converter (SRC) [97](Fig. 2.11) is proposed with partial ZVS to drive LEDs with independent current and dimming operation but requires a high component count. An integrated buck-boost SRC [98](Fig. 2.12) for multiple LED loads having a high gain feature is presented. In this

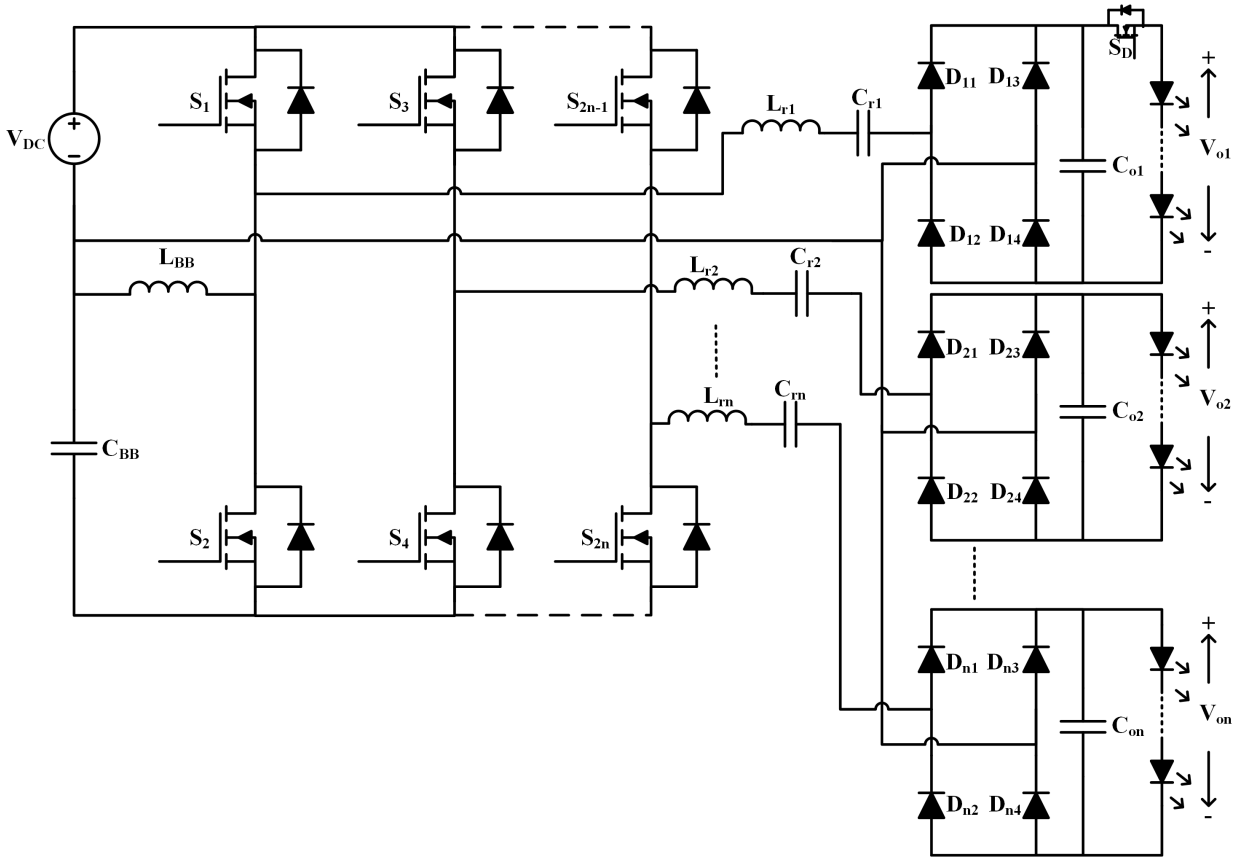

Figure 2.12: Buck-boost integrated Half-bridge LED Driver

paper, variable frequency control is used to regulate the LED currents, which makes the filter design difficult.

2.4 LED dimming

The adjustable illumination from an LED is called dimming. It is an important requirement for LED lighting applications. Dimming operation in LED driver saves good amount of power which further reduces the consumption of energy. Dimming can be achieved by Amplitude Modulation (AM) or Pulse-Width Modulation (PWM) schemes. In AM, illumination control is achieved by varying the operating currents of the LED strings [58, 59]. As the opearting current of LED changed, the color of the light may change in AM dimming. Hence AM dimming is not suitable for color sensitive lighting applications. Because of non-linear charcteristics of LED, wide range of dimming is not possible in AM dimming. PWM dimming methods have been widely used to overcome the limitations of AM [60–65]. In PWM dimming, the operating current of LED maintained constant, the average current through it is varied by turning

ON and OFF LEDs at low frequencies. With PWM dimming wide range of dimming can be achieved without any color change in the light output. Several PWM dimming schemes like turning on and off the LED strings through a series connected controlled switch [60], turning on and off the input voltage to the driver circuit [61], multi-phase PWM [62], pulse-code modulation (PCM) [63], double pulse width modulation (DPWM) [64], bi-level driving [65], etc., have been reported in literature.

2.5 Motivations and Objectives of the Thesis

From the literature review on driver circuits for light emitting diode (LED) lighting applications, the following observations are drawn.

i) The application of multiple output LED drivers is a cost-effective and more optimized solution compared to the use of several low power single output LED drivers

ii) Some of the configurations are not capable of providing soft switching feature.

iii) Some of the driver circuits are having high device current or voltage stress.

iv) Some configurations do not provide regulation of LED lamp current against input voltage fluctuations.

v) Some of the LED drivers are not able to drive multiple lighting loads.

vi) Only few circuits are having independent regulation and dimming feature.

vii) Some of configurations are not able to drive LED lamps of different power ratings.

Despite the availability of various converter architectures and control techniques, there is still room for further research in developing a compact LED driver to meet a variety of application requirements.

The proposed research work aims at design and development of multiple output DC-DC converter configurations for LED lighting applications with objectives to provide high power conversion efficiency, reduced device count and stress on the devieces, powering multiple lighting loads with dimming, zero-voltage switching, driving LED lamps of different power ratings, regulate LED lamp current against input voltage variations.

2.6 Contribution

This research work focuses on high efficiency DC-DC converter configurations with low voltage or current stress on switching devices, dimming control and current regulation for LED lighting applications. This necessitates use of soft-switching technique in DC-DC Converter configurations. Thee different LED driver configurations have been proposed. These configurations and their features are listed below

1. **Input voltage controlled full-bridge series resonant converter for LED driver application**

   Features:

   i) High power conversion efficiency.

   ii) Reduced device current stress.

   iii) Multiple LED lamps with dimming

   iv) Zero-voltage switching

2. **Dual Frequency Series Resonant Converter Based LED Driver**

   Features:

   i) Capability of driving LED lamps of different power ratings.

   ii) Independent lamp current regulation.

   iii) Independent illumination control.

3. **Independently Controllable Dual-Output Half-Bridge Series Resonant Converter for LED Driver Application**

   Features:

   i) Capability of driving LED lamps of different power ratings.

   ii) Independent lamp current regulation.

   iii) Independent illumination control.

   iv) Reduced number of componens.

   v) Zero voltage switching.

2.7 Conclusion

In this chapter, an overview of AC fed LED driver circuits has been presented. In section 2.1.2, DC fed LED drivers for single and multi-output LED based lighting applications have been discussed. Different illumination or dimming control methods have been explained in section 2.2.

The number of soft switched converters in the literature with reduced current stress for multiple output LED lighting applications are less in number. Converters with soft switching, dimming operation, ability to power multiple LED lamps and LED current regulation are also few. Also, some of configurations are not capable to drive LED lamps of different power ratings with independent dimming and regulation. Some of the LED drivers described in literature are not suitable for high power LED applications.

Hence there is sufficient scope for further research in development of multiple output LED driver circuits with soft switching, reduced current stress, current regulation, independent dimming control, and high efficiency. With this objective, Three different converter configurations have been proposed in this thesis.

In the next Three chapters, proposed converter configurations for LED based lighting applications are explained in detail.

Chapter 3

Input voltage controlled full-bridge series resonant LED driver application

Chapter 3

Input voltage controlled full-bridge series resonant converter for LED driver application

3.1 Introduction

In this chapter an Input voltage controlled full-bridge series is proposed to drive four LED loads. In this configuration, the output of the SRC is connected in series with the input, which reduces the power processed by SRC, hence the efficiency of the converter is enhanced. The LED currents are regulated by regulating the input voltage to the full-bridge by using phase-shift control. A 142 W prototype has been developed experimentally to confirm its working principle, performance and validity. The working principle of the proposed circuit is explained in section 3.2. The analysis and the current regulation and dimming control of the proposed converter are discussed in sections 3.3 and 3.5 respectively. The comparative analysis of proposed converter with exsiting similar kind of topologies is presented in section 3.6 . Experimental results and conclusions are provided in sections 3.7 and 3.8 respectively.

3.2 Circuit description and operating principle

The circuit diagram of the proposed LED driver is shown in Fig. 3.1. This circuit consists of a full-bridge inverter (FBI) having four MOSFETs ($S_1 - S_4$) with body diodes ($D_1 - D_4$) and snubber capacitors ($C_1 - C_4$) across it. A series resonant circuit formed by resonant inductor L_r, resonant capacitor C_r and high-frequency transformer (HFT) is connected between the output terminals($A\&B$) of the FBI and diode bridge rectifier. The diode bridge rectifier output is connected to a capacitive filter. The filtered output of the diode bridge rectifier is connected in series with the input voltage V_{DC}, which is applied as input to the FBI. Four LED loads each in series with an inductor is connected across each switch of the FBI.The inductors $L_1 - L_4$ are chosen in such a way that ripple currents through LED loads are within limits. Gating signals to the switches ($S_1 - S_4$) of FBI and the operating waveforms of the proposed

converter are shown in Fig. 3.2. Switches S_1 and S_2 are operated complimentarily with 180° pulse width. Similarly, Switches S_3 and S_4 are operated complimentarily with 180° pulse width. The gating signals of S_1 and S_3 are phase-shifted by an angle δ. The phase shift angle δ is 180° for a minimum value of input voltage V_{DC} and is varied to control the voltage applied to the FBI for variations in input voltage. The modes of operation of the proposed LED driver are explained in this section.

3.2.1 Mode: I

At time t_0, gate pulse to switch S_1 is applied, thereby it is start conducting, and it takes over the current carried by its body diode D_1. Since the body diode D_1 is conducting before the turn-on of the switch S_1, it is turned-on under zero voltage condition. The equivalent circuit in this mode is shown in Fig. 3.3a. In this mode, switches S_1 and S_4 are in conduction. Therefore the inductor currents, i_{01}, and i_{04} decrease linearly and i_{02}, and i_{03} increases linearly. The switch S_1 carries resonant circuit current and difference of the currents i_{02} and i_{01}. Similarly, switch S_4 carries resonant circuit current and difference of the currents i_{03} and i_{04}.

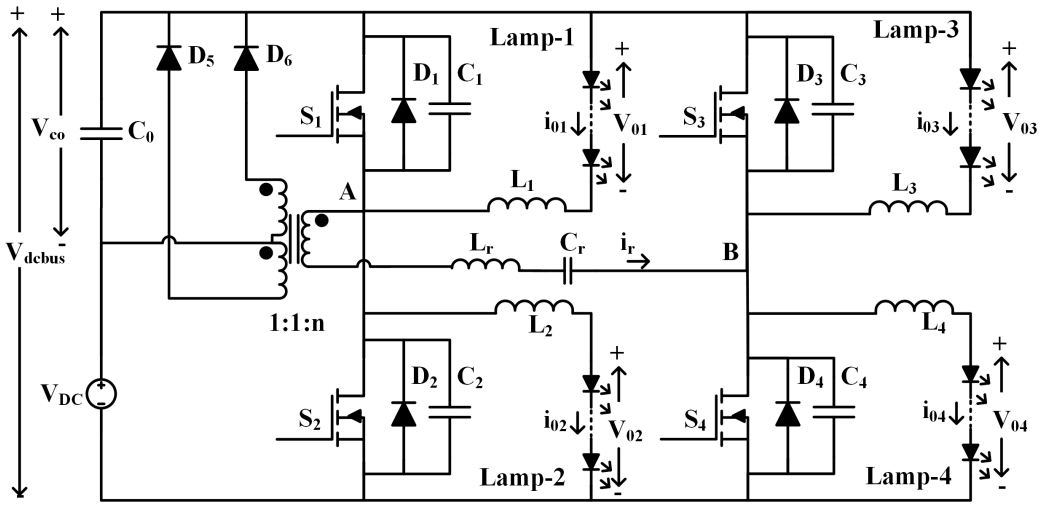

Figure 3.1: Circuit diagram of the proposed LED driver

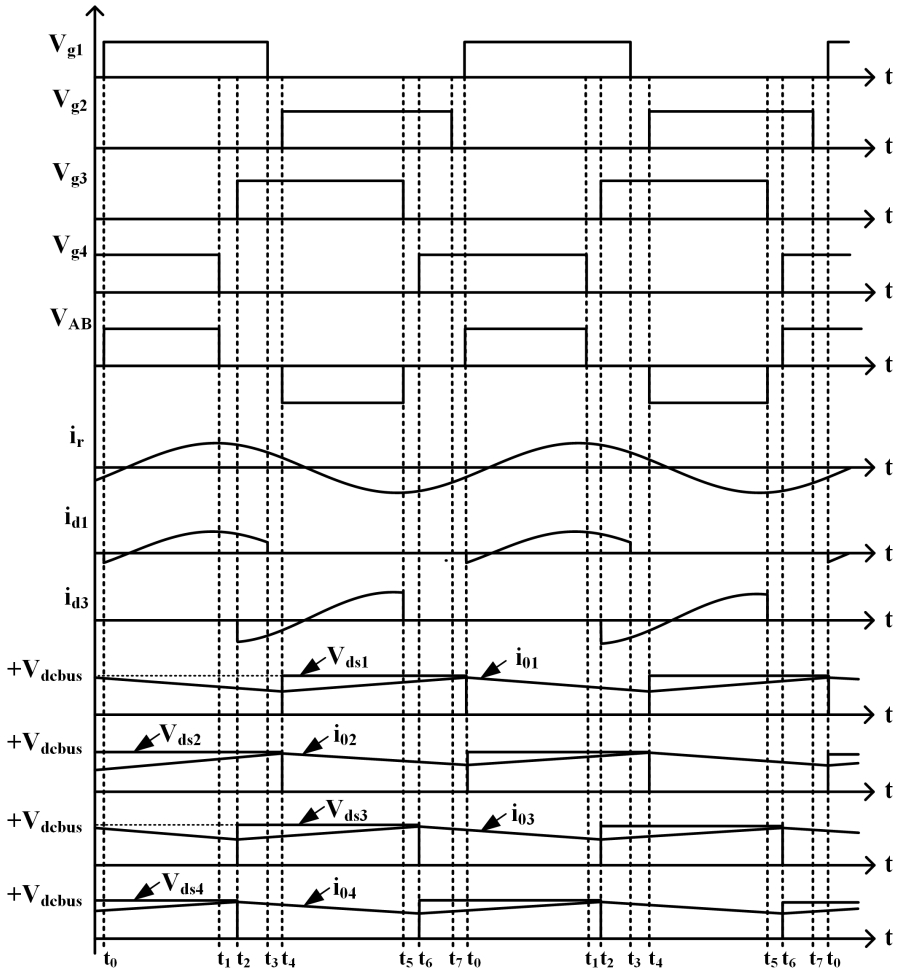

Figure 3.2: Operating waveforms of the proposed LED driver

3.2.2 Mode: II

This mode begins at time $t = t_1$ by removing gate pulse to switch S_4, thereby it is turned-off and snubber capacitor C_4 starts charging. At this time, resonant circuit current i_r is positive, because of this snubber C_3 discharges into resonant circuit. Once it is completely discharged, the body diode D_3 starts conducting. Due to the snubber capacitor C_4, the voltage across the switch S_4 raises slowly, which reduces turn-off losses of the switch. The equivalent circuit in this mode is shown Fig. 3.3b.

3.2.3 Mode: III

This mode begins at time $t = t_2$ by applying the gate pulse to switch S_3, thereby it is start conducting, and it takes over the current carried by its body diode D_3. Since the body diode D_3 is conducting before the turn-on of the switch S_3, it is turned-on at zero voltage. The equivalent circuit in this mode is shown in Fig. 3.3c. In this mode, switches S_1 and S_3 are in conduction. Therefore the inductor currents, i_{01}, and i_{03} decrease linearly and i_{02}, and i_{04} increases linearly. The switch S_1 carries resonant circuit current and difference of the currents i_{01} and i_{02}. Similarly, switch S_3 carries resonant circuit current and difference of the currents i_{04} and i_{03}.

3.2.4 Mode: IV

This mode begins at time $t = t_3$ by removing gate pulse to switch S_1, thereby it is turned-off and snubber capacitor C_1 starts charging. At this time, resonant circuit current i_r is positive, because of this snubber capacitor C_2 discharges into resonant circuit. Once it is completely discharged, the body diode D_2 starts conducting. Due to the snubber capacitor C_1, the voltage across the switch S_1 raises slowly, which reduces turn-off losses of the switch. The equivalent in this mode is shown Fig. 3.3d.

3.2.5 Mode: V

This mode begins at time $t = t_4$ by applying the gate pulse to switch S_2, thereby it is start conducting, and it takes over the current carried by its body diode D_2. Since the body diode D_2 is conducting before the turn-on of the switch S_2, it is turned on at zero voltage. The equivalent circuit in this mode is shown in Fig. 3.3e. In this mode switches S_2 and S_3 are in conduction. Therefore the inductor currents, i_{02}, and i_{03} decrease linearly i_{01} and i_{04} increase linearly. The switch S_2 carries resonant circuit current and difference of the currents i_{01} and i_{02}. Similarly, switch S_3 carries resonant circuit current and difference of the currents i_{04} and i_{03}.

3.2.6 Mode: VI

This mode begins at time $t = t_5$ by removing gate pulse to switch S_3, thereby its turned-off and snubber capacitor C_3 starts charging. At this time, resonant circuit current i_r is negative, because of this snubber capacitor C_4 discharges into resonant circuit. Once it is completely discharged, the body diode D_4 starts conducting. Due to the snubber capacitor C_3, the voltage across the switch S_3 raises slowly, which reduces turn-off losses of the switch. The equivalent in this mode is shown Fig. 3.3f.

3.2.7 Mode: VII

This mode begins at time $t = t_6$ by applying the gate pulse to switch S_4, thereby it is start conducting, and it takes over the current carried by its body diode D_4. Since the body diode D_4 is conducting before the turn-on of the switch S_4, it is turned-on at zero voltage. The equivalent circuit in this mode is shown in Fig. 3.3g. In this mode, switches S_2 and S_4 are in conduction. Therefore the inductor currents, i_{02}, and i_{04} decrease linearly and i_{01} and i_{03} increase linearly. The switch S_2 carries resonant circuit current and difference of the currents i_{01} and i_{02}. Similarly, switch S_4 carries resonant circuit current and difference of the currents i_{03} and i_{04}.

3.2.8 Mode: VIII

This mode begins at time $t = t_7$ by removing gate pulse to switch S_2, thereby it is turned-off and snubber capacitor C_2 starts charging. At this time, resonant circuit current i_r is negative because of this snubber capacitor C_1 discharges into resonant circuit. Once it is completely discharged, the body diode D_1 starts conducting. Due to the snubber capacitor C_2, the voltage across the switch S_2 raises slowly, which reduces turn-off losses of the switch. The equivalent in this mode is shown Fig. 3.3h.

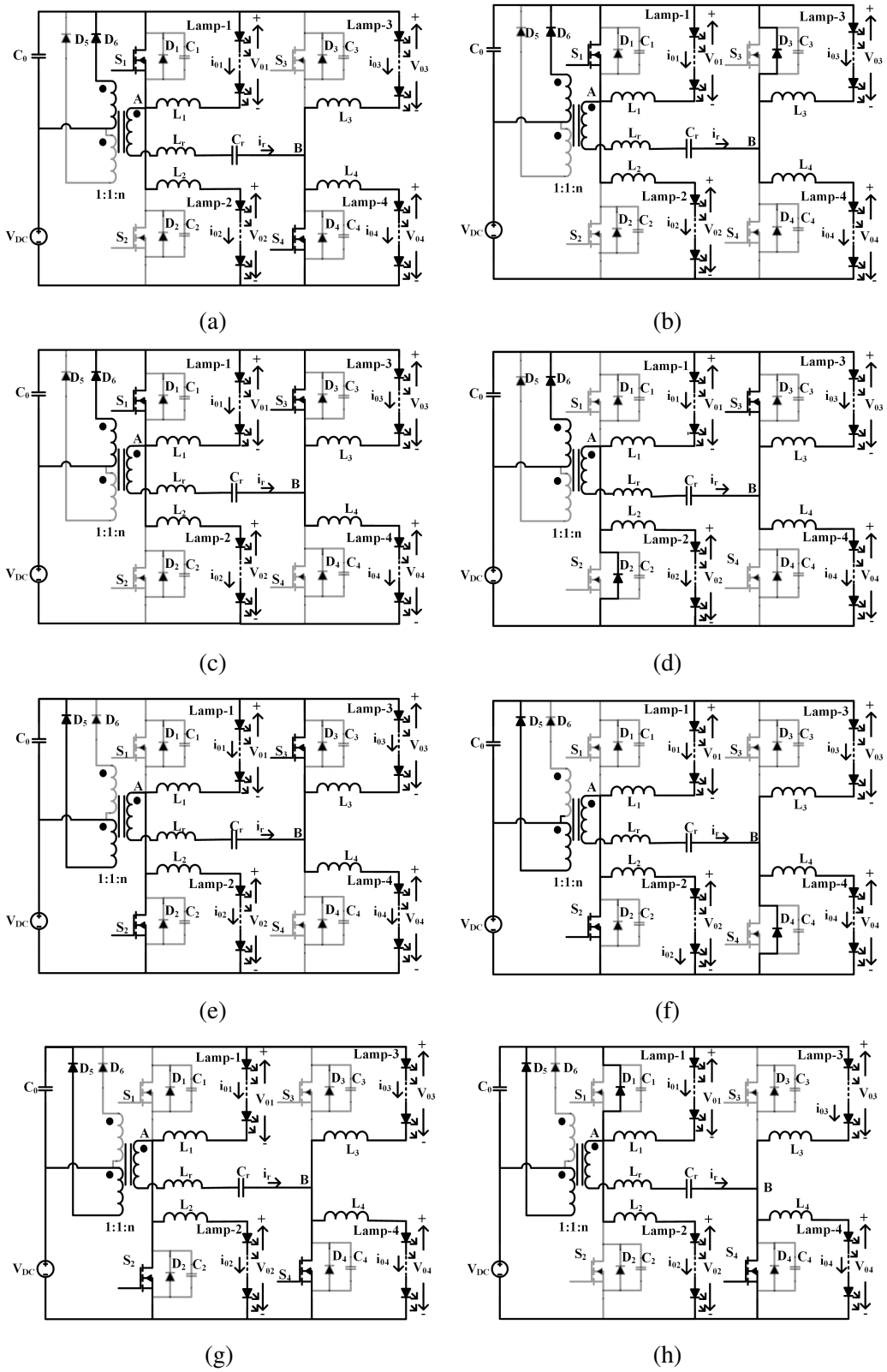

Figure 3.3: Equivalents circuits during (a) Mode-I (b) Mode-II (c) Mode-III (d) Mode-IV (e) Mode-V (f) Mode-VI (g) Mode-VII (h) Mode-VIII

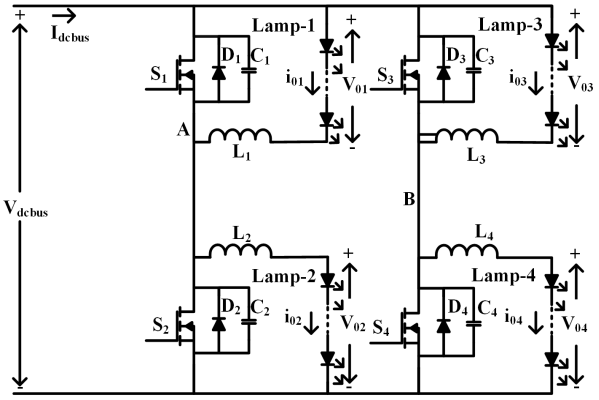

Figure 3.4: Equivalent circuit w.r.t LED loads

3.3 Analysis of the proposed LED driver

The following assumptions are made to simplify the analysis

i) All the devices used in the converter are ideal.

ii) LED currents are constant without any ripple.

iii) Q-factor of SRC is reasonably high so that the fundamental component of the analysis is carried out.

The simplified circuit w.r.t LED loads is shown in Fig. 3.4. When the switch S_1 is off and S_2 is on, voltage applied across the inductor L_1 is $(V_{dcbus} - V_{o1})$, and when the switch S_1 is on and S_2 is off, voltage applied across the inductor L_1 is $(-V_{o1})$, and both the switches operated complimentarily with 50% duty cycle, by applying volt-sec balance to inductor L_1, the voltage across the LED lamp-1 is given by

$$V_{o1} = \frac{V_{dcbus}}{2} \tag{3.1}$$

Similarly, all other LED lamp voltages are given by

$$V_{o1} = V_{o2} = V_{o3} = V_{o4} = V_o = \frac{V_{dcbus}}{2} \tag{3.2}$$

As all the output voltages are equal and all the LED loads are similar, the LED currents are given by

$$I_{o1} = I_{o2} = I_{o3} = I_{o4} = I_o \tag{3.3}$$

The LED current ripples are given by

$$\triangle I_{o1} = \triangle I_{o2} = \triangle I_{o3} = \triangle I_{o4} = \triangle I_o = \frac{V_{dcbus}}{2Lf_s} \tag{3.4}$$

Where, $L = L_1 = L_2 = L_3 = L_4$

At any time one switch in each leg of the FBI is off, the corresponding load current is flowing through the DC bus. Therefore the DC bus current is given by

$$I_{dcbus} = 2I_o \tag{3.5}$$

All the LED loads can be replaced with an equivalent resistance R_L across DC bus, and its value is given by

$$R_L = \frac{V_{dcbus}}{I_{dcbus}} = \frac{V_o}{I_o} = R_{LED} \tag{3.6}$$

Simplified circuit w.r.t series resonant circuit when an equivalent resistance R_L replaces all the LED loads is shown in Fig. 3.5. From the equivalent circuit, the DC bus voltage is given by

$$V_{dcbus} = V_{co} + V_{DC} \tag{3.7}$$

From Fig. 3.5, it is clear that the average output current of SRC is equal to input current from dc supply V_{DC}. As it is assumed that the converter is ideal output current of SRC is given by

$$I_{co} = I_{DC} = \frac{V_{dcbus} * I_{dcbus}}{V_{DC}} \tag{3.8}$$

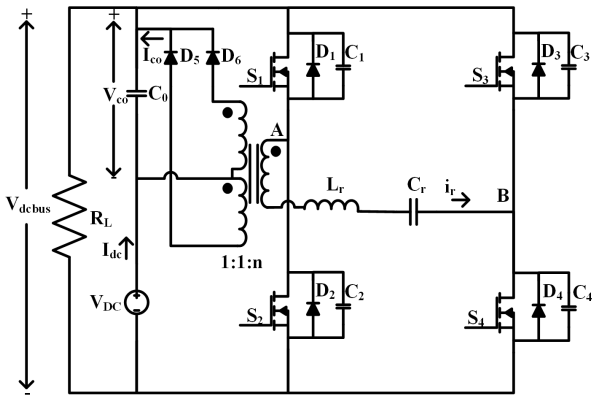

Figure 3.5: Equivalent circuit w.r.t series resonant circuit

Effective resistance R_{eff} seen by the SRC is given by

$$R_{eff} = \frac{V_{co}}{I_{co}} \tag{3.9}$$

From equs (3.6),(3.7),(3.8) & (3.9) we get

$$R_{eff} = G(1-G)R_L \tag{3.10}$$

Where, $G = \frac{V_{co}}{V_{dcbus}}$

From [99], the gain of the SRC with phase shift control is given by

$$G = \frac{V_{co}}{V_{dcbus}} = \frac{sin(\delta/2) * R_{aceff}}{|Z_{eq}|} \tag{3.11}$$

Where, R_{aceff} & $|Z_{eq}|$ are given by

$$R_{aceff} = \frac{8}{\pi^2} R_{eff} \tag{3.12}$$

$$|Z_{eq}| = \sqrt{{R_{aceff}}^2 + (X_{Lr} - X_{Cr})^2} \tag{3.13}$$

Where, $X_{Lr} = 2\pi f_s L_r$, $X_{Cr} = \frac{1}{2\pi f_s C_r}$

From the Fourier series analysis of V_{AB} the fundamental component (V_{AB1}) of V_{AB} is given by

$$V_{AB1} = \frac{4V_{dcbus}}{\pi} sin(\delta/2) sin(\omega_s t + \frac{\pi - \delta}{2}) \tag{3.14}$$

The output current I_{oc} of the SRC is the average value of rectified series resonant circuit current i_r. Hence the peak value (I_m) of i_r is given by

$$I_{oc} = \frac{2I_m}{\pi} \tag{3.15}$$

As the switching frequency (f_s) is greater than the resonant frequency (f_o), the series resonant circuit current i_r lags the voltage V_{AB1} by an angle Φ and is given by

$$\Phi = tan^{-1}(\frac{X_{Lr} - X_{Cr}}{R_{aceff}}) \tag{3.16}$$

From (3.14), (3.15) and (3.16) the series resonant circuit current i_r is given by

$$i_r = I_m sin(\omega_s t + \frac{\pi - \delta}{2} - \Phi) \tag{3.17}$$

When the switch S_1 is ON, it carries series resonant circuit current i_r and difference of the LED lamp-1 and LED lamp-2 currents. Since the LED lamp-1 and lamp-2 currents are equal and it is assumed that these currents are ripple free, the switch S_1 carries only the series resonant circuit current i_r. Hence the switch S_1 current at the instant when it is turned-on is given by

$$i_{d1turnon} = I_m sin(\frac{\pi - \delta}{2} - \Phi) \tag{3.18}$$

From eq(3.18) it is clear that for δ greater than $(\pi - 2\Phi)$), $I_{d1turnon}$ is negative and hence the switch S_1 is turned-on with ZVS. At the boundary of ZVS turn-on of S_1, $I_{d1turnon}$ becomes zero.

$$i_{d1turnon} = 0 = I_m sin(\frac{\pi - \delta}{2} - \Phi) \tag{3.19}$$

$$\frac{\pi - \delta}{2} = 0 \tag{3.20}$$

By combining equations (3.10), (3.11), (3.16) and (3.20) we get

$$G^4 - 3G^3 + 3G^2 - G + (\frac{\pi^2 (X_{Lr} - X_{Cr})}{8R_L})^2 = 0 \tag{3.21}$$

By solving (3.21), the valid value of G is the minimum value of G (G_{min}) at the boundary of ZVS turn-on of the switch S_1.

If the leading switch S_1 of the SRC with phase-shifted control is turn-on with ZVS then all other switches (S_2, S_3 and S_4) also turn-on with ZVS [100].

3.4 Design considerations

An LED driver with the following specifications is designed to test its performance. Input supply voltage, V_{DC} = 48V and $\pm$5% variations in input voltage; operating voltage of each LED lamp, V_o= 35.5V; operating current of each LED lamp, I_o = 1A; switching frequency, f_s=200kHz;

From eq 3.2, DC bus voltage is given by

$$V_{dcbus} = 2V_o \tag{3.22}$$

With V_o = 35.5V, the DC bus voltage V_{dcbus} is calculated as 71V.
From eq 3.4, the inductor values are given by

$$L = L_1 = L_2 = L_3 = L_4 = \frac{0.5V_o}{f_s \Delta I_o} \tag{3.23}$$

With ΔI_o=140 mA (i.e 14% of I_o), V_o=35.5 V and f_s=200 kHz, the inductor values L_1 to L_4 are calculated as 630 μH each.

The SRC is designed for rated V_{dcbus} and minimum input supply voltage V_{DC}(min). Therefore, the SRC output voltage should be maximum to maintain $Vdcbus$ at rated value. With V_o = 35.5V, I_o = 1 A, f_s = 200 kHz and by choosing f_s/f_r = 1.1, where $f_r = 1/(2\pi\sqrt{L_r C_r})$ and by solving equations (3.2), (3.6), (3.7), (3.10)–(3.13) the resonant circuit elements L_r and C_r are calculated as 106 μH and 6.9 nF, respectively.

3.5 Current regulation and Dimming control

The illumination levels of an LED lamp is proportional to the average current flowing through it. It can be changed by changing the average current through the LED lamp. This can be done by amplitude (AM) or pulse width modulation (PWM) of LED lamp current. In AM dimming, the amplitude of the operating current through the LED lamp is varied. This may cause a color change in the light output. In PWM dimming, the operating current of LED maintained constant, the average current through it is varied by turning ON and OFF LEDs at low frequencies. Due to the advantages such as no color change, smooth control, etc. in this paper, PWM dimming control is adopted. Fig. 3.6 shows the PWM dimming control scheme for the proposed LED driver. The gate pulses to the switches in the full-bridge inverter are the combination of high and low frequencies. During the low state of the low-frequency signal, the gate pulses to the switches in the full-bridge inverter are OFF, during this state the capacitor C_o discharges until the V_{dcbus} reduces to two times the threshold voltage of each LED lamp, thereby the current through LED lamps becomes zero, and the lamps are turned OFF.

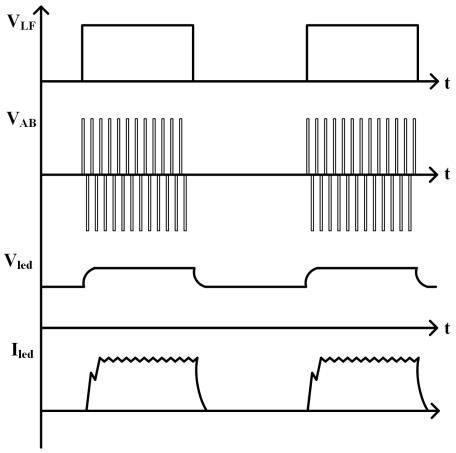

Figure 3.6: PWM dimming scheme

The lamps are turned ON again during the high sate of the low-frequency signal. The average current flowing through LED lamps is varied by varying the pulse width of the low-frequency signal. The amplitude of LED lamp current is regulated against the variations in input voltage V_{DC} by controlling the phase shift (δ) between the gate pulse of switch S_3 w.r.t S_1 such that the V_{dcbus} is maintained at nominal value and hence the LED currents.

3.6 Comparative analysis

Table 3.1 gives a comparison between the proposed LED driver and other multiple output soft-switched LED drivers presented in the literature. In [98] and [97] separate resonant converters are used to drive each load. Hence, in these converters, the component count is high when compared to the proposed converter. Although the active switches are less in [52], [93] and [101], these converters also use separate resonant circuits to drive different loads and require a higher number of passive components when compared to the proposed converter. The total component count of the proposed converter and the topologies presented in [82] and [83] are more or less the same. But, these converters use the hard switched buck-boost converter at the front end to regulate LED currents. Whereas the proposed converter utilizes an integrated soft switched converter, thus provides better efficiency compared to others with the same component count. From Table3.1 it is clear that the component count of the proposed converter is less when compared to the other multiple output LED drivers. The size of the converter is determined by the component count. Hence the size of the proposed LED driver is less when compared to the other topologies.

Table 3.1: Comparision table

Refrences	[98]	[52]	[93]	[50]	[101]	[97]	[82]	[83]	Proposed
No. of switches	2n+1	2	2	n	4	2n+2	n+2	n+4	n
No. of inductors	n+1	n (variabe)	n (variable)	n	2n+2	n+1	n+1 +(n-2)/2	2n +(n-2)/2	n +(n-2)/2
No. of capacitors	2n+1	2n	2n	2n-1	2n+2	2n	1	1	1
No. of HF transformers	0	n	0	0	1	0	0	0	1
No. of diodes	4n	2n	2n	n	4n	4n	1	1	2
Input voltage	48	380	48	150	400	48	66	31.2	48
No. of LED loads tested	2	1	1	2	2	2	4	2	4
Total power rating in watts	65	50	22.32	30	200	126	145	87	142
Peak efficiency	92.3	90.5	94	95.5	92.8	92.45	94.96	94.26	95.6

3.7 Results

To test the performance of the proposed concept, a 142 W LED driver with 48 V input is designed, simulated in Orcad PSPICE, and tested with an experimental prototype. The parameters used for simulation and experimentation are given in Table.3.2. Fig.3.7 shows a photograph of the experimental setup.

Table 3.2: Parameters of the proposed LED driver

Input voltage (V_{DC})	48 V
Switching frequency (f_s)	200 kHz
Dimming frequency (f_d)	200 Hz
Resonant inductor (L_r)	106 μH
Resonant capacitor (C_r)	6.9 nF
Filter capacitor (C_o)	10 μF
Inductances $L_1, L_2, L_3$and L_4	570 μH
Transformer turns ratio	2:2:3
No. of LEDs per string	11
No. of LED strings per lamp	2
Operating current of LEDs	0.5 A
MOSFETs used	IRF 540N
Diodes used	MBR10100

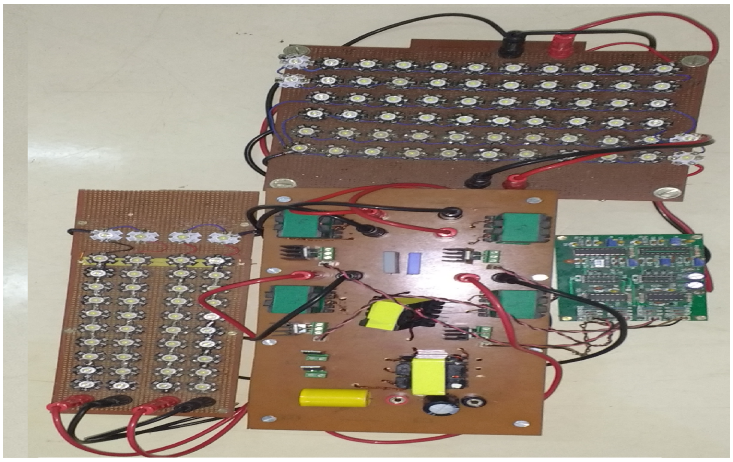

Figure 3.7: Experimental setup

The block diagram of the pulse generation circuit is shown in Fig. 3.8. High frequency (200 kHz) switching pulses are generated using phase shift resonant controller IC UC3875. This IC generates four pulses (A, B, C and D) with 50% duty cycle. The output pulses A&B and C&D are complimentary. Using this IC the phase shift between output pulses A&C can also

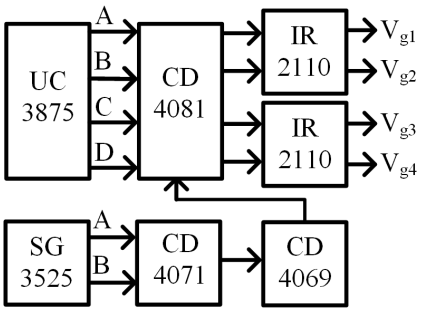

Figure 3.8: The block-diagram of the pulse generation circuit

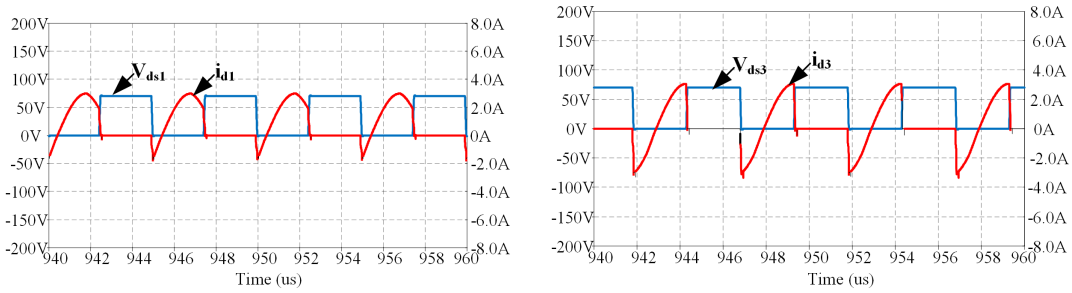

(a) (b)

Figure 3.9: Simulation waveforms of voltage and current (a) switch S_1 (b) switch S_3

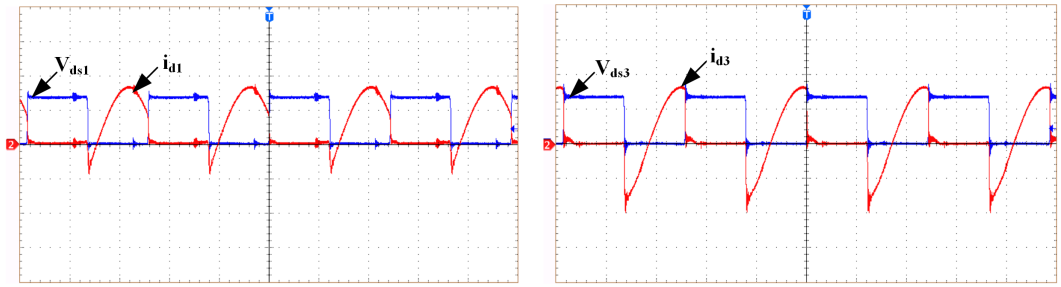

(a) (b)

Figure 3.10: Experimental waveforms of voltage and current (a) switch S_1 (b) switch S_3 (voltage: 50 V/div; current: 2 A/div; time: 2 μsec/div

be controlled. Low frequency (200 Hz) PWM dimming control pulse is generated using PWM control IC SG3525. AND operation of the high frequency switching pulses with low frequency dimming pulse is performed using quadruple AND gate IC CD4081. These signals are given to the MOSFET switches ($S_1 - S_4$) through gate driver IC IR2110. Simulation and experimental voltage and currents of the switches are shown in Fig.3.9 and Fig.3.10, respectively. From these figures, it is observed that the switch currents are negative at the time of turn-on. Hence the switches are turned-on at zero voltage. Simulation and experimental series resonant circuit

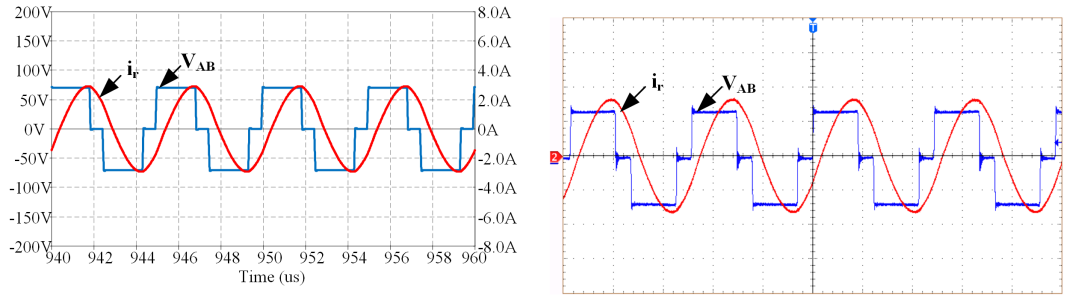

(a) (b)

Figure 3.11: SRC voltage V_{AB} and current i_r waveforms (a) Simulation (b) Experimental (voltage: 50 V/div; current: 2 A/div; time: 2 μsec/div

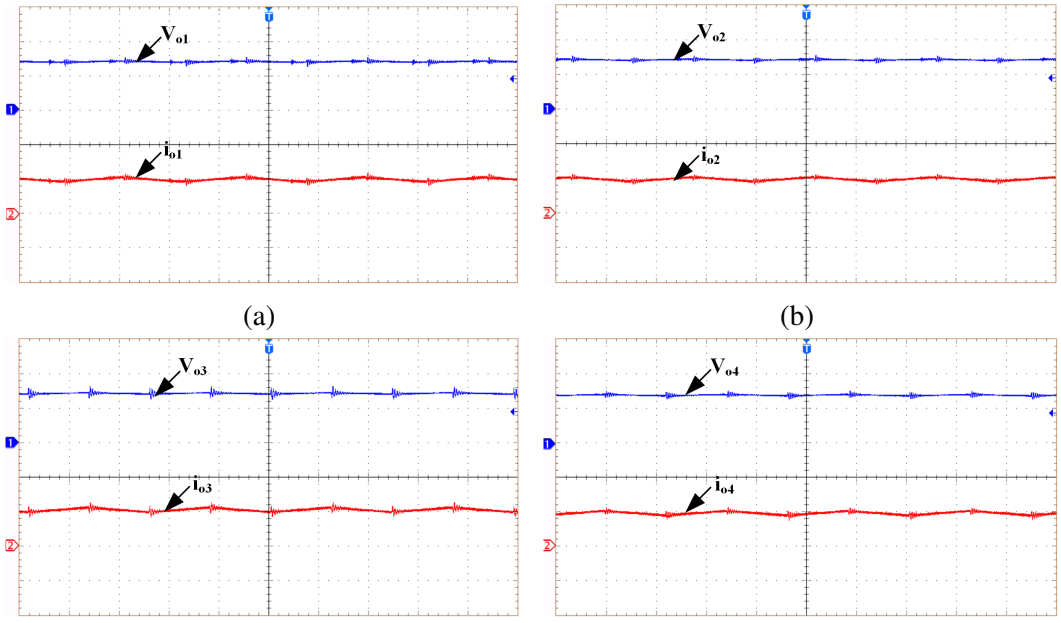

(a) (b)

(c) (d)

Figure 3.12: Voltage and current waveforms of LED lamps (a) lamp1 (b) lamp2 (c) lamp3 (d) lamp4 (Voltage: 25 V/div; Current: 1 A/div; time: 2 μsec/div)

voltage V_{AB}, and current i_r are shown in Fig.3.11a and 3.11b, respectively. From switch and SRC currents, it is observed that switch currents are approximately equal to the resonant circuit current during their turn on states. This is because each switch carries the series resonant circuit and two load components of currents, which are in the opposite direction and cancel each other. Hence, the switching and conduction losses of the converter are low, and the efficiency of the converter is high and is 95.6% at full illumination level. Fig.3.12 shows all the LED lamps' voltage, and current waveforms at full illumination level.

The proposed converter is also tested with different input voltages. In this converter, the

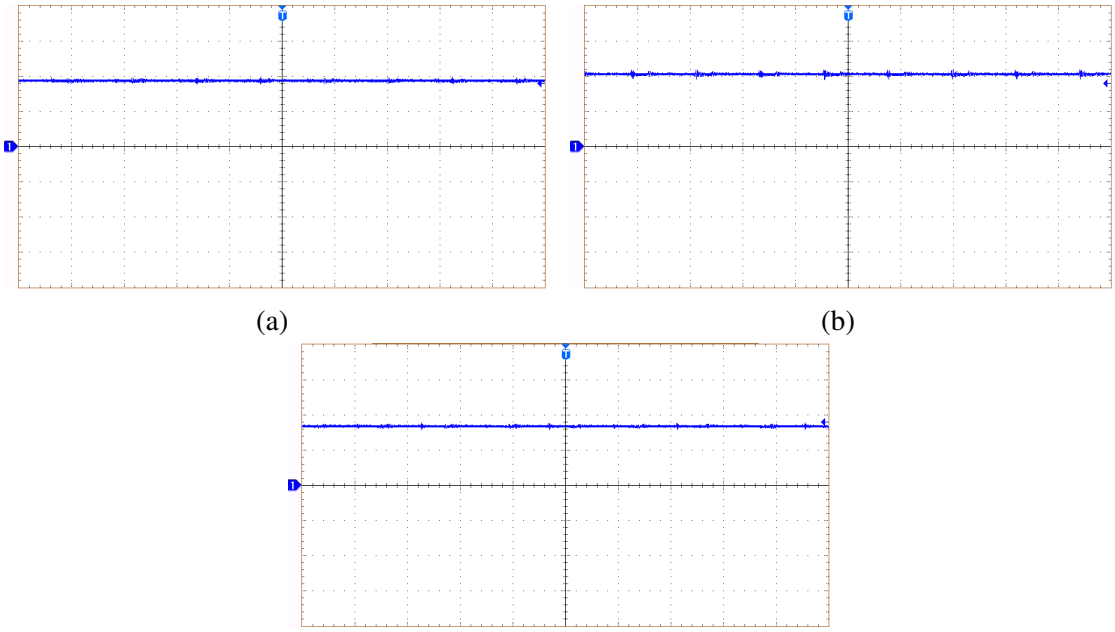

(a) (b)

(c)

Figure 3.13: Capacictor voltage V_{co} at different input voltages V_{DC} (a) at V_{DC}= 48 V (b) at V_{DC}= 45.6 V (c) at V_{DC}= 50.4 V (voltage: 12.5 V/div; time: 2 μsec/div

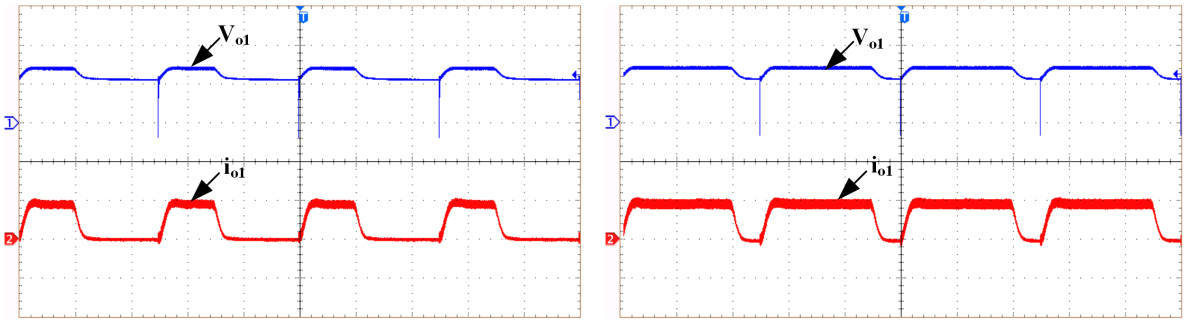

(a) (b)

Figure 3.14: Waveforms of Voltage and currents of LED lamp1 with (a) 40% of full illumination (b) 80% of full illumination (voltage: 25 V/div; current: 1 A/div; time: 2 msec/div

SRC output voltage V_{Co} is varied, by varying the phase between the gating signals of switches S_1 and S_3, In such a way that V_{dcbus} is maintained constant at 71 V. The output voltage V_{Co} of the SRC at different input voltages are shown in Fig.3.13. The efficiency of the proposed converter at input voltages 45.6 V, 48 V, and 50.4 V are found to be 93.14%, 94.7%, and 95.67%, respectively. To verify the dimming performance of the proposed LED driver LED lamp-1 voltage and current waveforms with 40% and 80% of full illumination levels are presented in Fig.3.14a and Fig.3.14b respectively. The variation efficiency w.r.t illumination levels of the lamps is shown in Fig.3.15.

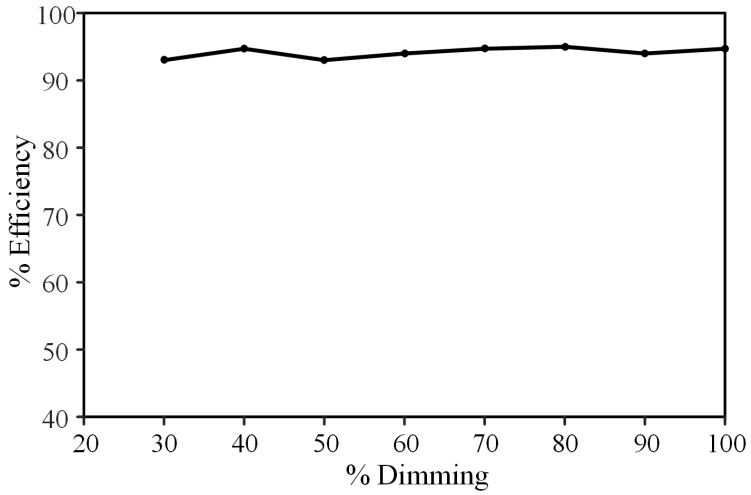

Figure 3.15: Variation of efficiency w.r.t %dimming

3.8 Conclusions

In this chapter, an integrated buck phase-shift controlled full-bridge converter is presented. This LED driver suitable for the applications, which requires equal wattage lamps like street lighting, auditorium lighting, etc. The proposed configuration is studied in detail for its performance. Modes of operations and analysis are explained clearly. To validate experiment results with simulation results, a 142 W prototype is implemented. Experimental results are in good agreement with simulation results.

The proposed configuration has the following advantages:

1. The current in bridge devices is almost independent lamp currents and carries only the series resonat circuit currents .
2. All the switches in the converter operated with ZVS.
3. Only part of the power is processed by the series resonant converter. Hence the efficiency of the proposed LED driver is high.
4. Dimming operation is achieved for all lamps.
5. Input voltage to the full-bridge is controlled for regulating LED lamp current.
6. High efficiency is obtained at both full and dimming levels.

7. Components count per lamp as well as the cost of the driver is less.

8. This configuration can be extended to multiple LED lamps by addition legs in bridge.

9. This configuration can be powered from battery operated systems.

The limitation of proposed converter is lack of independent dimming of LED lamps. The next chapter proposes a Dual frequency series resonant converter based LED driver with independent current regulation and dimming.

Chapter 4

Dual frequency series resonant converter based LED driver

Chapter 4

Dual frequency series resonant converter based LED driver

4.1 Introduction

In this chapter a Dual frequency series resonant converter is proposed to drive two LED loads independently. The proposed converter is operated simultaneously at two different frequencies. Two series resonant circuits are used to generate the two different frequency currents. Each lamp is powered through a series resonant circuit. Asymmetric duty cycle cntrol is used to regulate the LED currents independently, and PWM selective dimming is also implemented. A 48.75 W prototype has been developed experimentally to confirm its working principle, performance and validity. The working principle of the proposed circuit is explained in section 4.2. The analysis and parameters design are presented in sections 4.3 and 4.4 respectively. In section 4.5, the currentregulation and dimming control of the proposed converter are discussed. Experimental results and conclusions are provided in sections 4.6 and 4.7 respectively.

4.2 Circuit description and operating principle

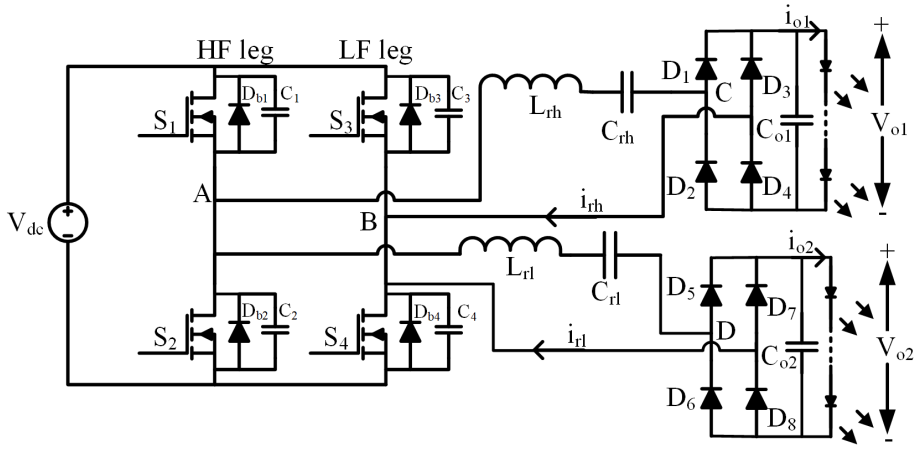

Figure 4.1: Circuit diagram of the proposed LED driver

The circuit diagram of proposed dual frequency series resonant LED driver is shown in Fig. 4.1. The switches S_1-S_4 form a full bridge inverter. Inductor L_{rh} , capacitor C_{rh} , diodes D_1-D_4 , filter capacitor C_{o1} and load-1 forms high frequency (HF) series resonant circuit. Similarly Inductor L_{rl}, capacitor C_{rl}, diodes D_5-D_8, filter capacitor C_{o2} and load-2 forms low frequency (LF) series resonant circuit. These two LF and HF series resonant circuits are connected in parallel across the inverter output terminals A and B.

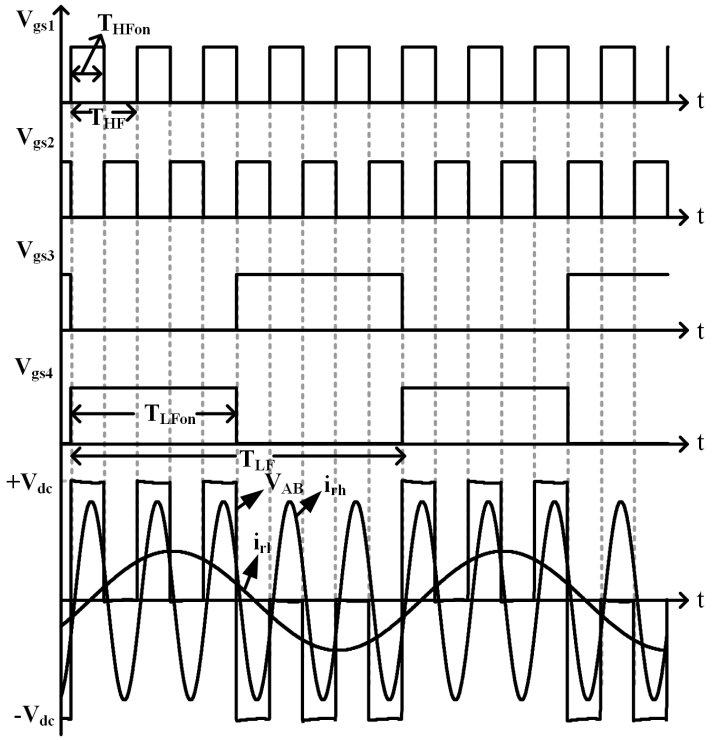

Figure 4.2: Operating waveforms of the proposed LED driver

The operating waveforms of proposed LED driver are shown Fig. 4.2. Switches S_1 and S_2 of the inverter are switching complimentarily with 50% duty ratio at high frequency (f_H) which is called HF leg of the inverter. The switches S_3 and S_4 in the other leg of the inverter are switching complimentarily with 50% duty ratio at low frequency (f_L) which is called LF leg of the inverter. Full-bridge inverter output voltage V_{AB} is a combination of HF voltage V_H and LF voltage V_L. L_{rh} and C_{rh} of HF series resonant circuit are chosen in such way that it will offer low impedance to only V_H component of V_{AB}. Hence, HF series resonant circuit allows only HF resonant current and it is rectified and feeds LED load-1. Similarly L_{rl} and C_{rl} of LF series resonant circuit are chosen in such way that it will offer low impedance to only V_L component of V_{AB}. Hence, LF series resonant circuit allows only LF resonant current and it is rectified and

feeds LED load-2. f_L and f_H should be chosen such that HF resonant circuit is not effected by LF and its harmonic components of V_{AB} voltage and vice versa. To make this happen, f_H should be chosen far greater than f_L and f_H should not be integer multiple of f_L.

4.3 Analysis of the proposed LED driver

The following assumptions are made to simplify the analysis

i) Q-factors of resonant circuits are high so that the each resonant converter allows single frequency sinusoidal currents.

ii) All the elements used in the converter are ideal.

iii) Dead times of the switches are neglected.

Voltage at the output of full-bridge inverter V_{AB} can be split into V_L and V_H as shown Fig. 4.3. From the Fig. 4.3 it is clear that V_L and V_H are square waves with frequency f_L and f_H respectively with amplitudes $V_{DC}/2$. Two series resonant circuits are connected at the output of inverter are tuned for LF and HF frequencies. Therefore the proposed converter can be equivalently analyzed as two half-bridge series resonant converter operating at LF and HF frequencies and conventional AC circuit analysis can be used to calculate static gain of the converter. Hence, the proposed converter is analyzed for HF series resonant converter and the same analysis can be applied for the other LF series resonant convreter. The HF series resonant circuit current (i_{rh}) is rectified and supplied to LED load-1, hence the peak value (I_{mh}) of i_{rh} is given by

$$I_{mh} = \frac{\pi}{2} I_{o1} \tag{4.1}$$

When i_{rh} is positive, D_1 and D_4 are conducting. Hence, the voltage V_{CB} is $+V_{o1}$. When i_{rh} is negative, D_2 and D_3 are conducting. Hence, the voltage V_{CB} is $-V_{o1}$. Therefore, the voltage V_{CB} is a square wave. The amplitude V_{CB1} of the fundamental component of V_{CB} is given by

$$V_{CB1} = \frac{4}{\pi} V_{o1} \tag{4.2}$$

As the voltage, V_{CB} and i_{rh} is in phase, the diode bridge rectifier along with filter capacitor and

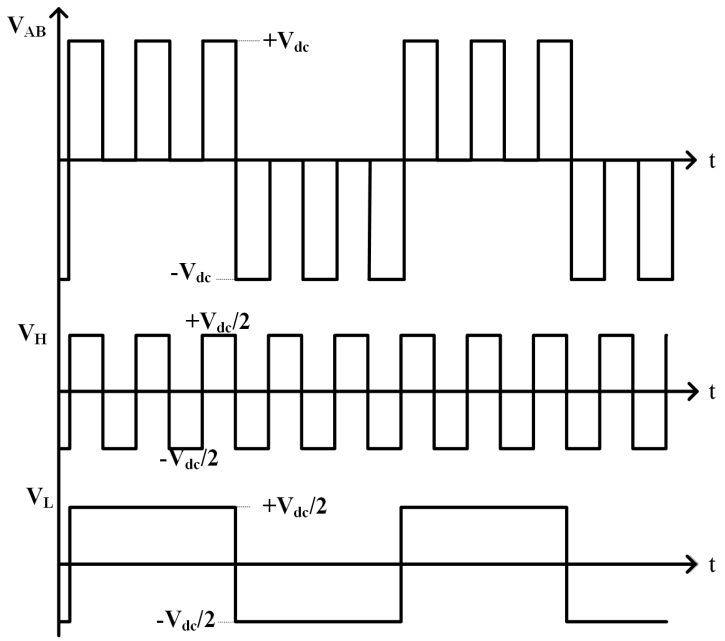

Figure 4.3: Equivalent waveforms of V_{AB}

LED load-1 can be replaced by resistor R_{ach}, whose value is given by

$$R_{ach} = \frac{V_{CB1}}{I_{mh}} = \frac{8}{\pi^2} R_{L1} \tag{4.3}$$

Where, $R_{L1} = V_{o1}/I_{o1}$

The amplitude V_{ABh1} of the HF component of V_{AB} is given by

$$V_{ABh1} = \frac{2}{\pi} V_{DC} \tag{4.4}$$

From the AC equivalent circuit of HF series resonant circuit shown Fig. 4.4, the converter voltage gain is given by

$$\frac{V_{CB1}}{V_{ABh1}} = \frac{R_{ach}}{\sqrt{R_{ach}^2 + (X_{Lrh} - X_{Crh})^2}} \tag{4.5}$$

Where,

Inductor reactance of HF series resonant circuit (X_{Lrh})= $2\pi f_H L_{rh}$,

Capacitor reactance of HF series resonant circuit (X_{Crh})= $\frac{1}{2\pi f_H C_{rh}}$

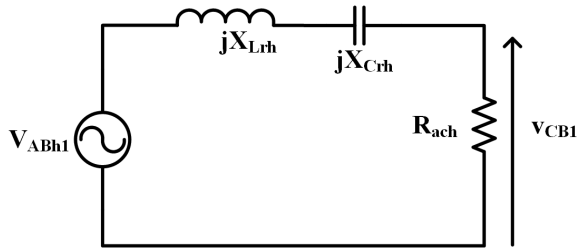

Figure 4.4: AC equivalent circuit of HF series resonant converter

From eqs (4.2), (4.3),4.4 and (4.5), the static gain of the HF series resonant circuit is given by

$$G_{HF} = \frac{V_{o1}}{V_{DC}} = \frac{R_{ach}}{\sqrt{R_{ach}^2 + (X_{Lrh} - X_{Crh})^2}} \tag{4.6}$$

Similarly, the static gain of LF series resonant converter is given by

$$G_{LF} = \frac{V_{o2}}{V_{DC}} = \frac{R_{acl}}{\sqrt{R_{acl}^2 + (X_{Lrl} - X_{Crl})^2}} \tag{4.7}$$

Where,

$(X_{Lrl})= 2\pi f_L L_{rl}$, $(X_{Crl})= \frac{1}{2\pi f_L C_{rl}}$, $R_{acl} = \frac{8}{\pi^2} R_{L2}$

4.4 Design considerations

To validate the operation of the proposed dual-output LED driver, a 48.75 Watt LED driver with the following specifications is designed. A 48 V_{DC} supply is used as input. 32.5 Watt LED load with a voltage of 16.25 V and current 2 A is used as load-1, which realized by four parallel connected LED strings with five series-connected LEDs in each string is used. 16.25 Watt LED load with a voltage of 16.25 V and current 1 A is used as load-2, which is realized by two parallel connected LED strings, with five series-connected LEDs in each string are used. To conrol the two LED loads independently the HF and LF switching frquencies are chosen as 150 kHz and 28 kHz respectively. To achieve ZVS turn on of the switches in a series resonant converter $\frac{f_s}{f_r}$ must be greater than one, and if the $\frac{f_s}{f_r}$ chosen high, then the analysis deviates from the fundamental component analysis. Hence, $\frac{f_H}{f_{rh}}$ and $\frac{f_L}{f_{rl}}$ are chosen as 1.033 and

1.056 respectively. For f_H=150 kHz the product of L_{rh} and C_{rh} is given by

$$L_{rh}C_{rh} = 1.2016x10^{-12} \tag{4.8}$$

With V_{o1}=16.25 V, I_{o1}=2 A, and V_{DC}=48 V, by solving equations (4.3), (4.6), and (4.8) the HF series resonant circuit elements L_{rh} and C_{rh} are calculated as 120 μH and 10 nF respectively. To limit the load-1 current ripple within 10% the filter capacitor C_{o1} is chosen as 10 μF. Similarly, the LF resonant circuit is also designed. The product of L_{rl} and C_{rl} is given by

$$L_{rl}C_{rl} = 3.607x10^{-11} \tag{4.9}$$

With V_{o2}=16.25 V, I_{o2}=1 A, and V_{DC}=48 V, by solving equations (4.7) and (4.9) the LF series resonant circuit elements L_{rl} and C_{rl} are calculated as 680 μH and 53 nF respectively. To limit the load-2 current ripple within 10% the filter capacitor C_{o2} is chosen as 10 μF

4.5 Dimming control

The illumination levels of an LED lamp is proportional to the average current flowing through it. It can be changed by changing the average current through the LED lamp. This can be done by amplitude (AM) or pulse width modulation (PWM) of LED lamp current. In AM dimming, the amplitude of the operating current through the LED lamp is varied. This may cause a color change in the light output. In PWM dimming, the operating current of LED maintained constant, the average current through it is varied by turning ON and OFF LEDs at low frequencies. Due to the advantages such as no color change, smooth control, etc. in this paper, PWM dimming control is adopted. In addition, the proposed converter provides individual dimming control of the two lamps. Fig. 4.5 shows the PWM dimming control scheme for the proposed LED driver. When the switch S_1 is OFF and S_2 is ON continuously, S_3 and S_4 are operated complimentarily at LF as shown in Fig. 4.5, produces LF voltage across A & B terminals of the inverter. As the HF series resonant circuit is tuned for HF frequency no current flows in it. Consequently lamp-1 turn-off, while lamp-2 operates normally. Similarly, to turn off the LED lamp-2 and operate the LED lamp-1 normally, the switch S_3 is OFF and S_4 is ON continuously, the switches S_1, and S_2 are operated complimentarily at HF frequency. In

this way, both the LED lamps are turned ON & OFF individually at a low frequency to control their brightness. The amplitude of LED lamp-1 and lamp-2 currents are regulated against the variations in input voltage V_{DC} by controlling the duty cycle D_{HF} of HF leg and duty cycle D_{LF} of LF leg respectively. Where D_{LF} and D_{HF} are given by

$$D_{HF} = \frac{T_{HFon}}{T_{HF}} \tag{4.10}$$

$$D_{LF} = \frac{T_{LFon}}{T_{LF}} \tag{4.11}$$

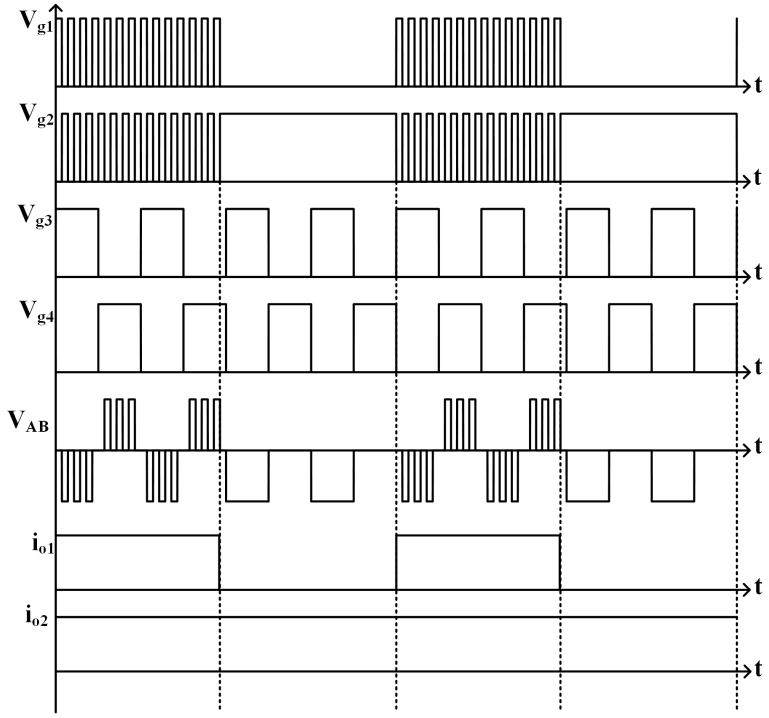

Figure 4.5: PWM dimming scheme

4.6 Results

To test the performance of the proposed concept, a 48.75 Watt (load-1 32.5 W, load-2 16.25 W) LED driver with 48 V input is designed, simulated in Orcad PSPICE, and tested with an experimental prototype. The parameters used for simulation and experimentation are given in Table 4.1. Fig. 4.6 shows a photograph of the experimental setup. Simulation and experimental inverter output voltage V_{AB} and its FFT waveforms are shown in Fig. 4.7. From the FFT of V_{AB} it

Table 4.1: Parameters of the proposed LED driver

Input voltage (V_{DC})	48 V
High switching frequency (f_H)	150 KHz
HF resonant inductor (L_{rh})	120 μH
HF resonant capacitor (C_{rh})	10 nF
HF output filter capacitor (C_{o1})	10 μF
Load-1 voltage (V_{o1})	16.25 V
Load-1 current (I_{o1})	2 A
Low switching frequency (f_L)	28 KHz
LF resonant inductor (L_{rl})	680 μH
LF resonant capacitor (C_{rl})	53 nF
LF output filter capacitor (C_{o1})	10 μF
Load-2 voltage (V_{o1})	16.25 V
Load-2 current (I_{o1})	1 A
Switches (S_1-S_4)	IRF540N
Diodes (D_1-D_8)	MBR10100
Dimming frequency	200 Hz

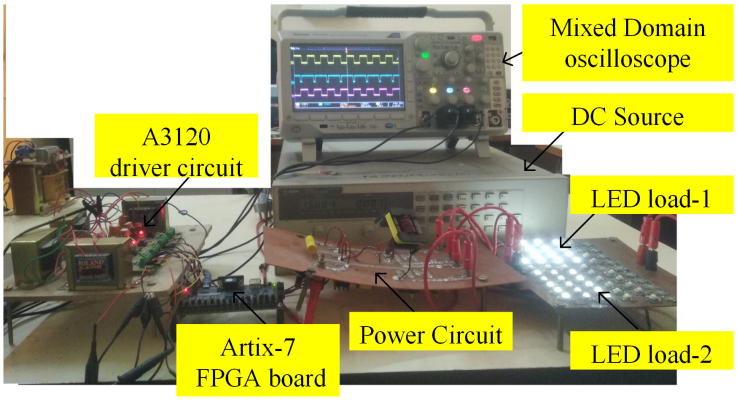

Figure 4.6: Experimental setup

is clear that the voltage V_{AB} contains two dominant components one is at LF and another is at HF frequencies. Fig. 4.8 and 4.9 shows the simulation and experimental HF and LF resonant circuit currents and its FFTs. From the FFTs of LF and HF resonant circuit currents it is clear that the LF and HF resonant circuits allows only LF and HF frequency currents respectively. Fig. 4.10 and Fig. 4.11 shows the simulation and experimental voltage and current waveforms of switchs S_1 and S_3 respectivey. From these figures it is clear that the switches are operating with partial ZVS. The output voltage and current waveforms of load-1 and load-2 at 100% illumination are shown in Fig. 4.12. To verify the independent dimming of the proposed converter PWM dimming with 200 Hz is implemented and the results are presented in Fig.s 4.13 and 4.14. Fig.

4.13 shows the experimental waveforms of load voltage and load currents with 40% and 80% illumination of load-1 and load-2 respectively. Fig.4.14 shows the experimental load voltage and load currents with 80% and 40% illumination of load-1 and load-2 respectively. Figs 5.11 and 5.12 prove the independent dimming operation of both the loads. Variation of Lamp-1 and Lamp-2 currents w.r.t duty cycle D_{LF} and D_{HF} are shown in Fig.5.13. From this figure, it is clear that Lamp-1 and Lamp-2 currents can be regulated independently by varying duty cycles D_{LF} and D_{HF} respectively

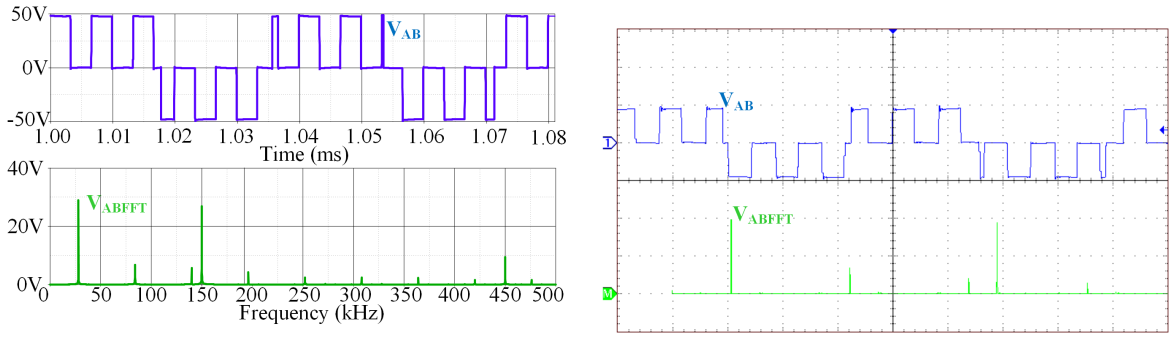

(a) (b)

Figure 4.7: Inverter output volatge V_{AB} and its FFT (a) Simulation waveforms (b) Experimental waveforms (V_{AB}: 50 V/div, time: 8 μs/div , V_{ABrms}: 10V/div, Frequency: 25 kHz/div)

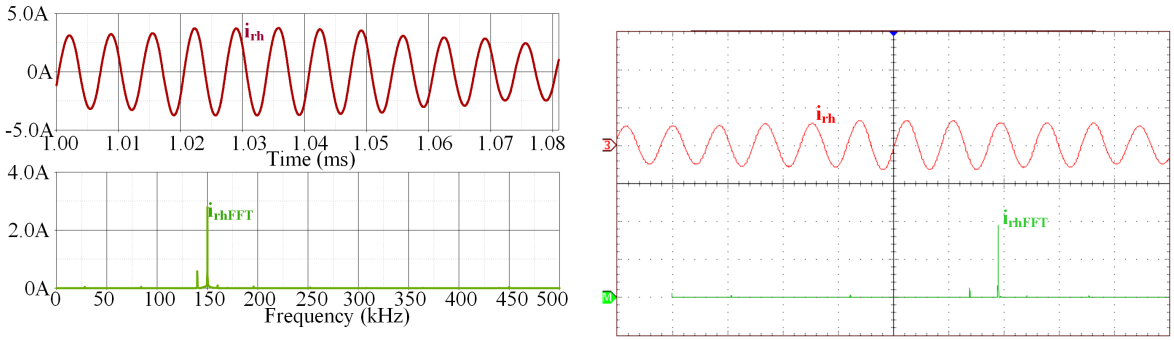

(a) (b)

Figure 4.8: Current i_{rh} and its FFT (a) Simulation waveforms (b) Experimental waveforms (i_{rh}: 5 A/div, time: 8 μs/div, i_{rhFFT}: 1 A/div, Frequency: 25 kHz/div)

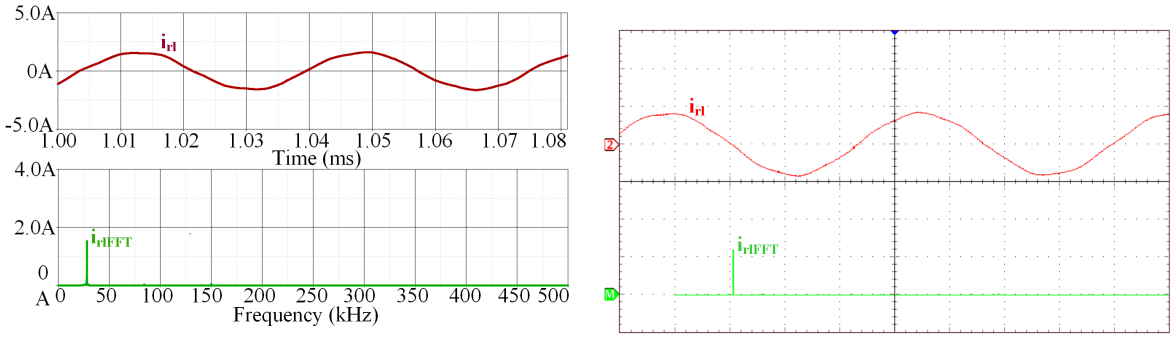

(a) (b)

Figure 4.9: Current i_{rl} and its FFT (a) Simulation waveforms (b) Experimental waveforms (i_{rl}: 2 A/div, time: 8 μs/div, i_{rlFFT}: 1 A/div, Frequency: 25 kHz/div)

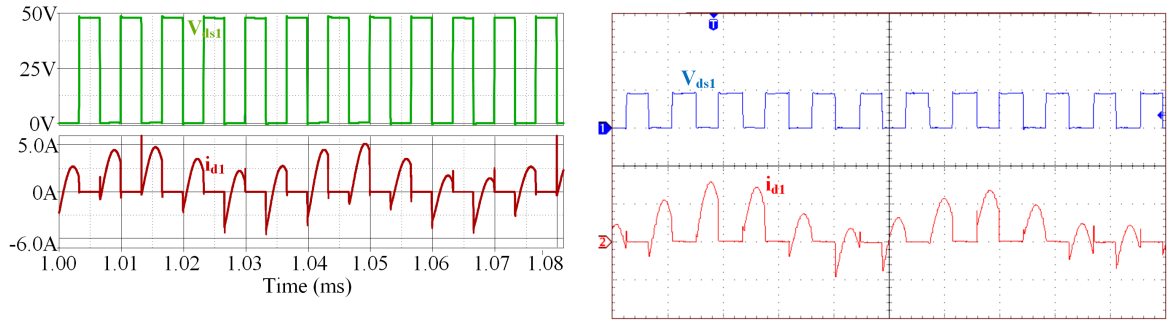

(a) (b)

Figure 4.10: Switch S_1 Voltage and Currents (a) Simulation waveforms (b) Experimental waveforms (V_{ds1}: 50 V/div, i_{ds1}: 3 A/div, time: 8 μs/div)

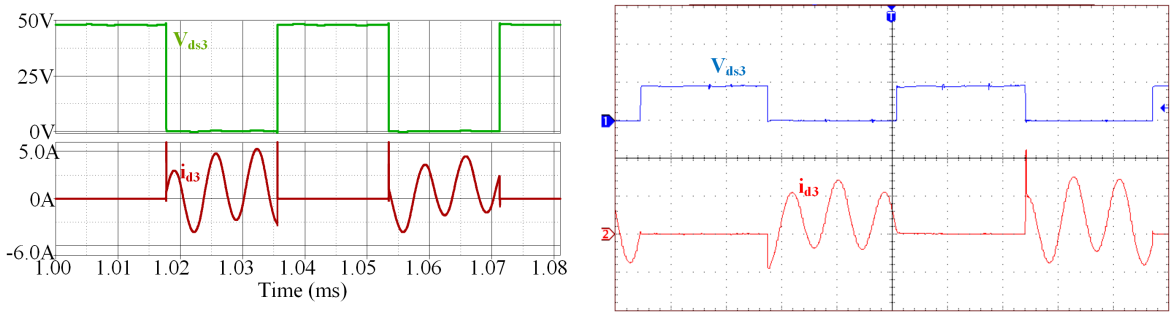

(a) (b)

Figure 4.11: Switch S_3 Voltage and Currents (a) Simulation waveforms (b) Experimental waveforms (V_{ds1}: 50 V/div, i_{ds3}: 3 A/div, time: 8 μs/div)

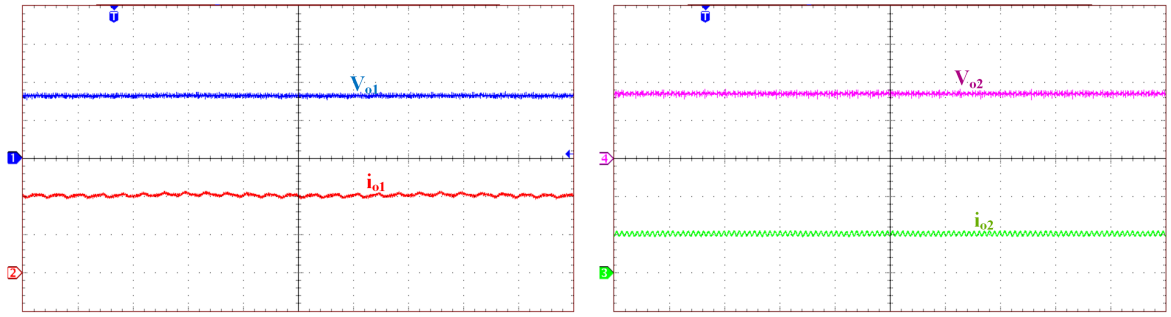

(a) (b)

Figure 4.12: Load voltage and current waveforms at full illuminations (a) Experimental load-1 voltage and current waveforms (V_{o1}: 10 V/div; i_{o1}: 1 A/div; time: 200 μs/div) (b) Experimental load-2 voltage and current waveforms (V_{o2}: 10 V/div; i_{o1}: 1 A/div; time: 200 μs/div)

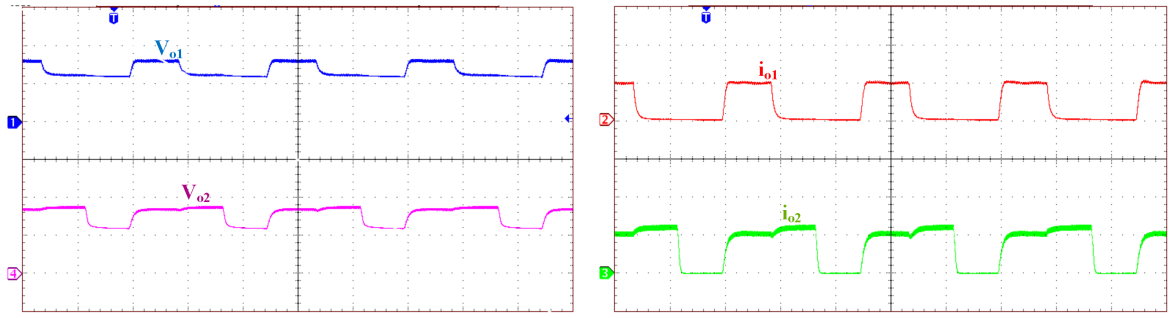

(a) (b)

Figure 4.13: Load voltage and current waveforms at 40% and 80% of full illuminations of Load-1 and Load-2 respectively (a) Experimental load voltage waveforms (V_{o1}: 10 V/div; V_{o2}: 10 V/div; time: 2 ms/div) (b) Experimental load current waveforms (i_{o1}: 2 A/div; i_{o2}: 1 A/div; time: 2 ms/div))

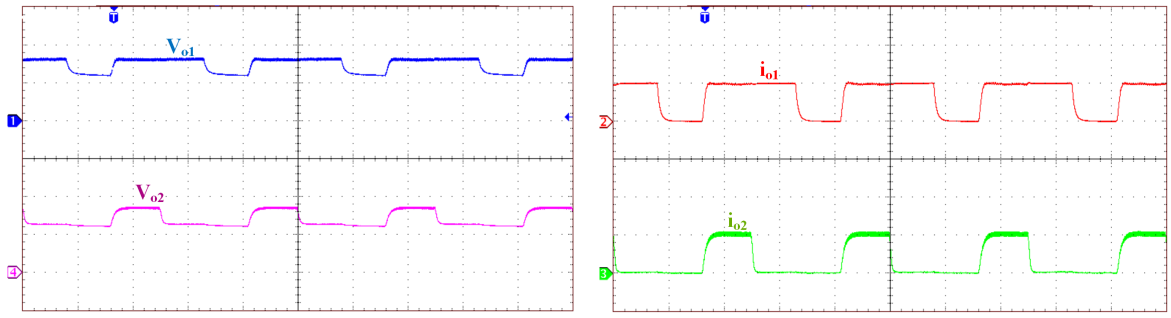

(a) (b)

Figure 4.14: Load voltage and current waveforms at 80% and 40% of full illuminations of Load-1 and Load-2 respectively (a) Experimental load voltage waveforms (V_{o1}: 10 V/div; V_{o2}: 10 V/div; time: 2 ms/div) (b) Experimental load current waveforms (i_{o1}: 2 A/div; i_{o2}: 1 A/div; time: 2 ms/div))

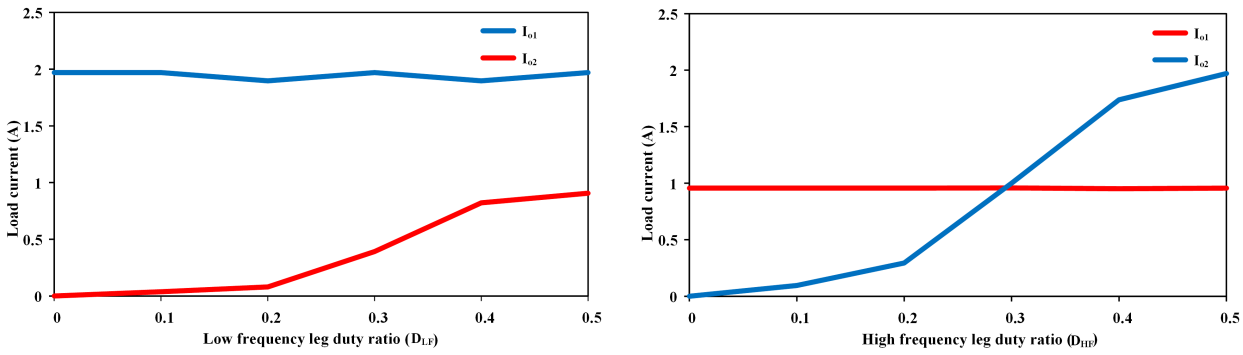

(a) (b)

Figure 4.15: Load currents Variations w.r.t duty cycle (a) variation of load currents w.r.t D_{LF} at D_{HF}=0.5 (b) variation of load currents w.r.t D_{HF} at D_{LF}=0.5

4.7 Conclusions

In this chapter, a dual-frequency series resonant converter has been developed to power two LED lamps with different power ratings. Asymetric duty cycle control is used to regulate the LED currents aganist input voltage variations. Principle of operation, analysis, design procedure and current regulation feature are explained in detail. Simulation and experimental results obtained of a 48.75 W prototype are presented.

This configuration has the following advantages;

1. Drives two LED lamps of different power rating with same input voltage.
2. Both LED lamps can be independently regulated at the required operating voltage and current.
3. Both LED lamps can be dimmed independently.
4. The proposed topology can be suitable for color mixing and multi color lighting applications.
5. It can be powered from low voltage dc grid or battery operated systems.

The limitations of this configuration is partial ZVS switching of the devices. The next chapter proposes an Independently controllable dual output converter for LED lighting application.

Chapter 5

Independently controllable dual output half-bridge series resonant converter for LED driver application

Chapter 5

Independently controllable dual output half-bridge series resonant converter for LED driver application

5.1 Introduction

In this chapter a Independently controllable dual output series resonant converter is proposed to drive two LED loads independently. In this configuration two half-bridge resonant converters are implemented with three switches, which reduces the switch count. Asymmetric duty cycle cntrol is used to regulate the LED currents independently, and PWM selective dimming is also implemented. A 50 W prototype has been developed experimentally to confirm its working principle, performance and validity. The working principle of the proposed circuit is explained in section 5.2. The analysis and parameters design are presented in sections 5.3 and 5.4 respectively. In section 5.5, the currentregulation and dimming control of the proposed converter are discussed. Experimental results and conclusions are provided in sections 5.6 and 5.7 respectively.

5.2 Circuit description and operating principle

The circuit diagram of the proposed dual-output LED driver is shown in Fig. 5.1. The capacitors C_{in1} and C_{in2} are charged to half of the input voltage. The three MOSFET switches $S_1 - S_3$, forms two independently controllable dual-output Half-bridge inverter (HBI), whereas switch S_2 is shared by the two HBIs. SRC-1, composed of inductor L_{r1}, capacitor C_{r1}, a diode bridge rectifier (having diodes $D_1 - D_4$), and filter capacitor C_{o1}, is connected across A and C terminals of HBI to feed LED load-1. Similarly, the SRC-2, composed of inductor L_{r2}, capacitor C_{r2}, a diode bridge rectifier (having diodes $D_5 - D_8$), and filter capacitor C_{o2}, is connected across B and C terminals of HBI to feed LED load-2. The functional waveforms of the proposed dual-output LED driver are shown in Fig. 5.2. To achieve independent operation of loads, the switches S_1 and S_3 should operate with greater than 50% duty cycles. There are three possible

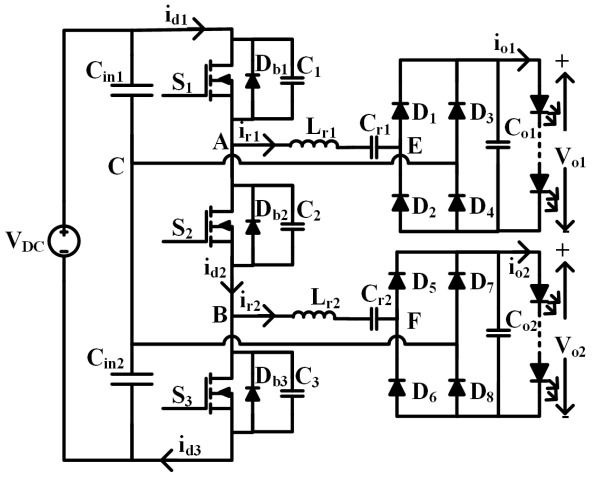

Figure 5.1: Circuit diagram of the proposed LED driver

combinations of the switches S_1 and S_3 as they are operating higher than 50% duty cycle and those are 1) S_1 OFF & S_3 ON, 2) S_1 ON & S_3 OFF and 3) S_1 ON and S_3 ON. The switch S_2 is ON only when either the switch S_1 or S_3 is ON and switch S_2 is OFF when S_1 and S_3 are ON. The detailed HBI voltages for different switching states of $S_1 - S_3$ are presented in Table 5.1. When switch S_1 is ON, either the switch S_2 or S_3 is ON. Therefore the voltage V_{AC} is V_{Cin1}. When the switch S_1 is OFF, both the switches S_2 and S_3 are ON. Therefore the voltage V_{AC} is -V_{Cin2}. i.e., the voltage V_{AC} can be regulated by controlling the duty cycle D_1 of the switch S_1. Similarly, when the switch S_3 is ON, either the switch S_1 or S_2 is ON. Therefore the voltage V_{BC} is -V_{Cin2}. When the switch S_3 is OFF, both the switches S_1 and S_2 are ON. Therefore the voltage V_{BC} is V_{Cin1} i.e., the voltage V_{BC} can be regulated by controlling the duty cycle D_3 of the switch S_3. Therefore the voltages V_{AC} and V_{BC} can be independently controlled by varying duty cycles D_1 and D_3 respectively. The SRC-1 and SRC-2 elements are selected in such a way that the respective SRC offers low impedance to the fundamental component of the corresponding HBI output. The operating modes of the proposed converter are explained in the following section.

Table 5.1: Voltages of HBI for different switching states of the proposed converter

S_1	S_3	S_2	V_{AC}	V_{BC}
OFF	ON	ON	-V_{Cin2}	-V_{Cin2}
ON	OFF	ON	+V_{Cin1}	+V_{Cin1}
ON	ON	OFF	+V_{Cin1}	-V_{Cin2}

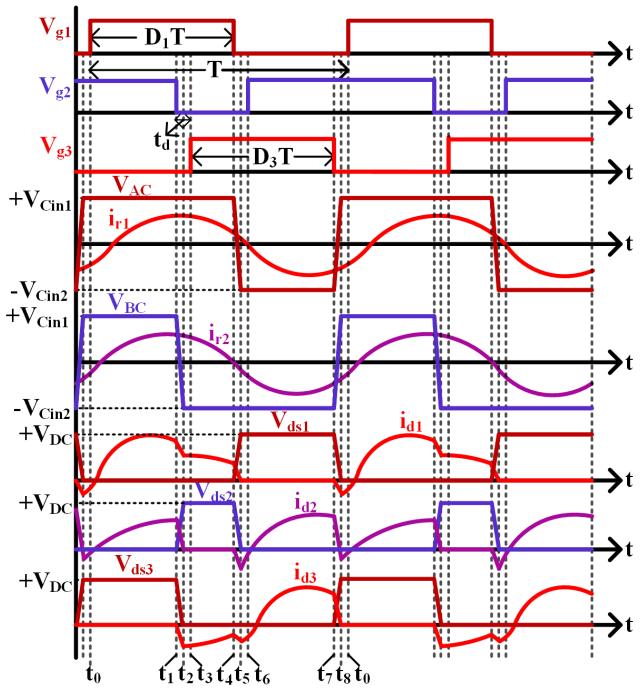

Figure 5.2: Functional Waveforms of the converter

5.2.1 Mode: I

Before this mode, D_{b1} is conducting. At $t = t_0$ S_1 is triggered and it conducts to take over the current carried by D_{b1}. Since D_{b1} is conducting before applying gate pulse to S_1, the switch S_1 is turned on with zero voltage. The analogous circuit for this mode is depicted in Fig. 5.3a. The switch S_1 current is given by

$$i_{d1} = i_{r1} + i_{r2} \tag{5.1}$$

The switch S_2 current is given by

$$i_{d2} = i_{r2} \tag{5.2}$$

5.2.2 Mode: II

When the triggering pulse of S_2 is removed at $t = t_1$, the current i_{r2} is positive. This makes the snubber capacitor C_2 is charging and C_3 discharging. This mode ends at $t = t_2$ when the capacitor C_2 is completely charged and C_3 completely discharged as depicted in Fig. 5.3b.

5.2.3 Mode: III

When the snubber capacitor C_3 discharges completely at $t = t_2$,the body diode D_{b3} of switch S_3 is forward biased and starts conducting. The analogous circuit for this mode is depicted in Fig. 5.3c.

5.2.4 Mode: IV

At $t = t_3$, S_3 is triggered and it conducts to takes over the current carried by D_{b3}. Since D_{b3} is conducting before applying gate pulse to S_3, the switch S_3 is turned on with zero voltage. The analogous circuit for this mode is depicted in Fig. 5.3d. The switch S_1 current is given by

$$i_{d1} = i_{r1} \tag{5.3}$$

The switch S_3 current is given by

$$i_{d3} = -i_{r2} \tag{5.4}$$

5.2.5 Mode: V

When the triggering pulse of S_1 is removed at $t = t_4$, the current i_{r1} is positive. This makes the snubber capacitor C_1 is charging and C_2 discharging. This mode ends at $t = t_5$ when the snubber capacitor C_1 is fully charged and C_2 completely discharged as depicted in Fig. 5.3e.

5.2.6 Mode: VI

When the snubber capacitor C_2 discharges completely at $t = t_5$, D_{b2} is forward biased and starts conducting. The analogous circuit for this mode is depicted in Fig. 5.3f.

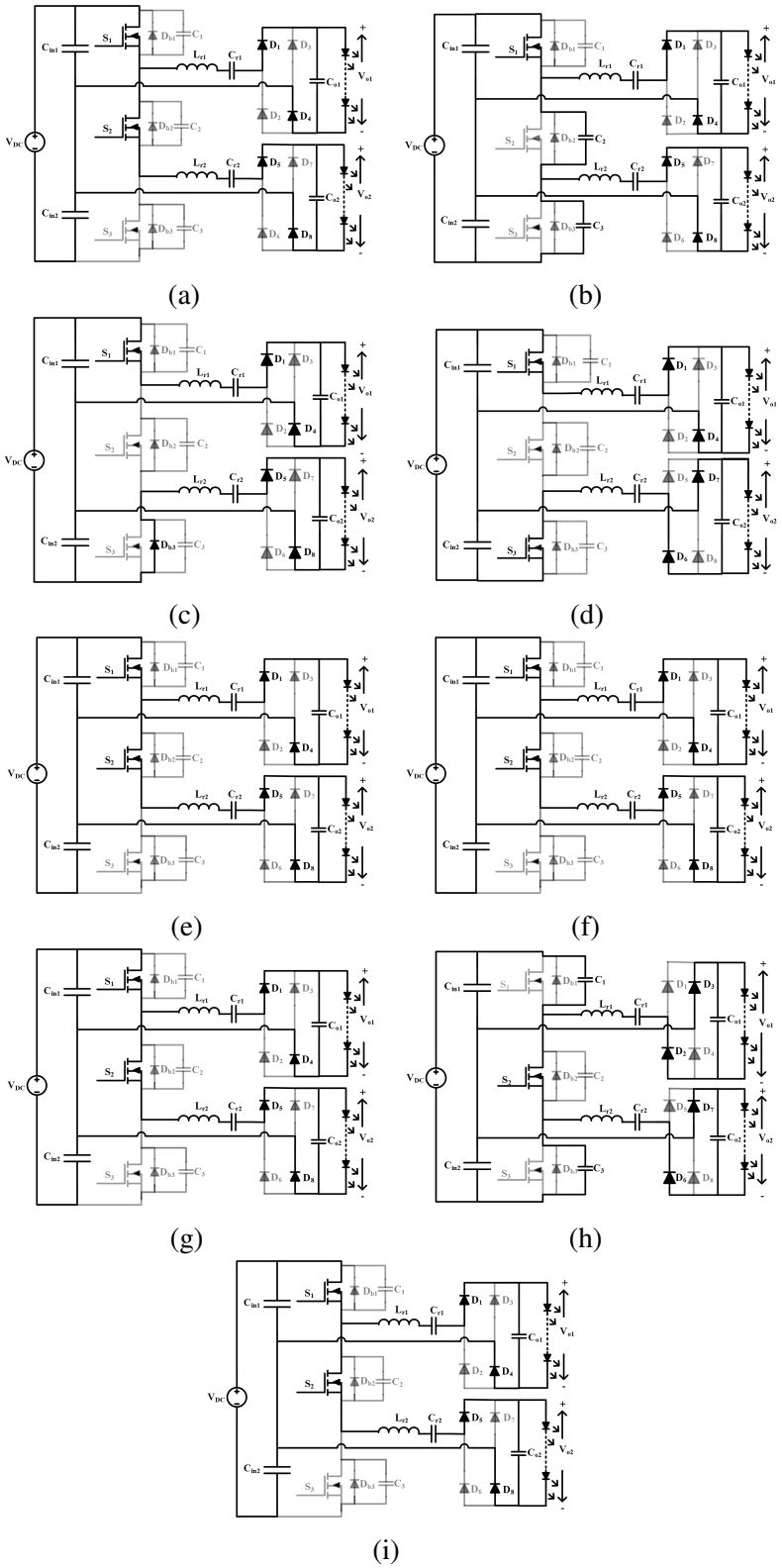

Figure 5.3: Equivalents circuits during (a) Mode-I (b) Mode-II (c) Mode-III (d) Mode-IV (e) Mode-V (f) Mode-VI (g) Mode-VII (h) Mode-VIII (i) Mode-IX

5.2.7 Mode: VII

At $t = t_6$, S_2 is triggered and it conducts to takes over the current carried by D_{b2}. Since D_{b2} is conducting before applying gate pulse to S_2, the switch S_2 is turned on with zero voltage. The analogous circuit for this mode is depicted in Fig. 5.3g. The switch S_2 current is given by

$$i_{d2} = -i_1 \tag{5.5}$$

The switch S_3 current is given by

$$i_{d3} = -(i_{r1} + i_{r2}) \tag{5.6}$$

5.2.8 Mode:VIII

When the switch S_3 is turned off at $t = t_8$, the sum of the resonant circuit currents ($i_{r1} + i_{r2}$) is negative. This makes the snubber capacitor C_3 is charging and C_1 discharging. This mode ends at $t = t_8$ when the snubber capacitor C_3 is fully charged and C_1 completely discharged as depicted in Fig. 5.3h.

5.2.9 Mode: IX

When the snubber capacitor C_1 discharges completely at $t = t_8$, D_{b1} is forward biased and starts conducting. The analogous circuit for this mode is depicted in Fig. 5.3i.

5.3 Analysis of the proposed LED driver

The following assumptions are made to simplify the analysis

i) All the components used in the converter are ideal.

ii) The converter is operating in a steady-state.

iii) The dead time t_d is neglected.

iv) The Q-factors of the resonant circuits are high, which confines the analysis to the fundamental frequency.

From Table 5.1 and Fig. 5.2 , the V_{AC} and V_{BC} voltages are switching between +V_{Cin1} and -V_{Cin2} , and these voltages can be independently regulated by separate duty cycles D_1 and D_3. Therefore, the proposed converter can be analyzied as two independent half-bridge converters. Hence, the proposed converter is analyzed for SRC-1 and the same analysis can be applied for the other SRC-2. The SRC-1 current (i_{r1}) is rectified and supplied to LED load-1, hence the peak value (I_{m1}) of i_{r1} is given by

$$I_{m1} = \frac{\pi}{2} I_{o1} \tag{5.7}$$

When i_{r1} is positive, D_1 and D_4 are conducting. Hence, the voltage V_{EC} is +V_{o1}. When i_{r1} is negative, D_2 and D_3 are conducting. Hence, the voltage V_{EC} is -V_{o1}. Therefore, the voltage V_{EC} is a square wave. The amplitude V_{EC1} of the fundamental component of V_{EC} is given by

$$V_{EC1} = \frac{4}{\pi} V_{o1} \tag{5.8}$$

As the voltage, V_{EC} and i_{r1} is in phase, the diode bridge rectifier along with filter capacitor and LED load-1 can be replaced by resistor R_{ac1} whose value is given by

$$R_{ac1} = \frac{V_{EC1}}{I_{m1}} = \frac{8}{\pi^2} R_{L1} \tag{5.9}$$

The amplitude V_{AC1} of the fundamental component of V_{AC} is given by

$$V_{AC1} = \frac{2}{\pi} sin(\pi D_1) V_{DC} \tag{5.10}$$

From the AC equivalent circuit of SRC-1 shown Fig. 5.4, the converter voltage gain is given by

$$\frac{V_{EC1}}{V_{AC1}} = \frac{R_{ac1}}{\sqrt{R_{ac1}^2 + (X_{Lr1} - X_{Cr1})^2}} \tag{5.11}$$

Where,

Inductor reactance of SRC-1 (X_{Lr1})= $2\pi f_s L_{r1}$,

Capacitor reactance of SRC-1 (X_{Cr1})= $\frac{1}{2\pi f_s C_{r1}}$

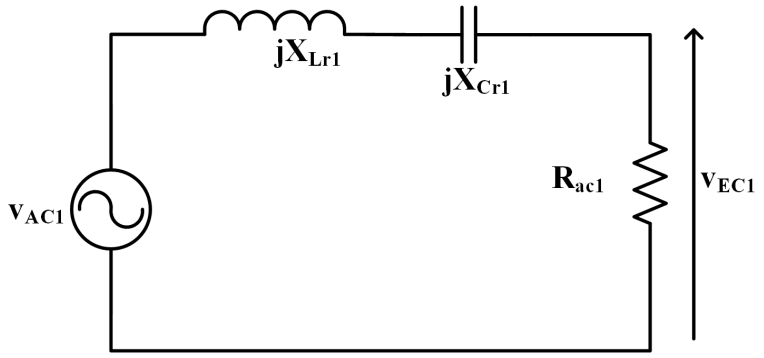

Figure 5.4: AC equivalent circuit of series resonant converter-1

From eqs (5.8), (5.9),5.10 and (5.11), the static gain of the SRC-1 is given by

$$G_1 = \frac{V_{o1}}{V_{DC}} = \frac{sin(\pi D_1)R_{ac1}}{\sqrt{R_{ac1}^2 + (X_{Lr1} - X_{Cr1})^2}} \tag{5.12}$$

Similarly, the static gain of resonant converter-2 is given by

$$G_2 = \frac{V_{o2}}{V_{DC}} = \frac{sin(\pi D_3)R_{ac2}}{\sqrt{R_{ac2}^2 + (X_{Lr2} - X_{Cr2})^2}} \tag{5.13}$$

Where,

$(X_{Lr2}) = 2\pi f_s L_{r2}$, $(X_{Cr2}) = \frac{1}{2\pi f_s C_{r2}}$, $R_{ac2} = \frac{8}{\pi^2} R_{L2}$

The resonant circuit currents are given by

$$i_{r1} = I_{m1} sin(\omega_s t + \frac{\pi}{2} - \pi D_1 - \Phi_1) \tag{5.14}$$

$$i_{r2} = I_{m2} sin(\omega_s t - \frac{\pi}{2} + \pi D_3 - \Phi_2) \tag{5.15}$$

Where, $I_{m1} = \frac{\pi}{2} I_{o1}$, $I_{m2} = \frac{\pi}{2} I_{o2}$, $\phi_1 = tan^{-1}(\frac{X_{Lr1} - X_{Cr1}}{R_{ac1}})$, $\phi_2 = tan^{-1}(\frac{X_{Lr2} - X_{Cr2}}{R_{ac2}})$

From Fig. 5.2 the instantaneous switch currents are given by

$$i_{d1} = \begin{cases} i_{r1} + i_{r2}, & 0 < t < (1 - D_3)T \\ i_{r1}, & (1 - D_3)T < t < D_1 T \\ 0, & D_1 T < t < T \end{cases} \tag{5.16}$$

$$i_{d2} = \begin{cases} i_{r2}, & 0 < t < (1-D_3)T \\ 0, & (1-D_3)T < t < D_1T \\ -i_{r1}, & D_1T < t < T \end{cases} \tag{5.17}$$

$$i_{d3} = \begin{cases} 0, & 0 < t < (1-D_3)T \\ -i_{r2}, & (1-D_3)T < t < D_1T \\ -(i_{r1}+i_{r2}), & D_1T < t < T \end{cases} \tag{5.18}$$

From eqs (5.16), (5.17), and (5.18) the turn-on currents of the switches are given by

$$i_{d1,turnon} = (i_{r1}+i_{r2})_{/t=0} \tag{5.19}$$

$$i_{d2,turnon} = (-i_{r1})_{/t=D_1T} \tag{5.20}$$

$$i_{d3,turnon} = (-i_{r2})_{/t=(1-D_3T)} \tag{5.21}$$

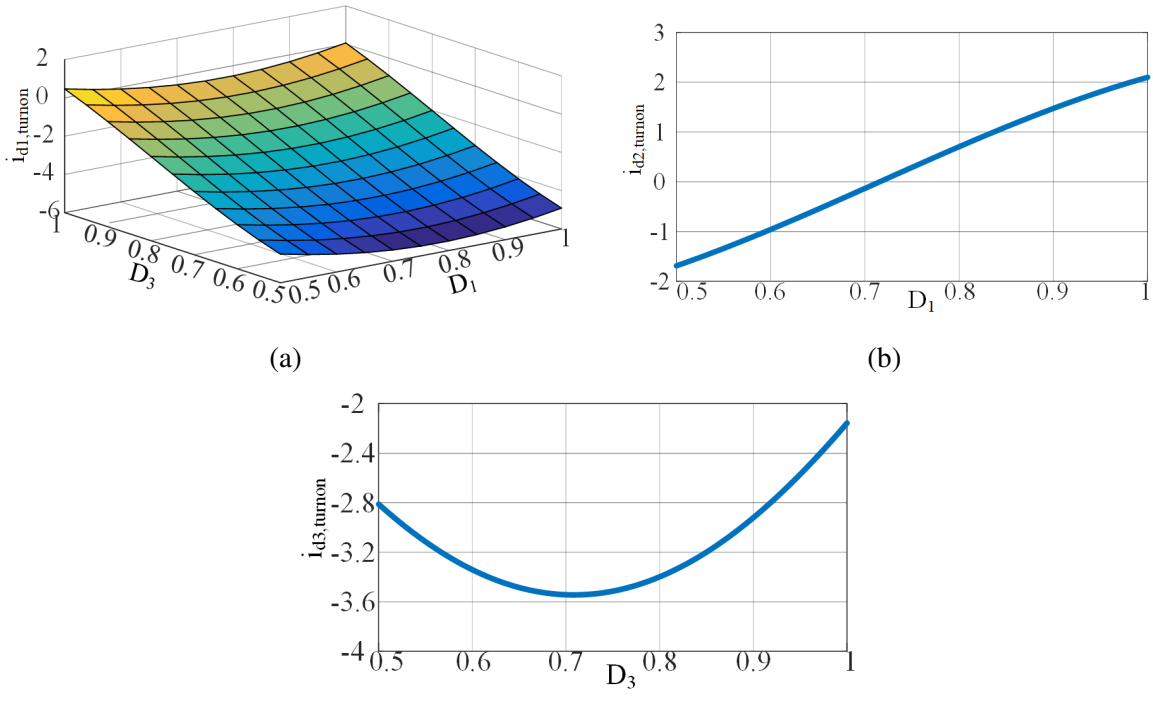

Figure 5.5: Variation of switch turn-on currents w.r.t duty cycles (a) Variation of $i_{d1,turnon}$ w.r.t D_1 and D_3 (b) Variation of $i_{d2,turnon}$ w.r.t D_2 (c) Variation of $i_{d3,turnon}$ w.r.t D_2

The plots of switch turn-on currents with duty cycle variation are given in Fig. 5.5. Switch turn-on currents need to be negative to achieve the ZVS turn-on of the switches. From Fig. 5.5 the duty cycles range for the ZVS turn-on of the switches can be observed.

5.3.1 Loss analysis

5.3.1.1 Conduction loss

Conduction losses are occurring in switching devices, resonant inductors, and rectifier diodes. Total conduction losses of the switching devices are given by

$$P_{cond,switch} = (I_{d1}^2 + I_{d2}^2 + I_{d3}^2)R_{dson} \tag{5.22}$$

Where, I_{d1}, I_{d2}, and I_{d3} are the R.M.S currents of switches S_1, S_2,and S_3 respectively; R_{dson} is the ON resistance of the switch.
Total conduction losses of the rectifier diodes are given by

$$P_{cond,diode} = 2V_f(I_{o1} + I_{o2}) \tag{5.23}$$

Where, V_f is the forward voltage drop of the rectifier diode.
Conduction losses of the resonant inductors are given by

$$P_{ind} = I_{r1}^2 R_{Lr1} + I_{r2}^2 R_{Lr2} \tag{5.24}$$

Where, I_{r1} and I_{r2} are the R.M.S resonant circuit-1 and resonant circuit-2 currents and R_{Lr1} and R_{Lr2} are the series resistances of the resonant inductors L_{r1} and L_{r2} respectively.

5.3.1.2 Switchig losses

Switching losses are taken place in switches and diodes. The rectifier diodes in the series resonant converter are turn-on and turn-off with zero currents. Hence, there are no switching losses in diodes. In the proposed converter the switches are turn-on with zero voltage. Hence, the turn-on losses of the switches are zero. Switch turn-off losses are only present in the proposed

converter. The total switching losses are given by

$$P_{sw} = V_{DC}(i_{d1off} + i_{d2off} + i_{d2off})(\frac{t_r + t_f}{2})f_s \tag{5.25}$$

Where, V_{DC} is the input voltage; i_{d1off}, i_{d2off}, and i_{d3off} are the turnoff currents of the switches S_1, S_2, and S_3 respectively; t_r and t_f are the rise time and fall times of the switches; f_s is the switching frequency.

5.4 Design considerations

To validate the operation of the proposed dual-output LED driver, a 50 Watt LED driver with the following specifications is designed. A 48 V_{DC} supply is used as input. 24 Watt LED load with a voltage of 16.25 V and current 1.5 A is used as load-1, which is realized by three parallel connected LED strings with five series-connected LEDs in each string is used. 26 Watt LED load with a voltage of 13 V and current 2 A is used as load-2, which is realized by four parallel connected LED strings, with four series-connected LEDs in each string are used. The converter is operated with a 100 kHz switching frequency (f_s). To make the switch S_2 OFF for minimum time in a switching period the minimum values of duty cycles D_1 and D_3 are chosen as 53%. The converter should be designed for minimum voltage. Hence, by considering 10% voltage variation in the input voltage the converter is designed for 44 V. To achieve ZVS turn on of the switches in a series resonant converter $\frac{f_s}{f_r}$ must be greater than one, and if the $\frac{f_s}{f_r}$ chosen high, then the analysis deviates from the fundamental component analysis. Hence, $\frac{f_s}{f_{r1}}$ and $\frac{f_s}{f_{r2}}$ are chosen as 1.13 and 1.1 respectively. For f_s=100 kHz the product of L_{r1} and C_{r1} is given by

$$L_{r1}C_{r1} = 3.2344x10^{-12} \tag{5.26}$$

With V_{o1}=16.25 V, I_{o1}=1.5 A, D_1=0.53, and V_{DC}=44 V, by solving equations (5.9), (5.12), and (5.26) the SRC-1 elements L_{r1} and C_{r1} are calculated as 49 μH and 66 nF respectively. To limit the load-1 current ripple within 10% the filter capacitor C_{o1} is chosen as 10 μF. Similarly, the resonant circuit-2 is also designed. The product of L_{r2} and C_{r2} is given by

$$L_{r2}C_{r2} = 3.064x10^{-12} \tag{5.27}$$

With V_{o2}=13 V, I_{o2}=2 A, D_3=0.53, and V_{DC}=44 V, by solving equations (5.13) and (5.27) the SRC-2 elements L_{r2} and C_{r2} are calculated as 58 μH and 53 nF respectively. To limit the load-2 current ripple within 10% the filter capacitor C_{o2} is chosen as 10 μF

5.5 Dimming control

Dimming control is necessary to adjust the illumination of the LED lamp. The LED lamp's light output directly depends on its average current. The average current through LED can be controlled by using amplitude modulation (AM) or pulse width modulation (PWM). In AM, the amplitude of the operating current is regulated to regulate the lamp brightness which adversely affects the color of the light from the lamp. Therefore this method is not suitable for color-sensitive applications. Whereas, in the PWM technique lamp will be ON & OFF with low frequency and maintains nominal current during the ON period. In PWM dimming, if the dimming frequency is not chosen properly then flickering will occur. To avoid flickering effect dimming frequency must be greater than 120 Hz [102]. Hence, to avoid color changing and flickering effect the proposed converter utilizes the PWM technique with 200 Hz dimming frequency for the dimming of the LED lamps. In addition, the proposed converter provides individual dimming control of the two lamps. The control pulses and model waveforms are depicted in Fig. 5.6. When the switch S_1 is ON continuously, S_2 and S_3 are operated at high frequency as shown in Fig. 5.6, produces DC voltage across A & C terminals and high-frequency ac voltage across B & C terminals. As the SRC-1 is tuned for switching frequency no current

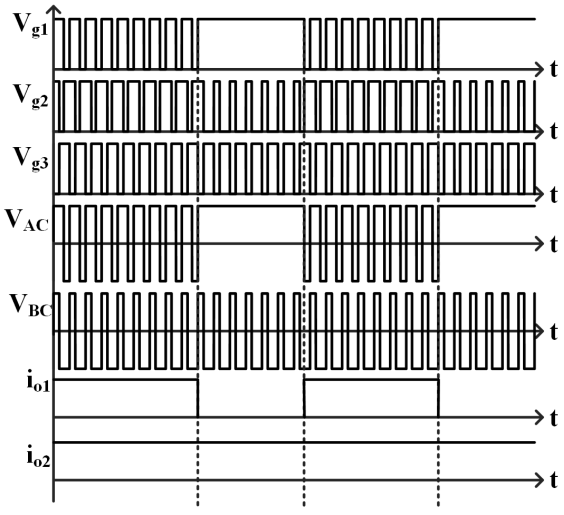

Figure 5.6: PWM Dimming Scheme

flows in it. Consequently lamp-1 turn-off, while lamp-2 operates normally. Similarly, to turn off the LED lamp-2 and operate the LED lamp-1 normally, the switch S_3 is made continuously ON, S_1, and S_2 are operated at high frequency. In this way, both the LED lamps are turned ON & OFF individually at a low frequency to control their brightness. The switching states for the dimming operation of the proposed converter are given in Table 5.2 .

Table 5.2: Details of switching states of SRC-1 & SRC-2 operations during dimming of LED-1 & LED-2 respectively

S_1	S_3	S_2	V_{AC}	V_{BC}	SRC-1	SRC-2
ON	D_3	$\bar{D}_3$	V_{Cin1}	Square wave	idle	Delivering power to Load-2
D_1	ON	$\bar{D}_1$	Square wave	-V_{Cin2}	Delivering power to Load-1	idle
ON	ON	OFF	V_{Cin1}	-V_{Cin2}	idle	idle

5.6 Experimental results

The operation of the propsed converter is tested with experimental prototype of 50 Watt load (load-1 26 Watt, load-2 24 Watt). The experimental results are presented in this section. Specifications and parameter values of the components used in the experimental prototype of the proposed LED driver are given in Table 5.3 . The control pulses for the proposed LED driver are generated using Basys3 Artix-7 FPGA board and A3120 based driver circuits are used to drive the MOSFET switches. The photograph of the experimental prototype is shown in Fig. 5.7.

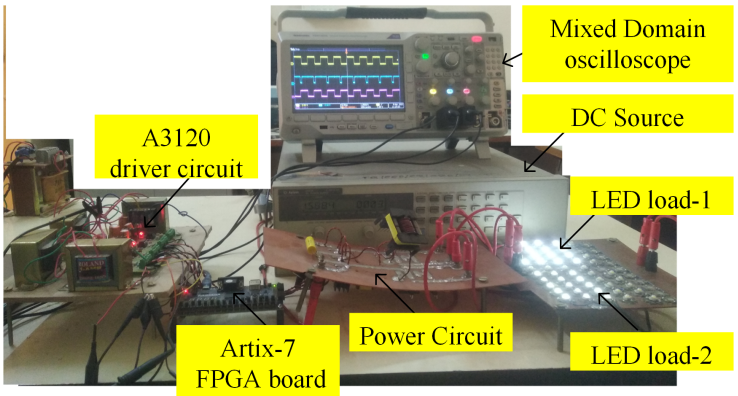

Figure 5.7: Experimental setup

Table 5.3: Components used in the proposed converter

Parameter	Description
DC input Voltage (V_{DC})	48 V
Resonant inductor (L_{r1})	49 μH
Resonant Capacitor (C_{r1})	66 nF/1500 V
No. of strings in LED lamp1	3
No. of LEDs in each string of LED lamp1	5
LED current per string of LED lamp1	0.5 A
Resonant inductor (L_{r2})	58 μH
Resonant Capacitor (C_{r2})	53 nF/1500 V
No. of strings in LED lamp2	4
No. of LEDs in each string of LED lamp2	4
LED current per string of LED lamp2	0.5 A
Switching frequency (f_s)	100 kHz
Filter capacitors (C_{o1} & C_{o2})	10 μF/250V
Switches (S_1-S_3)	IRF540N
Diodes (D_1-D_8)	MBR10100
Dimming frequency	200 Hz

The experimental waveforms of voltages V_{AC} and V_{BC}, currents i_{r1} and i_{r2} are shown in Fig. 5.8. Fig. 5.9 shows experimental waveforms of voltages and currents of all the switches in the proposed converter when the two loads are fully illuminated. From these waveforms, it is observed that all the switches in the converter are turned on with ZVS. Hence the switching losses of the converter are less.

The experimental waveforms of load voltages and load currents when both the loads are fully illuminated are shown in Fig. 5.10. To verify the independent dimming of the proposed converter PWM dimming with 200 Hz is implemented and the results are presented in Fig.s 5.11 and 5.12. Fig. 5.11 shows the experimental waveforms of load voltage and load current with 70% and 40% illumination of load-1 and load-2 respectively. Fig. 5.12 shows the experimental load voltage and load current with 40% and 70% illumination of load-1 and load-2 respectively. Figs 5.11 and 5.12 prove the independent dimming operation of both the loads. Experimental waveforms of all the switch voltages and currents when one load is ON and the other load is OFF are shown in Fig. 5.13 and Fig. 5.14. From these figures, it can be observed that all the switches are turn-on with ZVS even in the dimming operation also. Fig. 5.15 shows the transient response of the proposed converter. From this figure, it can be observed that the load change in one output is not affecting the operation of the other load. Variation of Lamp-1 and

Lamp-2 currents w.r.t duty cycles D_1 and D_3 are shown in Fig. 5.16. From this figure, it is clear that Lamp-1 and Lamp-2 currents can be regulated independently by varying duty cycles D_1 and D_3 respectively. The different losses occurring in the converter are calculated using the equations (5.22)-(5.25) and those are shown in Fig. 5.17a. From Fig. 5.17a it is observed that most losses occur in diode bridge rectifiers. The variation of efficiency with input voltage is shown in Fig. 5.17b. Variation of efficiency of the proposed LED driver w.r.t dimming percentage of the lamps is shown in Fig. 5.18. From Fig. 5.18 it is clear that the efficiency of the proposed LED driver is almost maintained constant throughout the dimming range and is near to 91%.

The proposed LED driver is compared with the recent multiple-output LED driver topologies and details are provided in Table IV. The component count per lamp of topologies [82] and [50] is less compared to the proposed topology, but independent current regulation and dimming are not possible. Independent dimming is possible in the topology presented [85], but this topology can drive LED loads with equal currents only. To regulate the LED currents independently variable inductor is used in each channel of configuration in [52]. The implementation of the variable inductor is difficult. The topologies presented in [97] and [98] can drive multiple LED loads with independent current control and dimming, but the component count of these topologies are higher when compared to the proposed LED driver. The topology presented in [91] uses fewer components and also uses a single closed loop to implement independent dimming control. However, the converter is operating with hard switching. Hence, the efficiency of the converter in [91] is less when compared to the proposed topology.

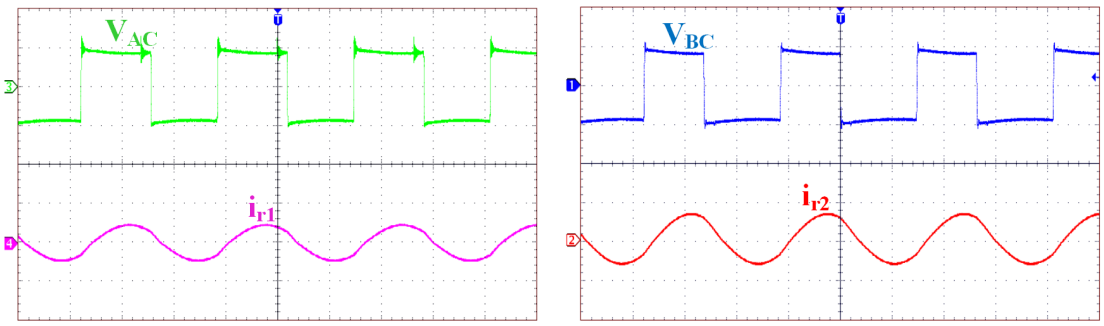

(a) (b)

Figure 5.8: Resonant circuit voltages and currents (a) Experimental waveforms of V_{AC}, i_{r1} (V_{AC}: 25 V/div; i_{r1}: 5 A/div; time: 4 μs/div) (b) Experimental waveforms of V_{BC}, i_{r2} (V_{BC}: 25 V/div; ir2: 5 A/div; time: 4 μs/div)

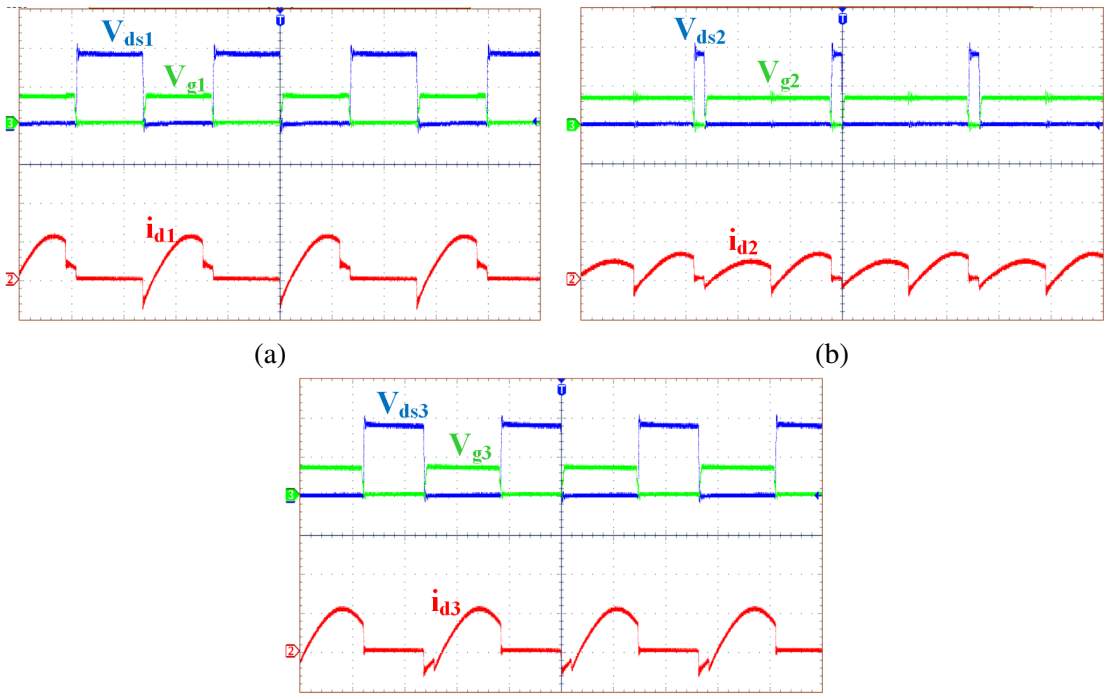

(a) (b)

(c)

Figure 5.9: Experimental voltage and current waveforms of the switches when both the loads are at full illumination (a) Waveforms of switch S_1 (V_{ds1}: 25 V/div; V_{g1}: 20 V/div; i_{d1}: 5A/div; time: 4 μs/div) (b) waveforms of switch S_2 (V_{ds2}: 25 V/div; V_{g2}: 20 V/div; i_{d2}: 5 A/div; time: 4 μs/div) (c) Waveforms of switch S_3 (V_{ds3}: 25 V/div; V_{g3}: 20 V/div; i_{d3}: 5 A/div; time: 4 μs/div)

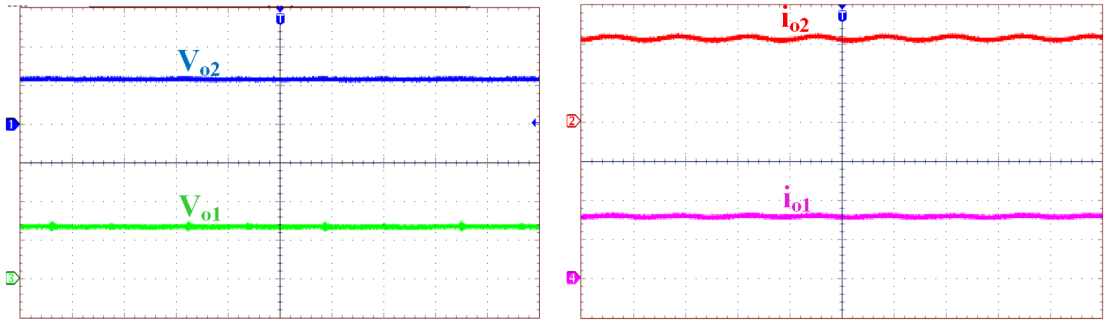

(a) (b)

Figure 5.10: Load voltage and current waveforms at full illumination (a) Experimental load voltage waveforms (V_{o1}: 12.5 V/div; V_{o2}: 12.5 V/div; time: 4 μs/div) (b) Experimental load current waveforms (i_{o1}: 1 A/div; i_{o2}: 1 A/div; time: 4 μs/div)

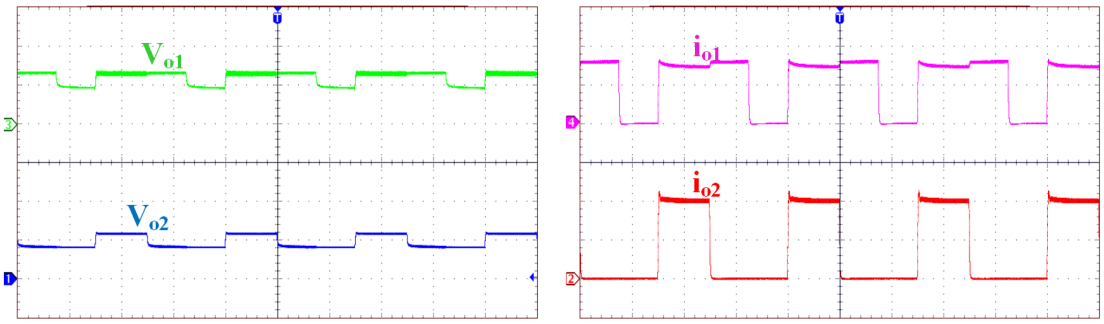

(a) (b)

Figure 5.11: Load voltage and current waveforms at 40% and 70% of full illuminations of Load1 and Load-2 respectively (a) Experimental load voltage waveforms (V_{o1}: 12.5 V/div; V_{o2}: 12.5 V/div; time: 2 ms/div) (b) Experimental load current waveforms (i_{o1}: 1 A/div; i_{o2}: 1 A/div; time: 2 ms/div)

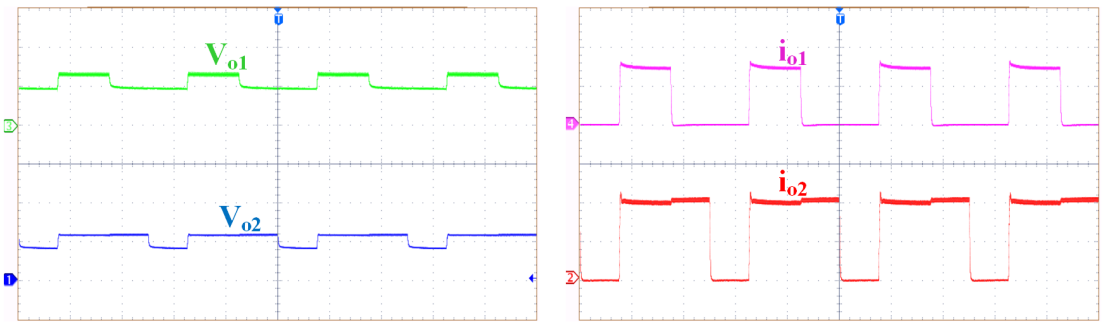

(a) (b)

Figure 5.12: Load voltage and current waveforms at 70% and 40% of full illuminations of Load1 and Load-2 respectively (a) Experimental load voltage waveforms (V_{o1}: 12.5 V/div; V_{o2}: 12.5 V/div; time: 2 ms/div) (b) Experimental load current waveforms (i_{o1}: 1 A/div; i_{o2}: 1 A/div; time: 2 ms/div)

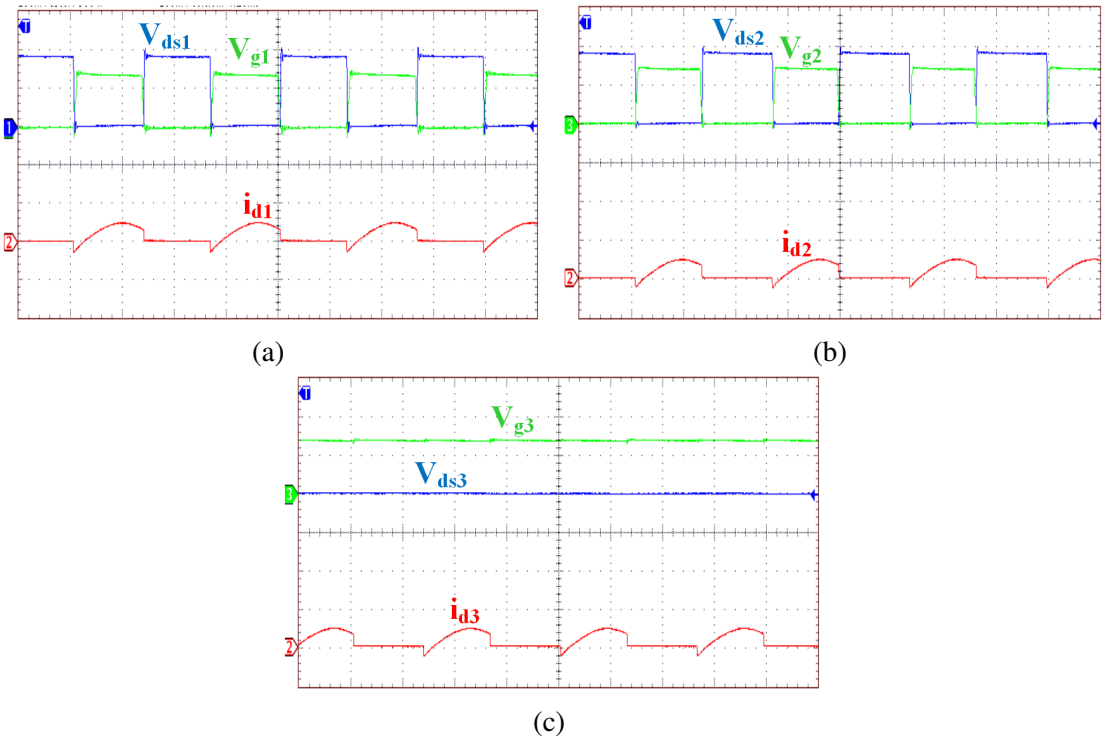

Figure 5.13: Experimental voltage and current waveforms of the switches when both the loads are at full illumination (a) Waveforms of switch S_1 (V_{ds1}: 25V/div; V_{g1}: 10 V/div; i_{d1}: 5 A/div; time: 4 μs/div) (b) waveforms of switch S_2 (V_{ds2}: 25V/div; V_{g2}: 10V/div; i_{d2}: 5A/div; time: 4μs/div) (c) Waveforms of switch S_3 (V_{ds3}: 25 V/div; V_{g3}: 10V/div; i_{d3}: 5A/div; time: 4 μs/div)

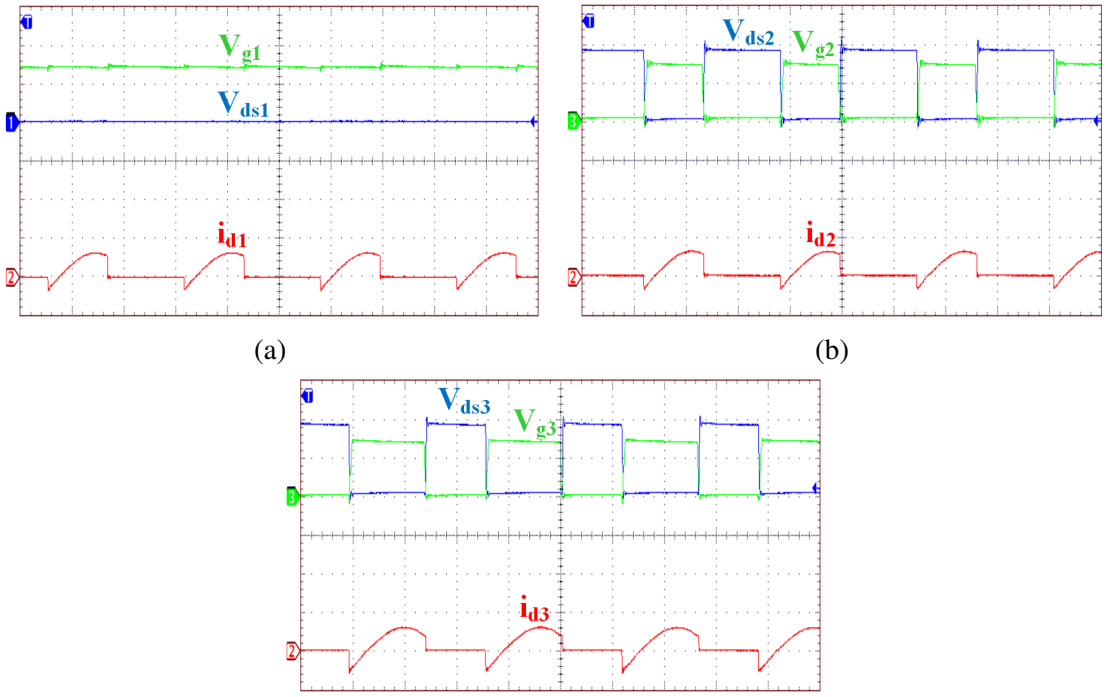

(a) (b)

(c)

Figure 5.14: Experimental voltage and current waveforms of the switches when both the loads are at full illumination (a) Waveforms of switch S_1 (V_{ds1}: 25V/div; V_{g1}: 10 V/div; i_{d1}: 5 A/div; time: 4 μs/div) (b) waveforms of switch S_2 (V_{ds2}: 25V/div; V_{g2}: 10V/div; i_{d2}: 5A/div; time: 4μs/div) (c) Waveforms of switch S_3 (V_{ds3}: 25 V/div; V_{g3}: 10V/div; i_{d3}: 5A/div; time: 4 μs/div)

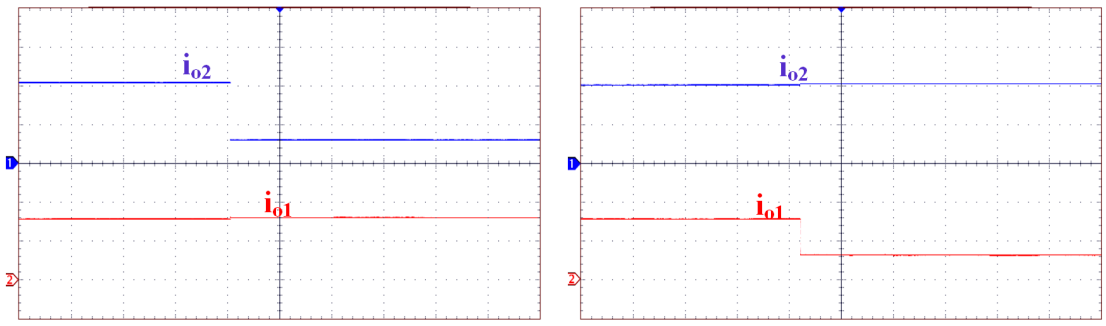

(a) (b)

Figure 5.15: Transient response of the converter for LED failures (a) LED load-1 is healthy LED load-2 changes from healthy to 75% LEDs are turned off (3 out of 4 LED strings are off) (i_{o1}: 1 A/div; i_{o2}: 1 A/div; time: 1 s/div) (b) LED load-2 is healthy LED load-1 changes from healthy to 66% LEDs are turned off (2 out of 3 LED strings are off) (i_{o1}: 1 A/div; i_{o2}: 1 A/div; time: 1 s/div)

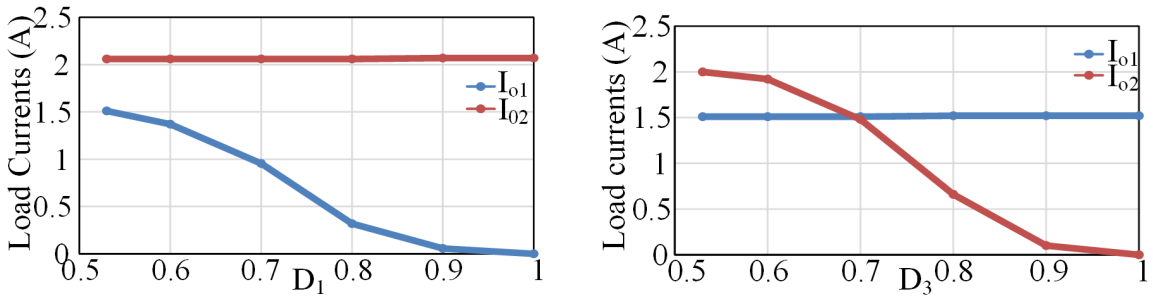

(a) (b)

Figure 5.16: Variation of load currents w.r.t duty ratios (a) Variation of Lamp-1 and Lamp-2 currents w.r.t D_1 at D_3 = 0.54 (b) Variation of Lamp-1 and Lamp-2 currents w.r.t D_3 at D_1 = 0.54

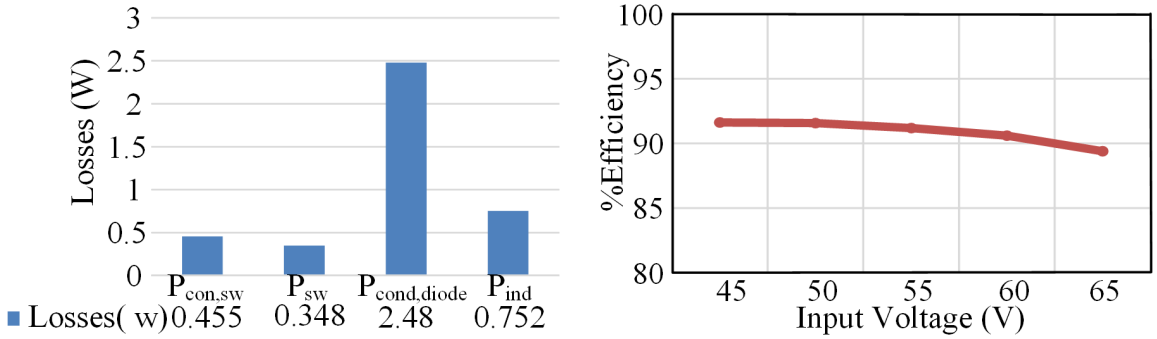

(a) (b)

Figure 5.17: (a) Loss distribution in the proposed converter at rated operating conditions (b) Variation of efficiency w.r.t input voltage

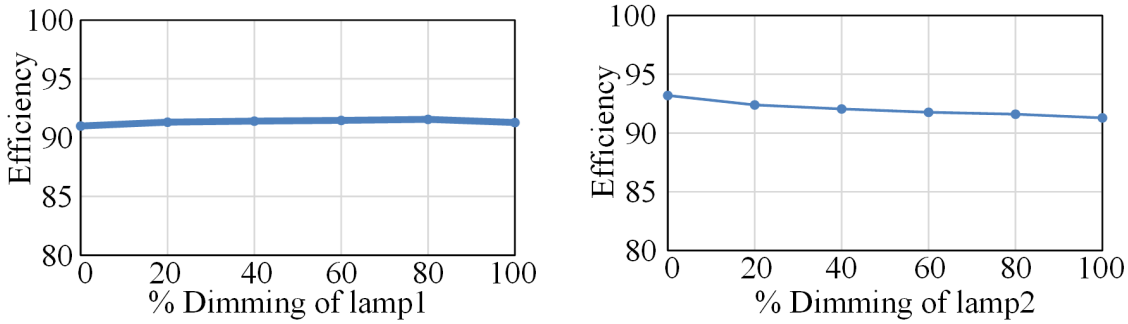

(a) (b)

Figure 5.18: Efficiency variations w.r.t percentage dimming (a) Efficiency w.r.t % dimming of Lamp-1 at full illumination of Lamp-2 (c) Efficiency w.r.t % dimming of Lamp-2 at full illumination of Lamp-1

Table 5.4: Comparision table

Refrences	Ref. [82]	Ref. [50]	Ref. [85]	Ref. [52]	Ref. [97]	Ref. [98]	Ref. [91]	Ref. [103]	Proposed
No. of switches	(n+2)	n	(2n+2)	2	(2n+2)	(2n+1)	(n+1)	(4n)	(n+1)
No. of inductors	(3n/2)	(n-1) 1(coupled)	2	n (Variable)	(n+1)	(n+1)	1	(n+1)	(2n)
No. of capacitors	1	(n+1)	(7n)	(2n)	(2n)	(2n+1)	n	(2n+1)	(2n+2)
No. of HF transformers	0	0	(n)	(n)	0	0	0	0	0
No. of diodes	1	n	(4n)	(2n)	(4n)	(4n)	(n+1)	(4n)	(4n)
No. of LED loads tested	4	2	2	1	2	2	2	1	2
Input voltage (volts)	48	150	400	380	48	48	48	18-120	48
Output voltages (volts)	33 (equal)	36, 7.2	–	25.4	42.25, 19.5	22.5, 39.6	–	22.5	16.25, 13
Total power (watts)	145	30	150	50	126	65	–	22.7	50
Peak efficiency	94.96	95.5	97.3	90.5	92.45	92.5	90	94	91.5
ZVS tur-on	Yes	Yes	Yes	Yes	Yes	Yes	No	Yes	Yes
Independent current regulation	No	No	No	Yes	Yes	Yes	Yes	–	Yes
Independent dimming	No	No	Yes	Yes	Yes	Yes	Yes	–	Yes

5.7 Conclusions

In this chapter, an Independently controllable dual-output series resonant converter has been developed to power two LED lamps with different power ratings. Two independent half-bridge series resonant converters are implimented with three switches, which reduces the switch count. Asymetric duty cycle control is used to regulate the LED currents aganist input voltage variatios. Principle of operation, analysis, design procedure and current regulation feature are explained in detail. Experimental results obtained from a 50 W prototype are presented.

This configuration has the following advantages;

1. Drives two LED lamps of different power rating with same input voltage.
2. All the switches are operated with ZVS.
3. Both LED lamps can be independently regulated at the required operating voltage and current.
4. Both LED lamps can be dimmed independently.
5. High efficiency is obtained at any dimming level of both LED lamps.
6. The proposed topology can be suitable for color mixing and multi color lighting applications.
7. It can be powered from low voltage dc grid or battery operated systems.

Chapter 6

Conclusions and future scope of research

Chapter 6

Conclusions and future scope of research

6.1 Conlcusions

In present lighting industry, Light Emitting Diode (LED) becomes a prominent light source for wide range of residential, industrial and commercial lighting applications. LED based lighting systems have gained remarkable attention over conventional lighting systems due to their several advantages such as energy efficient, high operating life, high brightness, environment friendly nature, and compactness. LEDs are current controlled or current driven devices. Hence LED based lighting systems require efficient constant current regulators. The essential requirements of LED driver circuits are: high efficiency, LED load current regulation, dimming control, compact size, high reliability etc.

Keeping in view the requirements of LED driver circuits, THREE driver circuit configurations for LED based lighting applications have been proposed in this thesis. All configurations provide zero-voltage switching (ZVS), dimming control and current regulation.

In first proposed configuration, an input voltage regulated full-bridge converter for LED driver application is presented. Proposed converter operates with constant duty ratio at 200 kHz. It powers four LED lamps. In this converter the output of full-bridge series resonant converter is concceted in series with the input voltage. Hence, part of the output directly supplied from input wthout processing thorugh series resonant converter. Therefore the efficiency of the converter high. Regulation of LED lamp current is achieved by phase controll of the full-bridge converter in order to main the input voltage to the full-bridge converter constant for variations in input voltage. The overall power conversion efficiency is high in this configuration. Dimming for all LED lamps is attained through on-off technique at high efficiency. This configuration is suitable for high power lighting applications. It also reduces components count per lamp as well as the cost of the driver. The number of LED lamps can be increased by adding legs in the bridge. The proposed converter can be powered from battery or PV operated systems.

In the second proposed configuration, a dual frequency series resonat converter propsed to power two LED lamps with different power ratings is presented. Proposed converter operates at two different frequencies simultaneously. Two series resonant circuits are used to generate two different frequency currents simultaneously for powering two different lamps. Both lamps are controlled against input voltage variations. Also, both LED lamps can be dimmed independently. In addition, it offers partial ZVS. High efficiency is achieved at any dimming level of both LED lamps. It can be powered from low voltage dc grid or battery operated systems.

In the third proposed configuration, an independently controllable dual-output series resonant converter for LED driver application is presented. In this converter two SRCs are independently powered with only three switches, this reduces the component count of the converter. This converter can drive two loads with equal or unequal voltages or currents. The two load currents are independently regulated using asymmetric duty cycle control and independent dimming of both the loads is also achieved in this converter. All the switches in the converter are operated with ZVS turn on. Hence, the switching losses of the converter are less. This converter is suitable for multi-color lighting applications.

A relative comparison among proposed three configurations is shown Table 6.1. It is observed that all the three proposed configurations offer high efficiency (>90%), soft switching operation, dimming control and good current regulation. All are suitable for multiple output lighting applications. In addition to the above mentioned advantages,each configuration is having its unique advantages and is suitable for particular applications.

Table 6.1: Comparision among the proposed configurations

Feature	Configuration-1	Configuration-2	Configuration-3
No. of components/lamp	Low	High	High
ZVS switching	Yes	Partial	Yes
Device current stress	Low	High	High
Power rating of lamps	Equal	Different	Different
Independent current regulation	No	Yes	Yes
Independent dimming	No	Yes	Yes
No. of lamps powered	4	2	2
Peak efficiency(%)	95.6	90	91.5

The additional advantages of configuration-1 are partial power processing and low circuit component count per lamp. The first configuration is suitable for the applications where multiple lamps with equal power are required like street lighting, auditorium lighting, etc. Both second and third confgurations can drive two LED lamps with independent regulation and dimming. These configurations are sutitable where multiple LED lamps with different ratings with independent controll are required like color mixing, mlti color lighting, etc.

6.2 Future scope of research

The thesis work encourage with the scope for further research on following issues

1. The proposed configurations presented in this thesis work can be further explored and extended to other application.

2. Control techniques that suit LED based lighting applications can be further explored.

3. The proposed circuits can be investigated for solar photo voltaic (PV) fed lighting applications.

4. The proposed circuits can be investigated for second stage of LED drivers operated from utility supply.

Bibliography

Bibliography

[1] G. of India Ministry of Power Central Electricity Authority, *All India Electricity Statistics*, ser. General Review 2021. New Delhi: Government of India, 2021.

[2] M. Shur and R. Zukauskas, "Solid-state lighting: Toward superior illumination," *Proceedings of the IEEE*, vol. 93, no. 10, pp. 1691–1703, 2005.

[3] J. Tsao, "Solid-state lighting: lamps, chips, and materials for tomorrow," *IEEE Circuits and Devices Magazine*, vol. 20, no. 3, pp. 28–37, 2004.

[4] W. Chen, S. Li, and S. Hui, "A comparative study on the circuit topologies for offline passive light-emitting diode (LED) drivers with long lifetime & high efficiency," in *2010 IEEE Energy Conversion Congress and Exposition*, 2010, pp. 724–730.

[5] S. Y. Hui, S. N. Li, X. H. Tao, W. Chen, and W. M. Ng, "A novel passive offline LED driver with long lifetime," *IEEE Transactions on Power Electronics*, vol. 25, no. 10, pp. 2665–2672, 2010.

[6] B. Lee, H. Kim, and C. Rim, "Robust passive LED driver compatible with conventional rapid-start ballast," *IEEE Transactions on Power Electronics*, vol. 26, no. 12, pp. 3694–3706, 2011.

[7] J. M. Alonso, D. Gacio, A. J. Calleja, J. Ribas, and E. L. Corominas, "A study on led retrofit solutions for low-voltage halogen cycle lamps," *IEEE Transactions on Industry Applications*, vol. 48, no. 5, pp. 1673–1682, 2012.

[8] J.-B. Baek and S. Chae, "Single-stage buck-derived LED driver with improved efficiency and power factor using current path control switches," *IEEE Transactions on Industrial Electronics*, vol. 64, no. 10, pp. 7852–7861, 2017.

[9] G.-C. Tseng, K.-H. Wu, H.-J. Chiu, and Y.-K. Lo, "Single-stage high power-factor bridgeless AC-LED driver for lighting applications," in *2012 International Conference on Renewable Energy Research and Applications (ICRERA)*, 2012, pp. 1–6.

[10] K. Modepalli and L. Parsa, "Lighting up with a dual-purpose driver: A viable option for a light-emitting diode driver for visible light communication," *IEEE Industry Applications Magazine*, vol. 23, no. 2, pp. 51–61, 2017.

[11] C.-A. Cheng, C.-H. Chang, T.-Y. Chung, and F.-L. Yang, "Design and implementation of a single-stage driver for supplying an LED street-lighting module with power factor corrections," *IEEE Transactions on Power Electronics*, vol. 30, no. 2, pp. 956–966, 2015.

[12] Z. Ye, F. Greenfeld, and Z. Liang, "Offline sepic converter to drive the high brightness white LED for lighting applications," in *2008 34th Annual Conference of IEEE Industrial Electronics*, 2008, pp. 1994–2000.

[13] F. Wang, L. Li, Y. Zhong, and X. Shu, "Flyback-based three-port topologies for electrolytic capacitor-less LED drivers," *IEEE Transactions on Industrial Electronics*, vol. 64, no. 7, pp. 5818–5827, 2017.

[14] A. Shrivastava, B. Singh, and S. Pal, "A novel wall-switched step-dimming concept in LED lighting systems using PFC zeta converter," *IEEE Transactions on Industrial Electronics*, vol. 62, no. 10, pp. 6272–6283, 2015.

[15] F. Sichirollo, J. M. Alonso, and G. Spiazzi, "A novel double integrated buck offline power supply for solid state lighting applications," in *2013 IEEE Industry Applications Society Annual Meeting*, 2013, pp. 1–8.

[16] J. Sebastian, D. G. Lamar, M. Arias, M. Rodriguez, and M. M. Hernando, "A very simple control strategy for power factor correctors driving high-brightness light-emitting diodes," in *2008 Twenty-Third Annual IEEE Applied Power Electronics Conference and Exposition*, 2008, pp. 537–543.

[17] K. Zhou, J. G. Zhang, S. Yuvarajan, and D. F. Weng, "Quasi-active power factor correction circuit for HBLED driver," *IEEE Transactions on Power Electronics*, vol. 23, no. 3, pp. 1410–1415, 2008.

[18] G.-C. Jane, Y.-L. Lin, H.-J. Chiu, and Y.-K. Lo, "Dimmable light-emitting diode driver with cascaded current regulator and voltage source," *IET Power Electronics*, vol. 8, no. 7, pp. 1305–1311, 2015. [Online]. Available: https://ietresearch.onlinelibrary.wiley.com/doi/abs/10.1049/iet-pel.2013.0908

[19] D. Camponogara, G. F. Ferreira, A. Campos, M. A. Dalla Costa, and J. Garcia, "Offline LED driver for street lighting with an optimized cascade structure," *IEEE Transactions on Industry Applications*, vol. 49, no. 6, pp. 2437–2443, 2013.

[20] F. Zhang, J. Ni, and Y. Yu, "High power factor AC-DC LED driver with film capacitors," *IEEE Transactions on Power Electronics*, vol. 28, no. 10, pp. 4831–4840, 2013.

[21] X. Qu, S.-C. Wong, and C. K. Tse, "Noncascading structure for electronic ballast design for multiple LED lamps with independent brightness control," *IEEE Transactions on Power Electronics*, vol. 25, no. 2, pp. 331–340, 2010.

[22] X. Wu, J. Yang, J. Zhang, and Z. Qian, "Variable on-time (VOT)-controlled critical conduction mode buck PFC converter for high-input ac/dc hb-led lighting applications," *IEEE Transactions on Power Electronics*, vol. 27, no. 11, pp. 4530–4539, 2012.

[23] U. R. Reddy, "Single-stage electrolytic capacitor less non-inverting buck-boost PFC based AC-DC ripple free LED driver," *IET Power Electronics*, vol. 10, pp. 38–46(8), January 2017. [Online]. Available: https://digital-library.theiet.org/content/journals/10.1049/iet-pel.2015.0945

[24] H.-C. Kim, M. C. Choi, S. Kim, and D.-K. Jeong, "An AC-DC LED driver with a two-parallel inverted buck topology for reducing the light flicker in lighting applications to low-risk levels," *IEEE Transactions on Power Electronics*, vol. 32, no. 5, pp. 3879–3891, 2017.

[25] S. Wang, X. Ruan, K. Yao, S.-C. Tan, Y. Yang, and Z. Ye, "A flicker-free electrolytic capacitor-less AC-DC LED driver," *IEEE Transactions on Power Electronics*, vol. 27, no. 11, pp. 4540–4548, 2012.

[26] M. Arias, D. G. Lamar, J. Sebastián, D. Balocco, and A. Diallo, "High-efficiency LED driver without electrolytic capacitor for street lighting," in *2012 Twenty-Seventh Annual*

IEEE Applied Power Electronics Conference and Exposition (APEC), 2012, pp. 1224–1231.

[27] D. Camponogara, D. R. Vargas, M. A. Dalla Costa, J. M. Alonso, J. Garcia, and T. Marchesan, "Capacitance reduction with an optimized converter connection applied to LED drivers," *IEEE Transactions on Industrial Electronics*, vol. 62, no. 1, pp. 184–192, 2015.

[28] D. G. Lamar, M. Arias, A. Rodriguez, J. Sebastian, A. Fernandez, and J. A. Villarejo, "A sustained increase of input current distortion in active input current shapers to eliminate electrolytic capacitor for designing AC-DC HBLED drivers for retrofit lamps applications," in *2016 IEEE Applied Power Electronics Conference and Exposition (APEC)*, 2016, pp. 1823–1830.

[29] Q. Hu and R. Zane, "LED driver circuit with series-input-connected converter cells operating in continuous conduction mode," *IEEE Transactions on Power Electronics*, vol. 25, no. 3, pp. 574–582, 2010.

[30] H. van der Broeck, G. Sauerlander, and M. Wendt, "Power driver topologies and control schemes for LEDs," in *APEC 07 - Twenty-Second Annual IEEE Applied Power Electronics Conference and Exposition*, 2007, pp. 1319–1325.

[31] S. Winder, *Power Supplies for LED Driving*. Newnes, 2017, vol. 2nd ed.

[32] Y. Hu and M. M. Jovanovic, "LED driver with self-adaptive drive voltage," *IEEE Transactions on Power Electronics*, vol. 23, no. 6, pp. 3116–3125, 2008.

[33] J. Garcia, A. J. Calleja, E. L. Corominas, D. G. Vaquero, and L. Campa, "Interleaved buck converter for fast pwm dimming of high-brightness LEDs," *IEEE Transactions on Power Electronics*, vol. 26, no. 9, pp. 2627–2636, 2011.

[34] W. Yu, J.-S. Lai, H. Ma, and C. Zheng, "High-efficiency DC-DC converter with twin bus for dimmable LED lighting," *IEEE Transactions on Power Electronics*, vol. 26, no. 8, pp. 2095–2100, 2011.

[35] A. Pollock, H. Pollock, and C. Pollock, "High efficiency LED power supply," *IEEE Journal of Emerging and Selected Topics in Power Electronics*, vol. 3, no. 3, pp. 617–623, 2015.

[36] K. I. Hwu and W. Z. Jiang, "Nonisolated two-phase interleaved LED driver with capacitive current sharing," *IEEE Transactions on Power Electronics*, vol. 33, no. 3, pp. 2295–2306, 2018.

[37] C. Zheng, W. Yu, J.-S. Lai, and H. Ma, "Single-switch three-level boost converter for PWM dimming LED lighting," in *2011 IEEE Energy Conversion Congress and Exposition*, 2011, pp. 2589–2596.

[38] P. Malcovati, M. Belloni, F. Gozzini, C. Bazzani, and A. Baschirotto, "A 0.18-µm cmos, 91LED drivers," *IEEE Transactions on Power Electronics*, vol. 29, no. 10, pp. 5392–5398, 2014.

[39] M. Tahan and T. Hu, "Multiple string LED driver with flexible and high-performance PWM dimming control," *IEEE Transactions on Power Electronics*, vol. 32, no. 12, pp. 9293–9306, 2017.

[40] Y. Wang, J. M. Alonso, and X. Ruan, "A review of LED drivers and related technologies," *IEEE Transactions on Industrial Electronics*, vol. 64, no. 7, pp. 5754–5765, 2017.

[41] A. P. M. Arias, A. Vázquez, and P. J. Sebastián, "An overview of the AC-DC and DC-DC converters for LED lighting applications," *Automatika*, vol. 53, no. 2, pp. 156–172, 2012. [Online]. Available: https://doi.org/10.7305/automatika.53-2.154

[42] W. Thomas and J. Pforr, "Buck-boost converter topology for paralleling HBLEDSs using constant-power operation," in *International Conference on Power Electronics and Drive Systems (PEDS)*, 2009, pp. 568–573.

[43] S. Y. Fan, S. Y. Tseng, Y. J. Wu, and J. D. Lee, "PV power system using buck/forward hybrid converters for LED lighting," in *2009 IEEE Energy Conversion Congress and Exposition*, 2009, pp. 2584–2591.

[44] M. A. D. Costa, G. H. Costa, A. S. dos Santos, L. Schuch, and J. R. Pinheiro, "A high efficiency autonomous street lighting system based on solar energy and LEDs," in *2009 Brazilian Power Electronics Conference*, 2009, pp. 265–273.

[45] H. Wu and Y. Xing, "Families of forward converters suitable for wide input voltage range applications," *IEEE Transactions on Power Electronics*, vol. 29, no. 11, pp. 6006–6017, 2014.

[46] C. Brañas, F. J. Azcondo, R. Casanueva, and F. J. Díaz, "Phase-controlled parallel-series resonant converter to drive high-brightness power LEDs," in *IECON 2011 - 37th Annual Conference of the IEEE Industrial Electronics Society*, 2011, pp. 2953–2957.

[47] E. Eloi dos Santos Filho, P. H. A. Miranda, E. M. Sá, and F. L. M. Antunes, "A LED driver with switched capacitor," *IEEE Transactions on Industry Applications*, vol. 50, no. 5, pp. 3046–3054, 2014.

[48] S. Zhi, Q. Luo, C. Zou, and L. Zhou, "Analysis and design of a multi-channel constant current LED driver based on high frequency AC bus," in *Proceedings of The 7th International Power Electronics and Motion Control Conference*, vol. 1, 2012, pp. 210–214.

[49] X. Chen, D. Huang, Q. Li, and F. C. Lee, "Multichannel LED driver with CLL resonant converter," *IEEE Journal of Emerging and Selected Topics in Power Electronics*, vol. 3, no. 3, pp. 589–598, 2015.

[50] U. Ramanjaneya Reddy and B. L. Narasimharaju, "A cost-effective zero-voltage switching dual-output LED driver," *IEEE Transactions on Power Electronics*, vol. 32, no. 10, pp. 7941–7953, 2017.

[51] X. Qu, S.-C. Wong, and C. K. Tse, "An improved LCLC current-source-output multi-string LED driver with capacitive current balancing," *IEEE Transactions on Power Electronics*, vol. 30, no. 10, pp. 5783–5791, 2015.

[52] J. M. Alonso, M. S. Perdigão, M. A. Dalla Costa, G. Martínez, and R. Osorio, "Analysis and experiments on a single-inductor half-bridge LED driver with magnetic control," *IEEE Transactions on Power Electronics*, vol. 32, no. 12, pp. 9179–9190, 2017.

[53] J. Liu, J. Zeng, R. Hu, and K. W. E. Cheng, "A valley-fill driver with current balancing for parallel LED strings used for high-frequency AC power distribution of vehicle," *IEEE Transactions on Transportation Electrification*, vol. 3, no. 1, pp. 180–190, 2017.

[54] J. Liu, W. Sun, and J. Zeng, "Precise current sharing control for multi-channel LED driver based on switch-controlled capacitor," *IET Power Electronics*, vol. 10, no. 3, pp. 357–367, 2017. [Online]. Available: https://ietresearch.onlinelibrary.wiley.com/doi/abs/10.1049/iet-pel.2016.0294

[55] X. Chen, D. Huang, Q. Li, and F. C. Lee, "Multichannel LED driver with CLL resonant converter," *IEEE Journal of Emerging and Selected Topics in Power Electronics*, vol. 3, no. 3, pp. 589–598, 2015.

[56] J.-W. Kim, J.-P. Moon, and G.-W. Moon, "Duty-ratio-control-aided LLC converter for current balancing of two-channel LED driver," *IEEE Transactions on Industrial Electronics*, vol. 64, no. 2, pp. 1178–1184, 2017.

[57] W. Feng, F. C. Lee, and P. Mattavelli, "Optimal trajectory control of LLC resonant converters for LED PWM dimming," *IEEE Transactions on Power Electronics*, vol. 29, no. 2, pp. 979–987, 2014.

[58] E. F. Schubert, *Light-emitting diodes*, 2nd Edision. Cambridge University Press, 2006.

[59] G. Harbers, S. J. Bierhuizen, and M. R. Krames, "Performance of high power light emitting diodes in display illumination applications," *Journal of Display Technology*, vol. 3, no. 2, pp. 98–109, 2007.

[60] Y. Yang, Z. Song, and Y. Gao, "A white LED driver based on dual mode switch dimming," in *2009 Symposium on Photonics and Optoelectronics*, 2009, pp. 1–4.

[61] X. Xu and X. Wu, "High dimming ratio LED driver with fast transient boost converter," in *2008 IEEE Power Electronics Specialists Conference*, 2008, pp. 4192–4195.

[62] M. Doshi and R. Zane, "Control of solid-state lamps using a multiphase pulsewidth modulation technique," *IEEE Transactions on Power Electronics*, vol. 25, no. 7, pp. 1894–1904, 2010.

[63] I. Ashdown, "Extended parallel pulse code modulation of LEDs," *Proceedings of SPIE - The International Society for Optical Engineering*, 09 2006.

[64] W.-C. Yang, Y.-J. Chen, and C.-S. Moo, "An efficient driver for dimmable LED lighting," in *2011 6th IEEE Conference on Industrial Electronics and Applications*, 2011, pp. 2331–2336.

[65] W.-K. Lun, K. H. Loo, S.-C. Tan, Y. M. Lai, and C. K. Tse, "Bilevel current driving technique for LEDs," *IEEE Transactions on Power Electronics*, vol. 24, no. 12, pp. 2920–2932, 2009.

[66] K. Ramakrishnareddy Ch, S. Porpandiselvi, and N. Vishwanathan, "An efficient full-bridge resonant converter for light emitting diode (LED) application with simple current control," *International Journal of Circuit Theory and Applications*, vol. 47, no. 12, pp. 2019–2031, 2019. [Online]. Available: https://onlinelibrary.wiley.com/doi/abs/10.1002/cta.2694

[67] C. K. R. Reddy, S. Porpandiselvi, and V. Satyakar Veeramallu, "Input controlled series-resonant converter for LED lighting application," in *2018 3rd International Conference on Communication and Electronics Systems (ICCES)*, 2018, pp. 608–612.

[68] M. Arias, I. Castro, D. G. Lamar, A. Vázquez, and J. Sebastián, "Optimized design of a high input-voltage-ripple-rejection converter for LED lighting," *IEEE Transactions on Power Electronics*, vol. 33, no. 6, pp. 5192–5205, 2018.

[69] T. N. Gücin, B. Fincan, and M. Biberoğlu, "A series resonant converter-based multichannel LED driver with inherent current balancing and dimming capability," *IEEE Transactions on Power Electronics*, vol. 34, no. 3, pp. 2693–2703, 2019.

[70] C. Ye, P. Das, and S. Kumar Sahoo, "Peak current control of multichannel LED driver with selective dimming," *IEEE Transactions on Industrial Electronics*, vol. 66, no. 5, pp. 3446–3457, 2019.

[71] D. Mounika and S. Porpandiselvi, "ADC controlled parallel loaded resonant half-bridge converter for LED lighting," in *2017 2nd International Conference on Communication and Electronics Systems (ICCES)*, 2017, pp. 1031–1036.

[72] Mounika, D and Porpandiselvi, S, "ADC controlled half-bridge LC series resonant converter for LED lighting," in *2017 2nd International Conference on Communication and Electronics Systems (ICCES)*, 2017, pp. 1037–1042.

[73] S. Borekci, N. C. Acar, and A. Kircay, "LED dimming technique without frequency and pulse width modulations," *International Journal of Circuit Theory and Applications*, vol. 46, no. 11, pp. 2028–2037, 2018. [Online]. Available: https://onlinelibrary.wiley.com/doi/abs/10.1002/cta.2523

[74] A. Malschitzky, F. Albuquerque, E. Agostini, and C. B. Nascimento, "Single-stage integrated bridgeless-boost nonresonant half-bridge converter for LED driver applications," *IEEE Transactions on Industrial Electronics*, vol. 65, no. 5, pp. 3866–3878, 2018.

[75] H. Ma, Y. Li, Q. Chen, L. Zhang, and J. Xu, "A single-stage integrated boost-LLC AC-DC converter with quasi-constant bus voltage for multichannel LED street-lighting applications," *IEEE Journal of Emerging and Selected Topics in Power Electronics*, vol. 6, no. 3, pp. 1143–1153, 2018.

[76] Y. Wang, Y. Wang, and D. Xu, "A single-stage bridgeless LED driver based on CLCL resonant converter," in *2017 IEEE Industry Applications Society Annual Meeting*, 2017, pp. 1–6.

[77] C.-A. Cheng and T.-Y. Chung, "A single-stage LED streetlight driver with PFC and digital PWM dimming capability," *International Journal of Circuit Theory and Applications*, vol. 44, no. 11, pp. 1942–1958, 2016. [Online]. Available: https://onlinelibrary.wiley.com/doi/abs/10.1002/cta.2203

[78] Y. Jeong, J.-K. Kim, J.-B. Lee, and G.-W. Moon, "An asymmetric half-bridge resonant converter having a reduced conduction loss for DC-DC power applications with a wide range of low input voltage," *IEEE Transactions on Power Electronics*, vol. 32, no. 10, pp. 7795–7804, 2017.

[79] L. Lin, J. Xu, Y. Chen, X. Wang, and J. Cao, "Asymmetrical hybrid-controlled half-bridge LCC resonant converter with low conduction loss and wide ZVS operation

range," *Electronics Letters*, vol. 53, no. 21, pp. 1422–1424, 2017. [Online]. Available: https://ietresearch.onlinelibrary.wiley.com/doi/abs/10.1049/el.2017.2659

[80] Y. Wang, X. Hu, Y. Guan, and D. Xu, "A single-stage LED driver based on half-bridge *CLCL* resonant converter and buck–boost circuit," *IEEE Journal of Emerging and Selected Topics in Power Electronics*, vol. 7, no. 1, pp. 196–208, 2019.

[81] S. P. V. V. K. Satyakar and C. K. R. Reddy, "Buck-boost based parallel resonant converter for multiple load LED lighting application," in *2018 Third International Conference on Electrical, Electronics, Communication, Computer Technologies and Optimization Techniques (ICEECCOT)*, 2018, p. 72–77.

[82] C. Kasi Ramakrishnareddy, P. Shunmugam, and N. Vishwanathan, "Soft switched full-bridge light emitting diode driver configuration for street lighting application," *IET Power Electronics*, vol. 11, no. 1, pp. 149–159, 2018. [Online]. Available: https://ietresearch.onlinelibrary.wiley.com/doi/abs/10.1049/iet-pel.2017.0021

[83] K. R. Ch, S. Porpandiselvi, and N. Vishwanathan, "An efficient ripple-free LED driver with zero-voltage switching for street lighting applications," *EPE Journal*, vol. 29, no. 3, pp. 120–131, 2019. [Online]. Available: https://doi.org/10.1080/09398368.2019.1570745

[84] L. W. Luo Q, Zhu B and Z. L, "High step-down multiple-output LED driver with the current auto-balance characteristic," *Journal of Power Electronics*, vol. 12, no. 4, pp. 519–527, 2012.

[85] C. Ye, H. W. Chan, D. Lan, P. Das, and S. K. Sahoo, "Efficiency improvement of multi-channel LED driver with selective dimming," *IEEE Transactions on Power Electronics*, vol. 35, no. 6, pp. 6280–6291, 2020.

[86] Y. Cikai, P. Das, S. S. Kumar, and M. Pahlevaninezhad, "A multi-channel LED driver with selective dimming," in *2018 IEEE Applied Power Electronics Conference and Exposition (APEC)*, 2018, pp. 2221–2226.

[87] S. Li, Y. Guo, S.-C. Tan, and S. Y. Hui, "An off-line single-inductor multiple-output LED driver with high dimming precision and full dimming range," *IEEE Transactions on Power Electronics*, vol. 32, no. 6, pp. 4716–4727, 2017.

[88] Y. Guo, L. Sinan, A. Lee, S.-C. Tan, C. Lee, and S. Hui, "Single-stage AC/DC single-inductor multiple-output LED drivers," *IEEE Transactions on Power Electronics*, vol. 31, 10 2015.

[89] Y.-J. Woo, H.-P. Le, G.-H. Cho, G.-H. Cho, and S.-I. Kim, "Load-independent control of switching DC-DC converters with freewheeling current feedback," *IEEE Journal of Solid-State Circuits*, vol. 43, no. 12, pp. 2798–2808, 2008.

[90] D. Ma, W.-H. Ki, and C.-Y. Tsui, "A pseudo-CCM/DCM SIMO switching converter with freewheel switching," *IEEE Journal of Solid-State Circuits*, vol. 38, no. 6, pp. 1007–1014, 2003.

[91] Z. Dong, C. K. Tse, and S. Y. R. Hui, "Current-source-mode single-inductor multiple-output LED driver with single closed-loop control achieving independent dimming function," *IEEE Journal of Emerging and Selected Topics in Power Electronics*, vol. 6, no. 3, pp. 1198–1209, 2018.

[92] X. L. Li, Z. Dong, and C. K. Tse, "Series-connected current-source-mode multiple-output converters with high step-down ratio and simple control," *IEEE Transactions on Power Electronics*, vol. 34, no. 10, pp. 10 082–10 093, 2019.

[93] M. Martins, M. S. Perdigão, A. M. S. Mendes, R. A. Pinto, and J. M. Alonso, "Analysis, design, and experimentation of a dimmable resonant-switched-capacitor LED driver with variable inductor control," *IEEE Transactions on Power Electronics*, vol. 32, no. 4, pp. 3051–3062, 2017.

[94] W. Chen and S. Y. R. Hui, "A dimmable light-emitting diode (LED) driver with mag-amp postregulators for multistring applications," *IEEE Transactions on Power Electronics*, vol. 26, no. 6, pp. 1714–1722, 2011.

[95] C. S. Wong, K. H. Loo, H. H.-C. Iu, Y. M. Lai, M. H. L. Chow, and C. K. Tse, "Independent control of multicolor-multistring LED lighting systems with fully switched-capacitor-controlled *LCC* resonant network," *IEEE Transactions on Power Electronics*, vol. 33, no. 5, pp. 4293–4305, 2018.

[96] G. Liang and H. Tian, "Novel single-inductor multistring-independent dimming LED driver with switched-capacitor control technique," *Journal of Power Electronics*, vol. 19, pp. 1–10, 01 2019.

[97] K. R. Ch, S. Porpandiselvi, and N. Vishwanathan, "A three-leg resonant converter for two output LED lighting application with independent control," *International Journal of Circuit Theory and Applications*, vol. 47, no. 7, pp. 1173–1187, 2019. [Online]. Available: https://onlinelibrary.wiley.com/doi/abs/10.1002/cta.2632

[98] V. K. S. Veeramallu, P. S., and N. B. L., "A buck-boost integrated high gain non-isolated half-bridge series resonant converter for solar PV/battery fed multiple load LED lighting applications," *International Journal of Circuit Theory and Applications*, vol. 48, no. 2, pp. 266–285, 2020. [Online]. Available: https://onlinelibrary.wiley.com/doi/abs/10.1002/cta.2720

[99] J. Burdio, F. Canales, P. Barbosa, and F. Lee, "Comparison study of fixed-frequency control strategies for ZVS DC-DC series resonant converters," in *2001 IEEE 32nd Annual Power Electronics Specialists Conference (IEEE Cat. No.01CH37230)*, vol. 1, 2001, pp. 427–432 vol. 1.

[100] R. U. Lenke, J. Hu, and R. W. De Doncker, "Unified steady-state description of phase-shift-controlled ZVS-operated series-resonant and non-resonant single-active-bridge converters," in *2009 IEEE Energy Conversion Congress and Exposition*, 2009, pp. 796–803.

[101] Q. Luo, S. Zhi, C. Zou, B. Zhao, and L. Zhou, "Analysis and design of a multi-channel constant current light-emitting diode driver based on high-frequency AC bus," *IET Power Electronics*, vol. 6, no. 9, pp. 1803–1811, 2013. [Online]. Available: https://ietresearch.onlinelibrary.wiley.com/doi/abs/10.1049/iet-pel.2012.0696

[102] B. Lehman and A. J. Wilkins, "Designing to mitigate effects of flicker in LED lighting: Reducing risks to health and safety," *IEEE Power Electronics Magazine*, vol. 1, no. 3, pp. 18–26, 2014.

[103] V. K. S. Veeramallu, S. Porpandiselvi, and B. L. Narasimharaju, "A nonisolated wide input series resonant converter for automotive LED lighting system," *IEEE Transactions on Power Electronics*, vol. 36, no. 5, pp. 5686–5699, 2021.

List of publications

International journal & conference publications:

[1] Hemasundara Rao. Kolla, Viswanathan. Neti, and Bhagwan. K. Murthy, "**Input voltage controlled full-bridge series resonant converter for LED driver application**," in *IET Power Electronics*, vol. 13, no. 19, Dec 2020, pp. 4532-4541, doi: 10.1049/iet-pel.2020.0554.

[2] N. Vishwanathan, Hemasundara Rao. Kolla, and Bhagwan. K. Murthy, " **Dual frequency series resonant converter based LED driver**," in *2019 National Power Electronics Conference (NPEC)*, Tiruchirappalli, India, 2019, pp. 1-4, doi: 10.1109/NPEC47332.2019.9034731 .

[3] Hemasundara Rao Kolla, N. Vishwanathan, and Bhagwan. K. Murthy, "**"Independently controllable dual-output half-bridge series resonant converter for LED driver application**," in *IEEE Journal of Emerging and Selected Topics in Power Electronics*, vol. 10, no. 2, pp. 2178-2189, April 2022, doi: 10.1109/JESTPE.2021.3120879.